

Review

Di-, oligo- and polymetallaynes: Syntheses, photophysics, structures and applications

Wai-Yeung Wong^{*}, Cheuk-Lam Ho

Department of Chemistry and Centre for Advanced Luminescence Materials, Hong Kong Baptist University, Waterloo Road, Kowloon Tong, Hong Kong, PR China

Received 14 December 2005; accepted 7 April 2006

Available online 25 April 2006

Contents

1. Introduction	2628
2. Structural variation systematics	2629
3. Effect of spacer groups	2630
3.1. Rigid-rod transition metal polyyne polymers of group 10 elements and their discrete molecular model oligomers	2630
3.1.1. Compounds with carbocyclic spacers	2630
3.1.2. Compounds with heterocyclic spacers	2641
3.1.3. Compounds with main group elements	2647
3.1.4. Compounds with metalloligand components	2653
4. Effect of auxiliary co-ligands on the metal group	2655
5. Effect of metal centers	2656
6. Summary and outlook	2670
Acknowledgements	2687
References	2687

Abstract

Rigid-rod transition metal acetylide polymers or polymetallaynes belong to a class of metallopolymers, which are technologically and scientifically important owing to their unique structures and optoelectronic properties. Fine-tuning of the desired physical and functional properties can be achieved by appropriate structural variations of the polymetallaynes involving the exploitation of different metal groups, auxiliary co-ligands around the metal coordination spheres or bridging spacers. This article reviews recent progress over the past decade in the developments of transition metal-based polymetallaynes and their related molecular model oligomers. These model compounds are considered as useful building blocks for the high-molecular-weight polymers and valuable insights concerning their molecular and electronic properties can be obtained through the detailed studies of these oligomers. The driving force for such research work derives from the possibility of coupling the chemical, electronic, optical and redox properties of transition metal complexes to those of the organic chromophores, thus affording novel metal-containing macromolecules with new material properties. Synthetic routes for the preparation of the metallopolymers as well as their photophysical and structural aspects are

Abbreviations: acac, acetylacetonate; COSY, correlated spectroscopy; Cp^{*}, bis(pentamethylcyclopentadienyl); Cy, cyclohexyl; D- π -A, donor- π -acceptor; DFT, density functional theory; dppe, bis(diphenylphosphino)ethane; dppm, bis(diphenylphosphino)methane; Fc, ferrocenyl group (η^5 -C₅H₅)(η^5 -C₅H₄)Fe; GPC, gel permeation chromatography; HOMO, highest occupied molecular orbitals; HRS, hyper-Rayleigh scattering; ICT, intramolecular charge-transfer; IE, ionization energy; IR, infrared spectroscopy; ISC, intersystem crossing; ITO, indium–tin-oxide; LED, light-emitting diodes; LLCT, ligand to ligand charge-transfer; LUMO, lowest occupied molecular orbitals; MALDI-TOF, matrix assisted laser desorption ionization time-of-flight; MMLCT, metal–metal to ligand charge-transfer; MLCT, metal to ligand charge-transfer; MNDO, modified neglect of differential overlap; NLO, non-linear optics; NMR, nuclear magnetic resonance; NOESY, nuclear overhauser effect spectroscopy; PEDOT, poly(3,4-ethylenedioxythiophene); PL, photoluminescence; PP, poly(*p*-phenylene)s; PPN, bis(triphenylphosphine)iminium; PPV, poly(*p*-phenylenevinylene)s; PSS, poly(styrenesulfonate); SAW, surface acoustic wave; *T*, transmittance; TEM, transmission electron microscopy; TGA, thermogravimetric analysis; TIPS, triisopropylsilyl; TLC, thin-layer chromatography; Tol, tolyl; TPA, two-photon absorption; UV–vis, ultraviolet–visible; XPS, X-ray photoelectron spectroscopy

^{*} Corresponding author. Tel.: +852 34117074; fax: +852 34117348.

E-mail address: rwylwong@hkbu.edu.hk (W.-Y. Wong).

summarized. Various up-and-coming applications of such family of compounds as molecular electronic, photonic and chemical sensing devices are also critically discussed in this review.

© 2006 Elsevier B.V. All rights reserved.

Keywords: Alkynyl; Crystal structures; Luminescence; Metallopolymers; Polyynes; Transition metals

1. Introduction

The incorporation of transition metal elements into a polymeric skeleton was shown to be an excellent and effective way of affording new metallopolymers with different properties from classical carbon-based polymers [1–5]. Such research work provides a good opportunity for coupling the chemical, electronic and optical properties of metal complexes to those of the organic chromophoric component, thus accessing novel polymers with new functional properties. These metal-based polymeric systems have demonstrated a wide range of interesting reactivity, optical, luminescent, magnetic and redox characteristics. Within the family of synthetic metal-containing polymers, polymers with direct metal–carbon σ -bonds in the main chain represent one of the most important categories of these materials [1,3]. Rigid-rod transition metal acetylide polymers or polymetallaynes were identified as the exciting and extensively investigated area of these metallopolymers [6–8].

One of the founding fathers of the oligo- and polymetallaynes is Hagihara who reported on the first synthesis of oligomeric and polymeric palladium(II) and platinum(II) acetylide compounds stabilized by tertiary phosphine ligands in the 1970s [9–12]. Since then, the chemistry of group 10 metal-containing polymetallaynes and their molecular model compounds have gained much research momentum, owing to their anticipated applications in molecular electronics, photonics and optical sensing (Fig. 1). In the early 1990s, numerous reports by Lewis and co-workers described the synthesis of rigid-rod metal-containing polyynes using bis(trimethylstannylacetylide) precursors [13–16]. The linear geometry of the alkynyl unit and its unsaturated character have made metal alkynyls very promising and versatile structural building blocks for molecular wires and organometallic oligomeric and polymeric alkynyl materials and the current interest in these materials is largely due to their electrical conductivities, rich luminescence properties, non-linear optical (NLO) properties, liquid crystallinity and photovoltaic behavior [6].

Organometallic materials are of particular interest in applications that demand light emission, for example as the active materials in light-emitting diodes (LEDs) and optical oxygen sensors [17–21]. This interest derives from the fact that incorporation of heavy metals into an organic conjugated framework can elicit large effects on the electronic and optical properties of the materials. In light of this, the search for new metalloorganic functional materials suitable for optoelectronic applications continues to attract much current attention as they have the potential to act as new systems for electronically important materials in various domains. Organic polymers are cheap to fabricate over large areas. If such materials can also provide electronic functionality, they would offer a very attractive route for the development of devices, which are necessarily large area (e.g. displays, photovoltaic cells, etc.). The current world-wide interest in conjugated polymer electroluminescence is driven by the perceived potential for the low-cost fabrication of large-area LEDs through simple processing methods. In such devices, light emission is believed to result from radiative decay of singlet excitons, created by electron–hole recombination within the organic layer. Triplet excitons are also produced, either by direct recombination of the charge carriers, or indirectly, through intersystem crossing from the singlet to the triplet manifold. The characterization of both the singlet and triplet excitations is thus of prime importance for understanding the mechanisms of LEDs based on conjugated polymers and thereby improving their macroscopic emission characteristics. In this context, polymetallayne systems have been widely studied as model systems to explain aspects of the photophysics of excited states in such conjugated polymers. Thus, in contrast to hydrocarbon conjugated polymers, the triplet excited state is accessible to experiment. In particular, poly(aryleneethynylene)s and their corresponding conjugated ethynylated materials and polymers of transition metals have been thoroughly investigated in this context. While intensive studies of conjugated polymers over the past few decades allow us to clarify some fundamental issues about the nature of the singlet excited states [22–25], yet still relatively little is known about the nature of triplet excited states in these materials. Much of the recent work has shown that electronic triplet states play a crucial role in optical and electrical processes within conjugated molecules with direct implications for their technological applications [26–33]. It has been recognized that the ultimate efficiency of LEDs is controlled by the fraction of triplet states generated or harvested [34–38]. It is therefore desirable to understand the photophysics of the triplet excited states and how they change with the chemical structure so that the relative separation of the energy bands can be manipulated and hence, the energy of the triplet excited state can be harvested directly. In this regard, there has been growing attention on the experimental and theoretical aspects for the

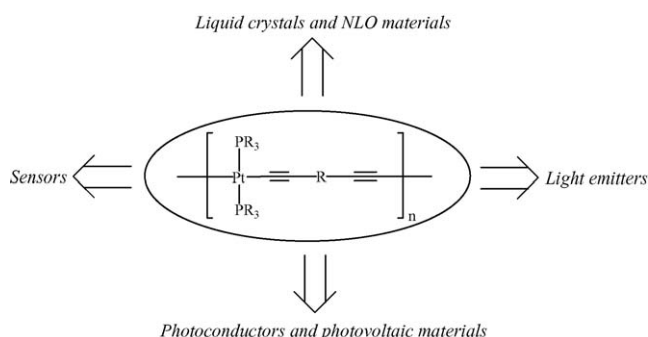


Fig. 1. Applications of polyplatinaynes in various domains of materials science.

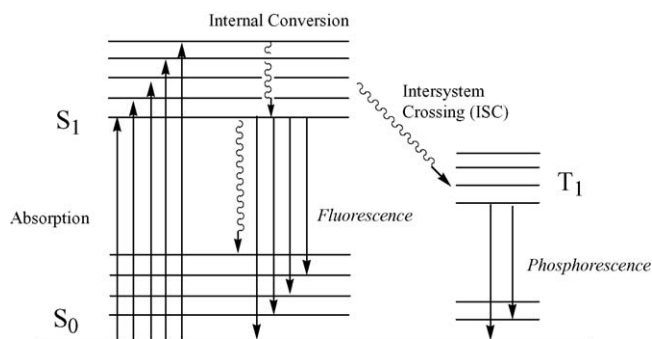


Fig. 2. The Jablonski diagram for a photoluminescence system.

energy levels of singlet and triplet states in conjugated polymers. Upon absorption of photons by a molecule, there are two possible radiative decay pathways, viz., fluorescence ($S_1 \rightarrow S_0$) and phosphorescence ($T_1 \rightarrow S_0$) (Fig. 2). The relative positions of singlet and triplet excited states strongly govern the intersystem crossing (ISC) rate into the triplet manifold. For organic systems, this provides a major nonradiative decay mechanism and reduces the luminescence efficiency. In accordance with the energy gap law, the ISC rate depends exponentially on the energy gap to the nearest triplet excited state [39]. Knowledge on the spatial extent of the singlet and triplet energy levels is thus critical in rational materials design. Transition metal-containing polyynes were widely employed as a research vehicle for studying the triplet excited states in conjugated polymers directly in which the heavy metals increase the spin–orbit coupling, rendering the spin-forbidden phosphorescence (triplet emission) partially allowed. The propensity of heavy transition elements such as Ir(III) and Pt(II) to mix singlet and triplet excited states leads to molecule-based materials, which feature high phosphorescence yields and relatively long emission lifetimes [18]. In fact, the triplet emission is extremely efficient, approaching 100% efficiency at low temperatures. This would render them ideal materials for high-efficiency LEDs. In LEDs, the ability to harvest light emission from both singlet and triplet excitons can result in devices that operate with high quantum efficiency.

2. Structural variation systematics

The general structure for the prototype polymetallayne is shown in Fig. 3, in which the polymer has a linear backbone comprised of the metal center M, the spacer group R and the auxiliary ligand L on the metal center. The polymer for much of this work is based on the group 10 platinum metal with the formulation *trans*-[–Pt(PBu₃)₂C≡C(*p*-C₆H₄)C≡C–]_n **1** and since then, a wide variety of relevant derivatives have been prepared where alkynyl units are bonded to various central spacer groups

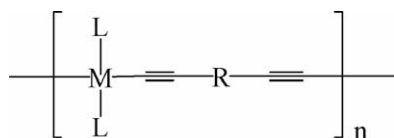


Fig. 3. General skeleton of transition metal polyne polymer.

[1,6,7]. All of these materials prepared are generally soluble in organic solvents and both the degree of solubility and the polymer length can be fine-tuned by appropriate choice of M, R or L units. This favorable feature accounts for the preference of the organometallic polymers over purely organic polymers where solubility is often a major problem when it comes to preparing films for optoelectronic measurements whereas little can be done to hurdle this obstacle. The tremendous progress in chemical synthesis has led to an extremely versatile route for producing a large range of application-tailored conjugated polymers of this kind in the literature. In order to achieve this target, many research groups have devoted their synthetic efforts to the three key areas, viz., variation of the M, R and L groups in such polymer structure (Fig. 3).

This article reviews current research work carried out on rigid-rod and in several occasions, hyperbranched transition metal polyne polymers and their corresponding monodisperse oligomers. The oligometallaynes can generally be considered as models and building blocks for the high-molecular-weight polymers and important information on their molecular and electronic properties can be obtained through the detailed studies of these model compounds. The polymeric compounds to be discussed are classified according to the types of metal groups, co-ligands on the metals and the central spacer units. The review will concentrate upon the developments from 1995 to 2005, but include significant earlier references where necessary for discussion. Most of the materials before 1995 are not covered in this article as they are periodically reviewed elsewhere [1,2,6]. The survey here also will not include discrete metal alkynyl compounds such as metal-acetylide cyclines, heterocyclines, catenane and polyhedral structures which are not of direct relevance to the topic in this review. Gladysz et al. and others have provided leading references to the modern literature of oligoynediyl and polyynediyl systems $M(C\equiv C)_nM$ [40–43]. Herein, oligomeric and polymeric metal alkynyl systems of the late transition metals are discussed, and particular attention is focused on the electronic absorption spectroscopy and photoluminescence behavior, electronic structures, thermal stability and structural aspects of these polymetallaynes. A detailed account of the evolution of the first excited singlet and triplet states on the electronic structure and conjugation length of the spacer groups of these metal polyne polymers is also given and the interplaying factors that influence the spatial extent of the lowest-lying singlet and triplet energy levels for the chemical tailoring of the singlet–triplet gap in polymetallaynes are described. All the metal polyynes and their molecular model compounds reported were characterized as fully as possible using conventional spectroscopic techniques. While the IR spectroscopy is useful for confirming the presence of the acetylenic unit in the complexes, there is little change in its position over a wide range of metals or spacer groups, and so it does not provide information as to the electronic properties of the coordinating moieties. The molecular weights of most of the soluble polymers were determined by GPC against polystyrene calibration. While GPC does not give absolute values of molecular weights but provides a measure of hydrodynamic volume, there is probably appreciable differences in the hydrodynamic behavior of rigid-rod type polymers in solu-

tion from those for flexible polymers. So, we would anticipate an overestimation of molecular weights, leading to certain systematic errors in the GPC measurements. But, the end group analysis in the NMR spectra can also help in examining the degree of polymerization (DP). The thermal stability of the polymers was studied by thermogravimetric analyses (TGA). Practical utilization of these metallocopolymers in different domains are critically discussed in this review.

3. Effect of spacer groups

3.1. Rigid-rod transition metal polyyne polymers of group 10 elements and their discrete molecular model oligomers

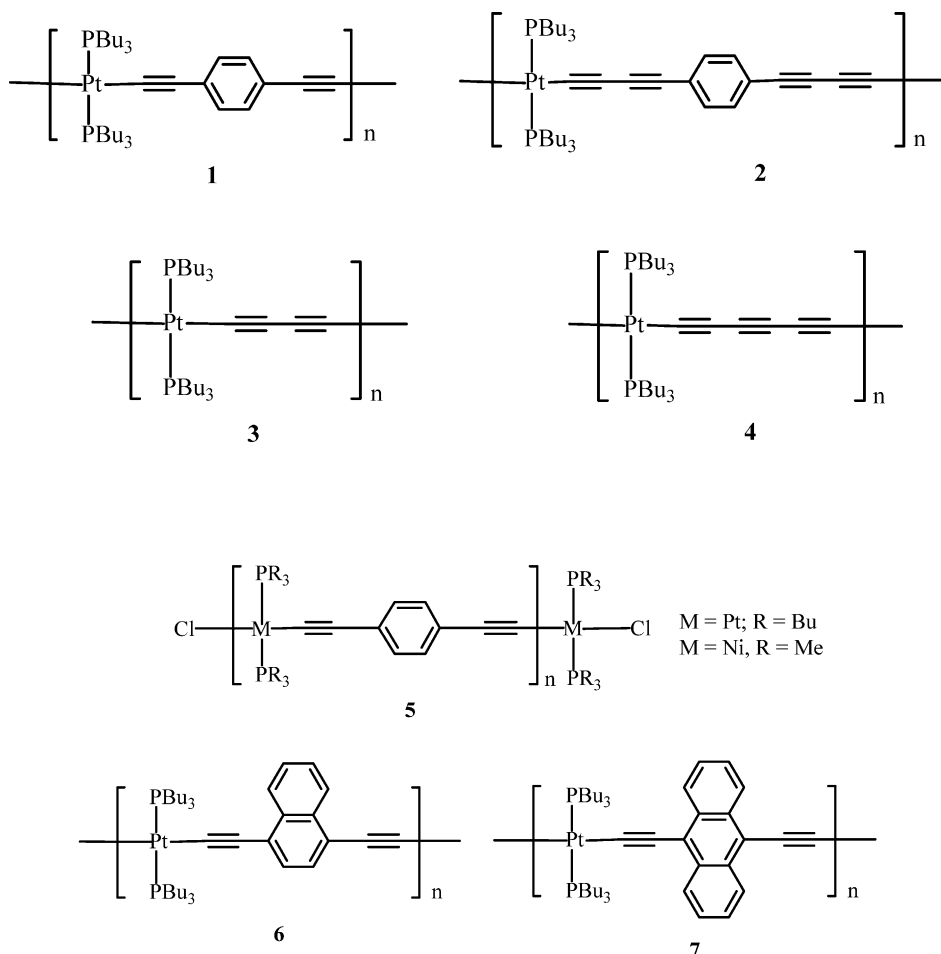
The synthetic tailoring of the organometallic σ -acetylide polymers to produce materials of variable optical bandgaps can be categorized according to the types of the metal groups, the central spacer units and the auxiliary ligands on the metals while keeping the rigid-rod nature of the polyyne backbone. Plenty of investigations have indicated that changing the nature of the spacer system has a significant effect on the size of the bandgap in the Pt-containing polyyne polymer, so the main synthetic aim will be to prepare new polymers, and their molecular precursors, with a list of different spacer groups ranging from some simple aromatic units, heteroaromatic groups, some group 14 main group elements and various inorganic/organometallic fragments. The following sections will give a summary of the recent research efforts devoted to the developments of group 10 metallocopolymers.

3.1.1. Compounds with carbocyclic spacers

Since the pioneering work by Hagihara et al. on the prototype compound of group 10 metals spaced by the phenylene ring **1** [9–12] followed by the versatile extension of the method to group 8 metals developed by the Lewis group in Cambridge [13–16], there has been considerable growing attention in the synthesis and detailed optical and spectroscopic characterization of this class of materials in the scientific community. First of all, it was shown that vibrational spectroscopy can help delineate structural properties of conjugated acetylenic polymers which are of pivotal importance to their function as electronic materials. A detailed vibrational spectroscopic investigation of rigid-rod platinum(II) acetylide polymers containing variable acetylenic microstructures **2–4** was provided [44]. In general,

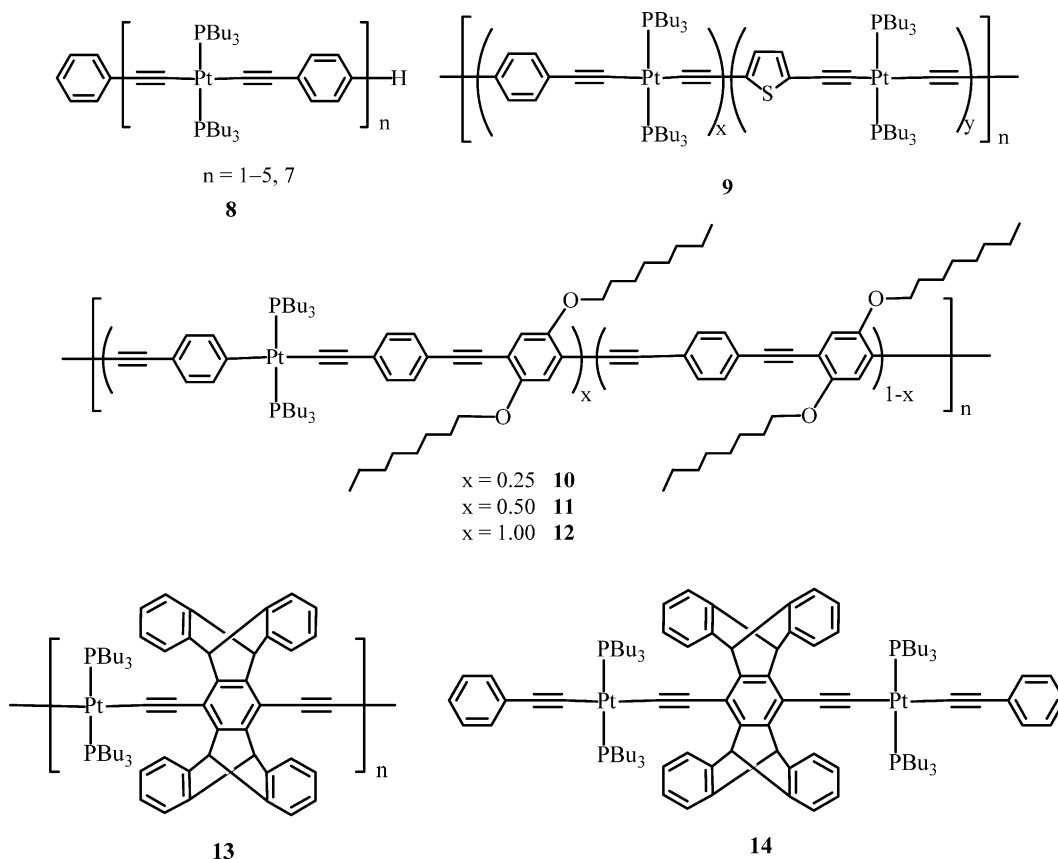
the vibrational data suggest that the backbone is essentially alternating $-\text{C}\equiv\text{C}-$ in nature, without any contribution from allene-type structures ($=\text{C}=\text{C}=$) typical for purely organic chains. The interruption of the acetylenic linkages with phenylene spacers reduces the extent of π -conjugation. The near-IR FT-Raman spectra of the polymers show resonance enhancement of selected vibrations, which take place along the polymer main chain. Vibrations in these rigid-rod compounds are strongly coupled to the electronic transitions of the delocalized polymeric backbone. These materials can exhibit strong and substituent-sensitive fluorescence in their FT-Raman spectra. Beljonne and co-workers have carried out a thorough experimental and theoretical study of the electronic excitations in **5** with two different group 10 metals [45]. The effect of the metal on the nature of the lowest singlet S_1 and triplet excited states T_1 is characterized. The authors have also analyzed the chain-length dependence of the $S_0 \rightarrow S_1$, $S_0 \rightarrow T_1$, and $T_1 \rightarrow T_n$ transition energies. According to both the experimental data and theoretical results obtained by the Hartree–Fock semiempirical modified neglect of differential overlap (MNDO) level, the lowest triplet exciton T_1 was shown to be heavily localized on a single C_6H_4 ring while the S_1 and T_n states extend over a few repeating units. The T_1 state was estimated to be ~ 0.6 eV below the S_1 state in the polymer. A Huang–Rhys analysis of the phosphorescence spectrum of these molecules was carried out which led to the conclusion that much more significant lattice distortions are calculated in the phenylene rings than the $\text{C}\equiv\text{C}$ units in both S_1 and T_1 states. These results were also confirmed by a theoretical modeling of the geometric relaxation process.

Since the use of fused-ring spacers were shown to be a powerful strategy to produce low bandgap conjugated polymers, platinum polyyne and diynes containing naphthalene and anthracene condensed carbocyclic systems **6** and **7** were synthesized and optically characterized [46]. The relative order of thermal stability follows the order: **7** > **6** > **1**. From the optical data, it is apparent that the electron-rich naphthalene and anthracene rings create strong donor–acceptor interactions between the Pt(II) units and conjugated organic groups along the rigid polyyne backbone. The bandgaps decrease as the size of the aromatic spacer increases, in line with there being greater delocalization within the anthryl group as compared to the phenylene spacer. For compounds that contain an anthracene unit, there is no evidence of observing any phosphorescence in thin films and the reason for this has been briefly discussed.



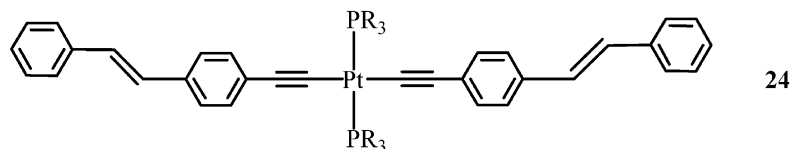
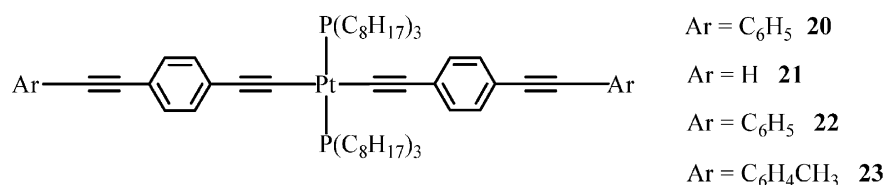
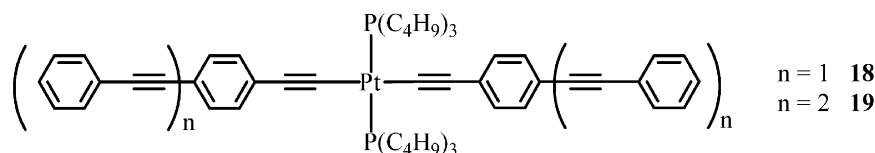
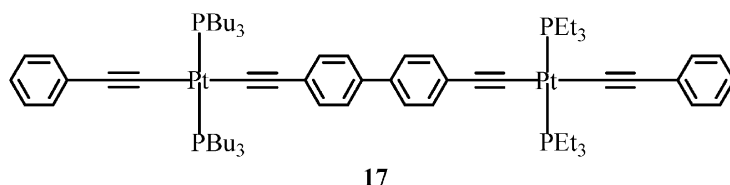
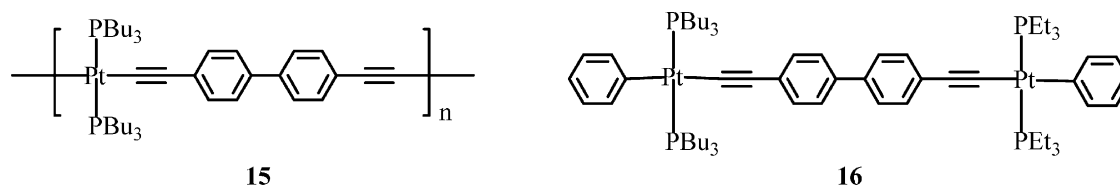
More recently, Schanze et al. have extensively reviewed the excited state properties of a series of Pt-acetylide oligomers, polymers and copolymers with a major focus placed on understanding structure–property relationships for the triplet state in such π -conjugated systems [47]. Several monodisperse Pt-acetylide oligomers of the form shown in **8** were prepared using an iterative-convergent approach. Absorption and emission data of these compounds are in line with the notion that S_1 is delocalized while T_1 is rather localized. An inverse square law between the oligomeric chain length and the energies of the Franck–Condon S_1 state, the relaxed S_1 state and the relaxed T_1 state was established in each case [48]. The findings are in good agreement with the theoretical results estimated for oligomers of linear polyenes, poly(*p*-phenylene)s (PP) and poly(*p*-phenylenevinylene)s (PPV) on the basis of a simple analytical Hückel model [49,50]. A series of platinum-containing poly(*p*-phenyleneethynylene)-type polymers **9–12** were prepared in which the content of Pt-acetylide repeat unit was varied [51]. The materials absorb strongly in the near UV region due to optical transitions involving ($\pi\pi^*$) character. The singlet exciton in the Pt-acetylide chain is delocalized over several repeat units, however, the triplet state is spatially confined on a chromophore consisting of two $[-\text{Pt}-\text{C}\equiv\text{C}-\text{C}_6\text{H}_4-\text{C}\equiv\text{C}-]$ units. Variation of the loading of the Pt-acetylide unit in the copolymers showed that the effect of spin–orbit coupling induced by the Pt-center decreases rapidly as the loading of the metal in the

backbone decreases. The mechanisms pertaining to the dynamics of intrachain energy transfer in these copolymers were discussed. Intrachain energy transfer could take place via either 1,4-phenylene \rightarrow 2,5-thienylene singlet energy transfer followed by ISC, or ISC followed by the triplet energy transfer from 1,4-phenylene to 2,5-thienylene [51]. The authors also found that the singlet exciton migrates rapidly, whereas the triplet exciton moves more slowly. They also examined recently the effect of aggregation or interchain interaction on the triplet excited state in Pt-acetylide materials by comparing the optical properties of **1** with another derivatized polymer **13** incorporating the pentyptycene unit [52]. The interchain interaction is precluded by the sterically demanding pentyptycene moiety in **13** and its photophysics is being dominated by the intrachain triplet exciton. It was shown that the solid-state phosphorescence spectrum of **13** is nearly superimposable with the emission profile of a single crystal of the model compound **14**. Such observation was also supported by the X-ray crystal structure analysis of **14** in which the Pt-acetylide chains are well separated by ~ 12 Å due to the sterically bulky spacer units. There is also a discussion on the effects of aggregation in **13** caused by the π – π stacking of the phenylene units and the introduction of low-lying excitations derived from $d\sigma^* \rightarrow p\sigma/\pi^*$ MMLCT (metal–metal to ligand charge transfer) transitions due to interchain Pt–Pt interactions.



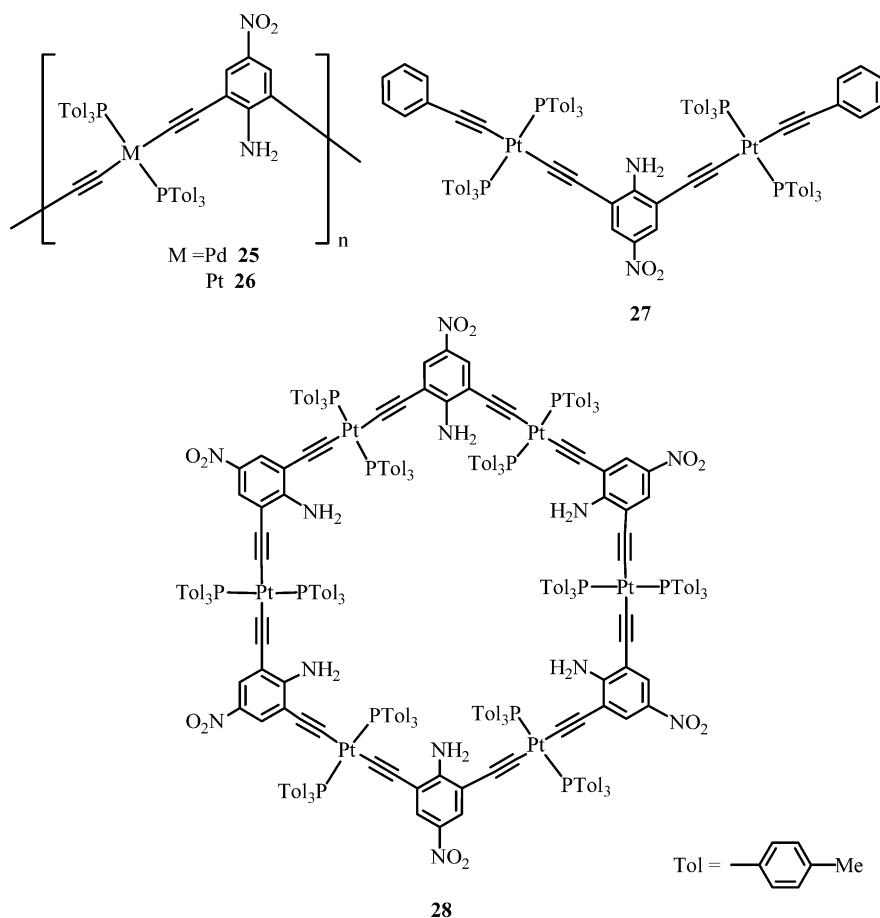
The synthesis, optical and structural properties of another Pt(II) polyyne containing biphenyl moiety **15** as well as its molecular diyne **16** were reported recently [53]. Another related highly ethynylated dinuclear Pt(II) tethers **17** was also reported by Russo and co-workers [54]. Such 4,4'-biphenyl-decorated system has also been extended to the Au(I) and Hg(II) congeners (vide infra). The influence of the metal center on the spatial extent of S_1 and T_1 excited states was characterized in detail. The ligand-based phosphorescence emissions can be harvested by the heavy-atom effect of these transition metals, which facilitates efficient intersystem crossing from the S_1 state to the T_1 state. Cooper et al. also synthesized a family of discrete platinum-containing phenylacetylene oligomers **18** and **19** and their molecular structure-spectroscopic property correlations were developed [55]. The extent of delocalization in these molecules was measured by studying the sensitivity of the electronic state energies to the number of repeat phenyl-ethynyl units. The S_0 and T_1 states were shown to be more localized over the chromophore than the S_1 and T_n states, and the charge-transfer character predominates in the $S_0 \rightarrow S_1$ and $T_1 \rightarrow T_n$ transitions. The authors further refined the investigations and a comprehensive study was performed using steady-

state absorption, steady-state emission, picosecond pump-probe, and nanosecond laser flash photolysis techniques to understand the effects of increased conjugation and the influence of platinum on the electronic structure [56]. As the conjugation length increases, the followings are observed: (i) a smaller phosphorescence quantum yield; (ii) a longer triplet lifetime; (iii) a reduced spin-orbit coupling effect; and (iv) a red-shift of absorption bands and an increase in the molar extinction coefficient. The glass-forming behavior of some platinum acetylide complexes **20–23** were described [57]. They are all liquids at room temperature and form glasses upon cooling. The presence of the long-chain trioctylphosphine ligands inhibited crystallization during cooling and they displayed glass-transition temperatures over the range of -67 to -82 °C. The photophysics and photochemistry of **20** was compared to those for the stilbene-containing molecule **24** [58]. The radiative decay was enhanced in **20** because the acetylene bridge in **20** does not undergo twisting in the excited state. But, the rapid nonradiative decay pathway in **24** is believed to originate from twisting of the olefinic bond in the stilbene moiety.

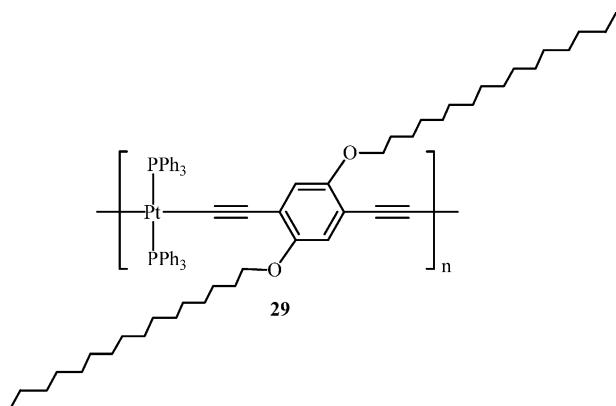


Some organometallic platinum(II) and palladium(II) acetylide polymers spaced by 2,6-diethynyl-4-nitroaniline bridge **25** and **26** were isolated in 70–75% yields and the geometrical model complex **27** was also obtained for the Pt(II) system for spectral comparison with those of the polymers [59]. In the polymerization reaction for the Pt(II) species, a cyclic hexanuclear hexagonal structure **28** was also proposed by the authors as a side product. Instead of exhibiting the rod-like zig-zag structure typical for group 10 polymetallaynes bearing simple phenyl or biphenyl rings, the polymer structures of **25** and **26** were shown to consist of a sequence of organic spacers

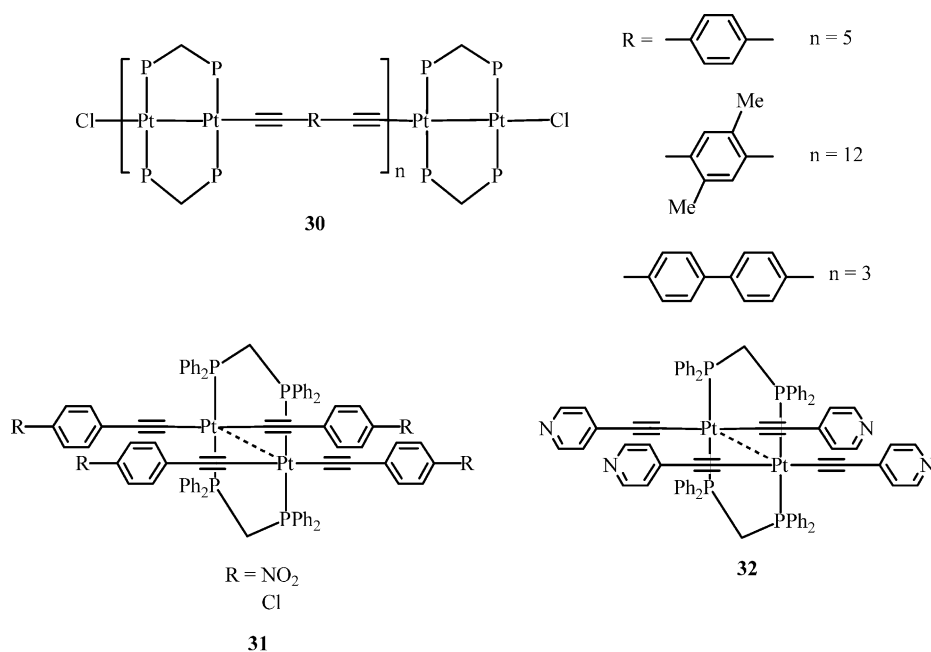
bound to metal centers, arranged in a helical configuration, with chain length corresponding to ~8 repeat units for **25** and ~16 repeat units for **26**. The polymer structure was elucidated using 2D COSY and NOESY NMR spectroscopy. Optical absorption studies and X-ray photoelectron spectroscopy (XPS) measurements indicated that only a limited extent of charge delocalization through the metal centers along the chain was apparent, presumably caused by the 1,3-conjugation for the alkyne units which precludes a fully delocalized π structures for these systems. This is in contrast to what was observed in other rod-like macromolecular structures.



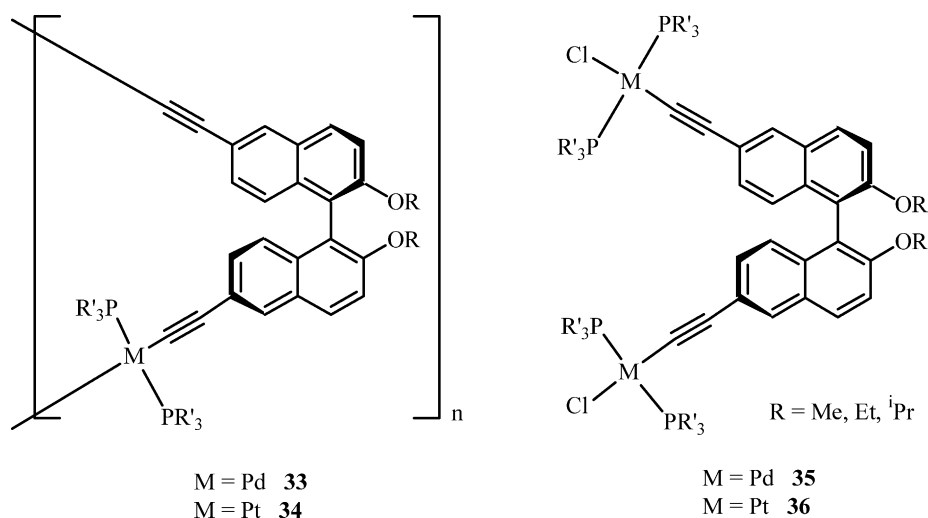
A new Pt(II) polyyn polymer **29**, prepared from the reaction of *cis*-[Pt(PPh₃)₂Cl₂] with 1,4-diethynyl-2,5-dihexadecyloxybenzene using the “extended one pot” polymerization route, was tested for its sensing properties and showed fast and reproducible response to relative humidity variations and methanol vapor in surface acoustic wave (SAW) sensors [60]. A SAW sensor was fabricated from polymer **29** as a sensitive membrane and the polymer was deposited as thin film on the surface of SAW delay lines on three different piezoelectric substrates. High sensitivity and reproducibility were recorded for such devices. The acoustic characterization of the polymer film was also studied with the aid of theoretical results obtained by the perturbation theory.



Puddephatt et al. reported the synthesis of some yellow oligomers **30** with Pt–Pt bonds in the main chain from the reaction of [Pt₂Cl₂(μ-dppm)₂] with some dialkynes HC≡CRC≡CH under NaOMe/MeOH basic conditions [61]. Since the compounds are insoluble in organic solvents, no molecular weight data are available. The XPS spectra of **30** afford Pt 4f 7/2 binding energies ranging from 72.2 to 72.4 eV, which are very close to that for the model complex [Pt₂(C≡CPh)₂(μ-dppm)₂] (72.8 eV). The syntheses, crystal structures and luminescent properties of novel face-to-face diplatinum(II) alkynyl compounds **31** and **32** bearing different aromatic moieties were reported by Yam and co-workers [62,63]. The synthetic utility of **31** and **32** for the construction of a variety of rigid supramolecular and oligonuclear assemblies was demonstrated. Experimental evidence indicates the presence of weak Pt···Pt interactions in these compounds.



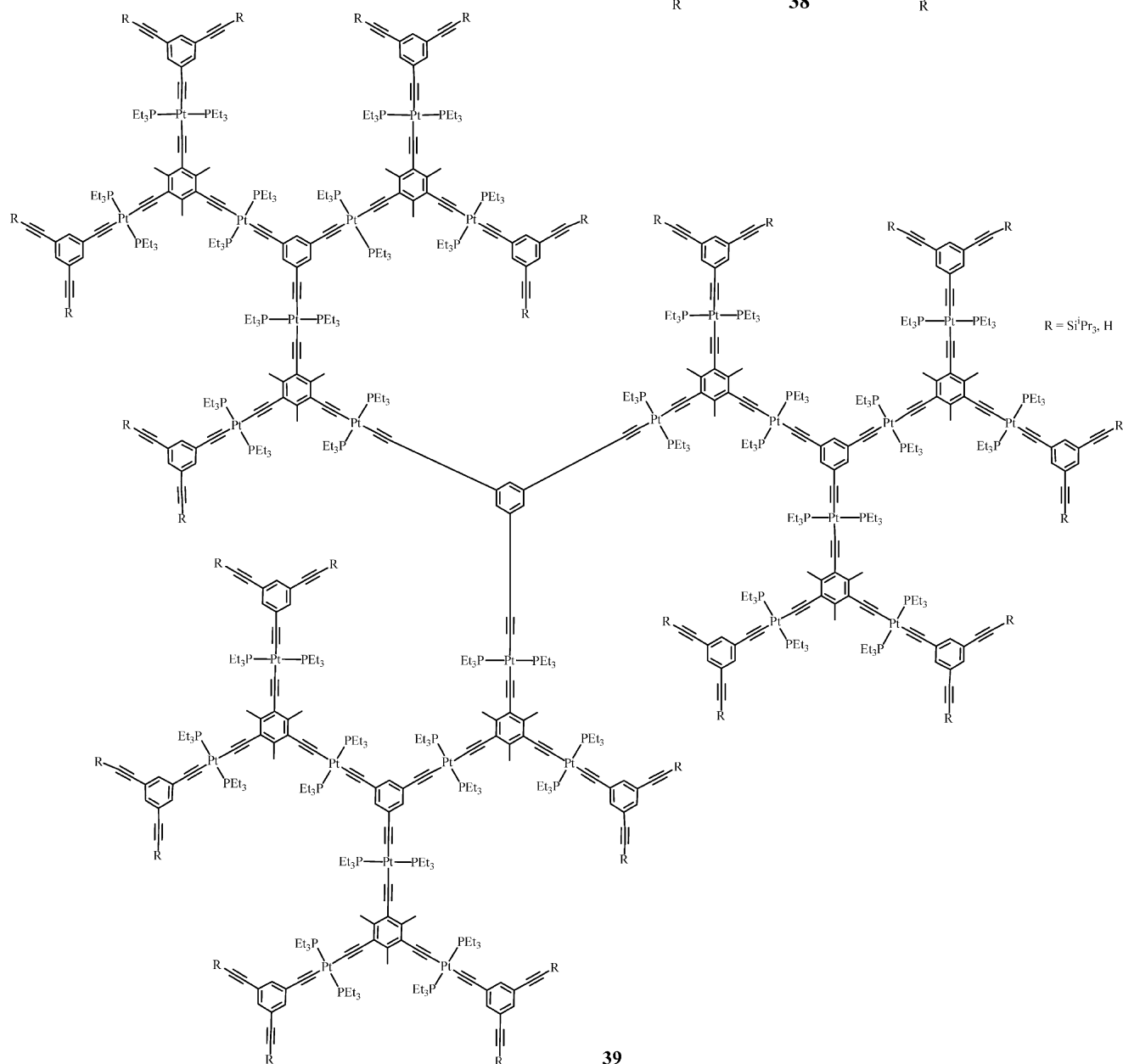
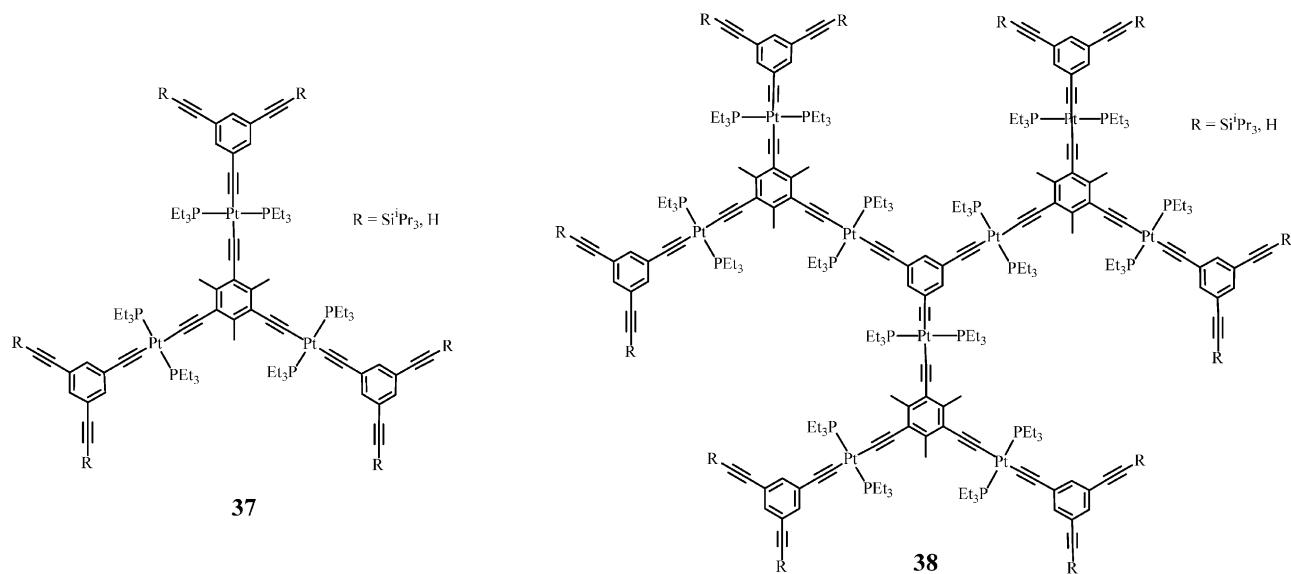
The synthesis of several high-molecular-weight platinum polyynyl polymers carrying chiral (*R*)-1,1'-bi-2-naphthol bridges **33** and **34** was described [64]. These represent the first examples of organometallic acetylene polymer with an optically active backbone. They display much larger specific negative optical rotations than both the free alkyne precursors and their corresponding model compounds **35** and **36**. These results support the fact that the main chain of the polymers adopts a one-handed helical conformation and induces the helical chirality of the polymers.

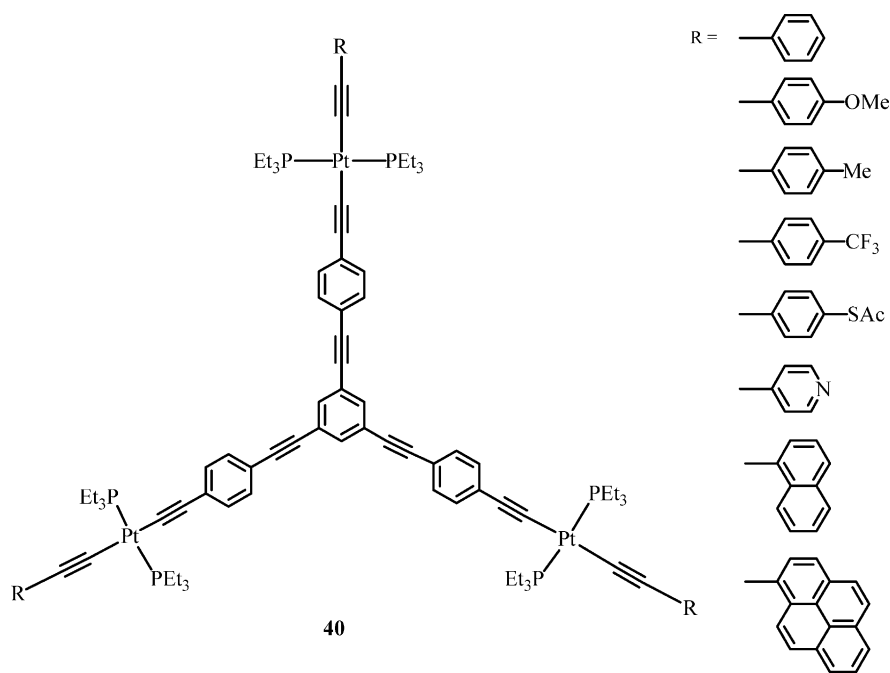


Large Pt-acetylide dendrimers of precise compositions up to the sixth generation were synthesized by a divergent approach and the dendrons **37**–**39** represent the structures of the first three generations [65]. The diameter of the largest nanosized den-

dimer exceeds 10 nm. There were also reports by the group of Yam on the synthesis and luminescence properties of multi-nuclear organo-platinum and -palladium oligomers and dendrimers. A series of carbon-rich platinum(II) complexes of branched alkynyls **40** were prepared and characterized by photoluminescence spectroscopy [66]. The energy transfer properties of these molecules were also carefully examined and assigned to be derived from predominantly intraligand triplet states, either of the central (C≡CC₆H₄C≡C)₃C₆H₃ core or the peripheral

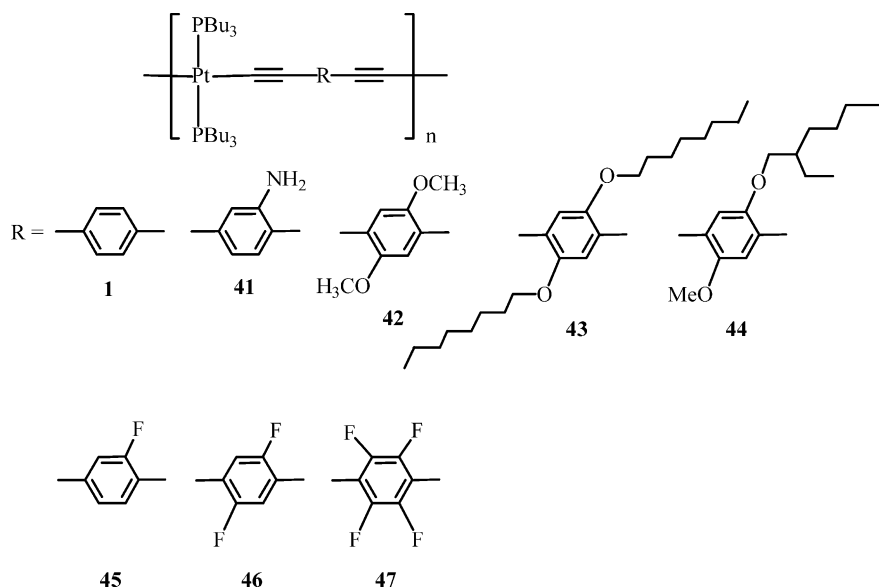
polyaromatic alkynyl units. Fine-tuning of the direction of energy transfer becomes viable through rational synthetic design. Analogous work has been partly extended to the palladium counterpart as well [67].



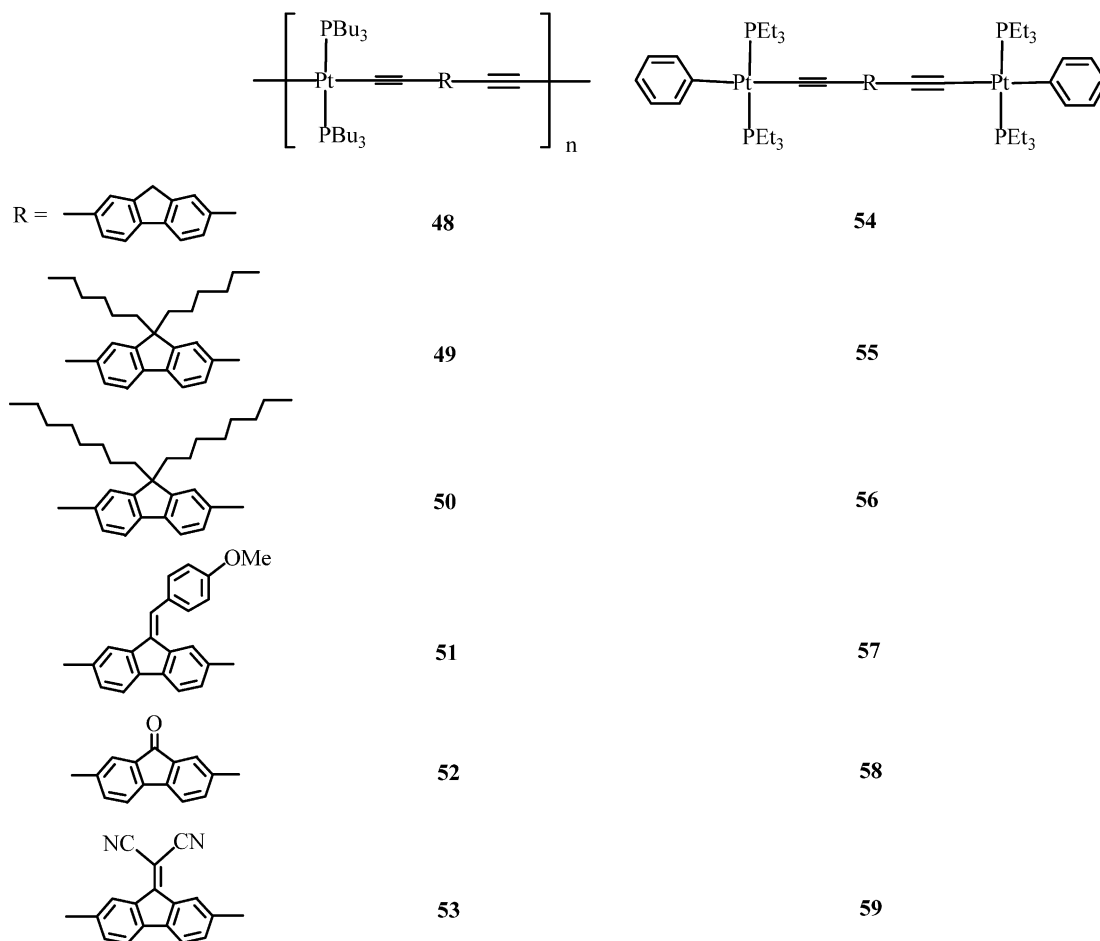


A new family of platinum(II) polyyne polymers functionalized with substituted 1,4-diethynylbenzene derivatives **41–47** were synthesized and optically characterized by absorption and photoluminescence studies [68]. Thermogravimetry showed that polyynes **41** and **42** with the amino- and methoxy-substituents have the lowest thermal stability while the fluorinated ones **45–47** exhibit increasing thermal stability with increasing extent of fluorination. The high thermal decomposition temperature observed for **44** is believed to be caused by the presence of the octyloxy chains that can favor stronger interchain van der Waals interactions. Substitution by methoxy or fluorine groups causes a small red-shift of ca. 6–20 nm in the absorption spectra, signifying only slightly more conjugated backbone. In regard to the emission properties, it is interesting to see that the relative intensity of triplet emission increases strongly with the fluorine content in such system.

One special current topic is concerned with the use of fluorene spacers in which functionalization at the 9-position of fluorene is feasible. Since the first report in 1998 [69], much attention was paid to the fluorene-based materials of this kind in polymetallaynes and alike [70]. The ease of modification and knowledge of the structure–property relationships of polyfluorene homopolymers and copolymers continue to make the fluorene-containing compounds very attractive candidates in the development of new functional materials for optoelectronics and chemosensing applications. It was demonstrated that substituted oligo- and poly(2,7-fluorene) derivatives hold great promises as active components for organic and polymeric LEDs due to their high thermal and chemical stability and high emission quantum yields [71–76]. The fluorene structural motif offers a rigidly planar biphenyl



group in the backbone. The versatility of preparing new polyplatinaynes of fluorene derivatives has been demonstrated by insertion of different peripheral groups on the fluorene ring and variation of the 9-substituents can affect the optical and photophysical properties of these materials. In this connection, a series of diethynyl fluorene-based precursors can be used as the synthons to produce thermally stable polymeric complexes (**48–53**) of platinum(II) as well as their binuclear model complexes **54–59** according to the classical dehydrohalogenative coupling procedures [69,77–80]. These platinum polyynes are generally organic-soluble and exhibit high DP values. The latter compounds were investigated as model complexes for the electronic and structural properties of the parent polymers. ^{31}P NMR spectroscopy has provided an exceptional tool for the determination of the configuration at the metal centers in each case. The three-dimensional structures of **54**, **57** and **59** were confirmed by single-crystal X-ray diffraction studies (Figs. 4–6).



By changing the substituents at C-9 position of fluorene ring, the optical bandgap (or onset of absorption), and the absorption and emission properties of these metal-containing polymers can be chemically modified, leading to diverse optoelectronic properties. These materials can display a variety of colors and optical energy gaps (E_g) in the solid states (Table 1). The dependence of the S_1 and T_1 electronic states on the electronic structure of the fluorene spacer groups was examined in detail. In the majority of

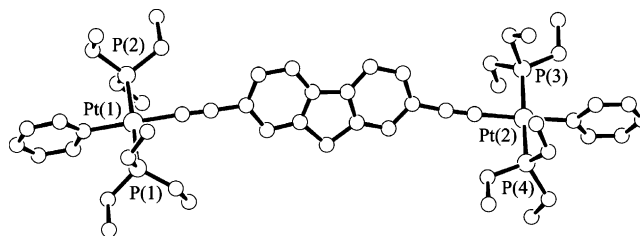
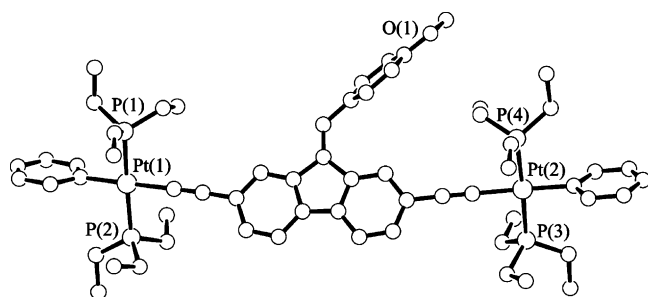
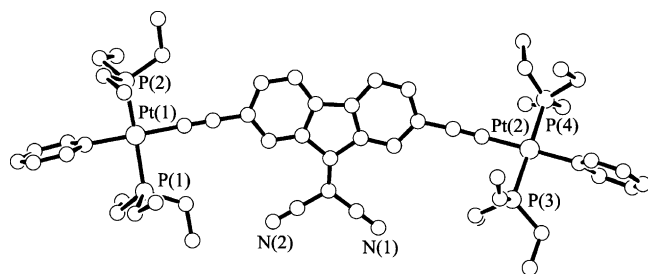


Fig. 4. X-ray crystal structure of **54**.

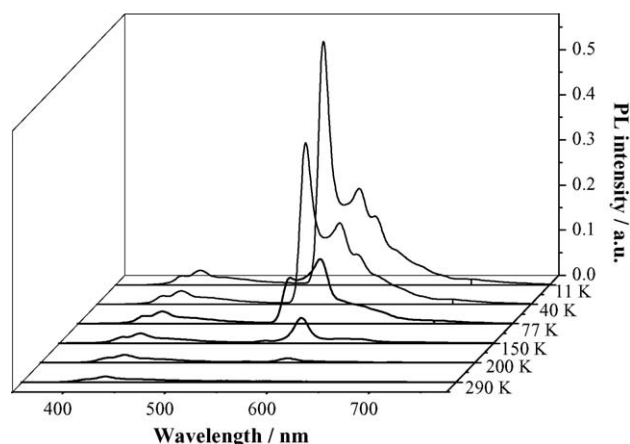
cases, the versatility of preparing new metal complexes of fluorene derivatives has been demonstrated by insertion of different peripheral groups on the fluorene ring and variation of the 9-substituents can affect the optical and photophysical properties of these materials.

The lowest energy absorption peaks of **48–53** in the near UV region have their origins mostly in the $\pi-\pi^*$ transitions of the bridging fluorenyleneethynylene ligands for these materials and the red-shift upon coordination of the platinum-phosphine units is consistent with there being an increase in conjugation length over the molecule through the metal center. Gratifyingly, the lowest energy absorption peak in **53** with two strong electron-withdrawing cyano side groups exhibits an unprecedented large

Fig. 5. X-ray crystal structure of **57**.Fig. 6. X-ray crystal structure of **59**.

red-shift as compared to other fluorene derivatives, showing the importance of donor–acceptor interaction in this class of polymetallaynes [80]. The E_g value of **53** is estimated to be 1.58 eV which, to our knowledge, is the lowest among any of the polyplatinaynes known to date and represents a significant step forward in the development of low bandgap materials. So, electron-withdrawing substituents at the periphery exert a more significant electronic effect on narrowing the bandgaps of these polymers than electron-donating groups. Hence, the energy of the S_1 state varies significantly with the nature of the fluorene ring and is highest for **48–50**.

The emission behavior of **48–53** are comprehensively analyzed and mirrors their absorption features in that the emission maxima are a function of the spacer group. The photoluminescence (PL) spectra of **48–50** feature two emission bands at 11 K attributable to the fluorescence and the phosphorescence bands [77,78]. The lower-lying triplet emission was found to be strongly temperature dependent in contrast to the singlet emission (Fig. 7). The lowest triplet excited state remains strongly localized, as indicated from the small energy difference between triplet emissions in the binuclear model complexes and in the polymers **48–50**. However, triplet emission was not observed over the measured temperature range for **51–53**. Our results sug-

Fig. 7. Temperature dependence of the PL spectra of **49**.

gest that reduced conjugation in **48–50** effectively facilitates the ISC rate to render phosphorescence readily measurable using optical spectroscopic techniques.

Raithby et al. further compared the photophysical properties of several platinum(II) polyynes **48**, **50** and **52** with their organic co-polyynes [78]. Since the nonradiative decay rate for the triplet emission (k_{nr})_P is equal or larger than the corresponding radiative decay rate (k_r)_P, the PL quantum efficiencies of the platinum polyynes are reduced from those for the organic polymers. Optical measurements reveal that the anchoring of octyl side chains on the fluorenyl spacer reduces interchain interaction in the polyynes while a fluorenonyl spacer affords a donor–acceptor motif along the rod-like backbone.

The photoconductive properties of **49**, **52** and **53** were studied by the single-layer photocells in the sandwich-type structure of ITO/Pt polyyne/Al (Fig. 8) [77,80]. These polymers show moderate photoconductivity. A photocurrent quantum yield of 0.01% was estimated in most cases, which does not vary much with variation of the central fluorene ring.

The optical-limiting behavior of selected platinum(II) fluorene-based polyynes was investigated by the Z-scan technique using the setup shown in Fig. 9. We have demonstrated that the platinum polyyne polymers **49**, **51** and **53** are excellent optical limiters to nanosecond laser pulse at 532 nm, whose results are comparable to or even better than those of the benchmark fullerene C₆₀ and phthalocyanine dyes (Fig. 10) [79]. Examination of their photophysics suggest that these polyplatinaynes follow two different optical-limiting mechanisms. One exploits

Table 1
Colors and optical bandgaps of platinum(II) diethynylfluorene-based polyynes

Platinum(II) polyyne	Color	E_g (eV)	References
48	Off-white	2.90	[69,78,117]
49	Off-white	2.92	[77]
50	Off-white	2.92	[78]
51	Red-orange	2.17	[79]
52	Red	2.10	[69]
53	Deep blue	1.58	[80]

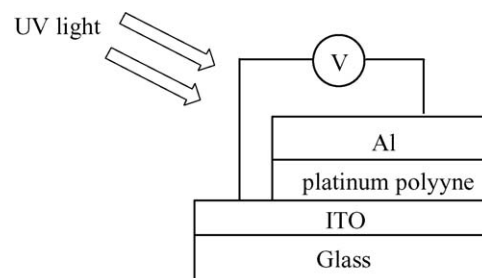


Fig. 8. Schematic diagram of a platinum(II) polyyne-based photocell.

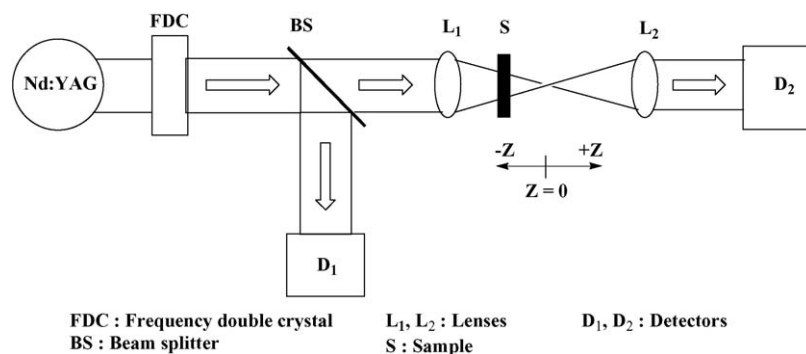
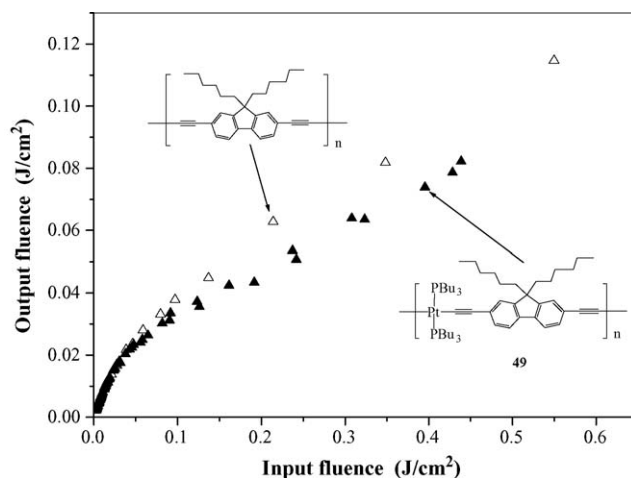
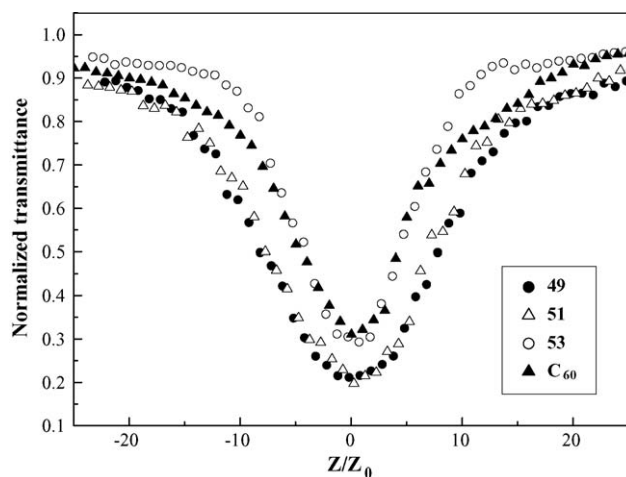
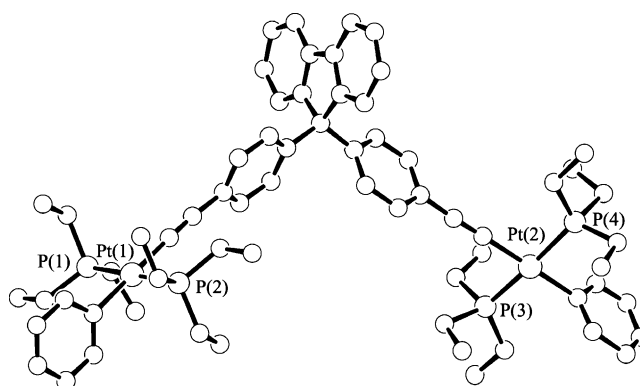


Fig. 9. Experimental setup for the measurement of optical-limiting properties.

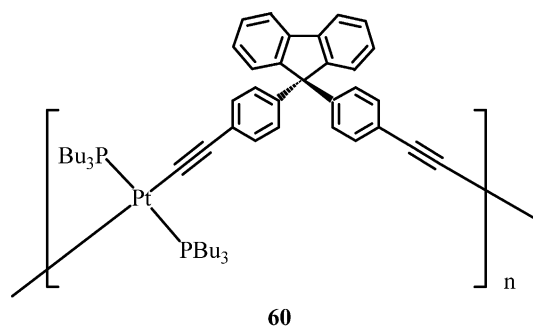
the heavy metal effect to increase the triplet state yield through strong spin–orbit coupling while the second is to make suitable D- π -A components in the conjugation path of the metal polyynes to facilitate the formation of intramolecular charge transfer (ICT) states. The optical-limiting thresholds for these polymetallaynes range from 0.06 to 0.13 J/cm² at the linear transmittance of 82%. In order to investigate the effect of heavy metal on the optical-limiting action of poly(aryleneethynylene)s, the purely organic poly(2,7-diethynyl-9,9-dihexylfluorene) polymer was prepared and their optical-limiting behavior was also studied. Fig. 11 compares the input-output curves for the organic and organometallic polyynes and the former material has its optical-limiting response weaker than that of **49**. The light energy transmitted started to deviate from Beer's law with increasing input light fluence, and the polymer solution became increasingly less transparent as the fluence rose. So, the transmittances of the samples were found to decrease as the laser fluence increases, characteristic of optical limiting. Thus, the optical-limiting capabilities of the organic polyyne can be markedly improved through insertion of heavy metal ion to the polyyne main chain.

Recently, the synthesis and luminescent properties of a metal polyyne containing the conjugation-interrupting diphenylfluorene unit **60** appeared in the literature [81]. The crystal structure of its model diyne complex **61** was also determined which also

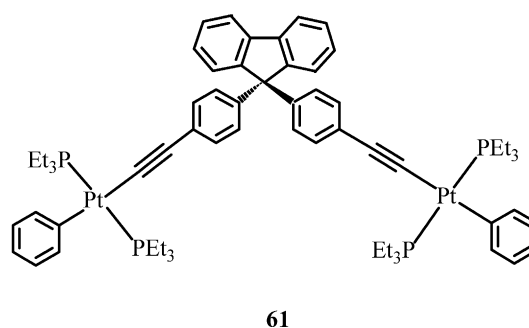
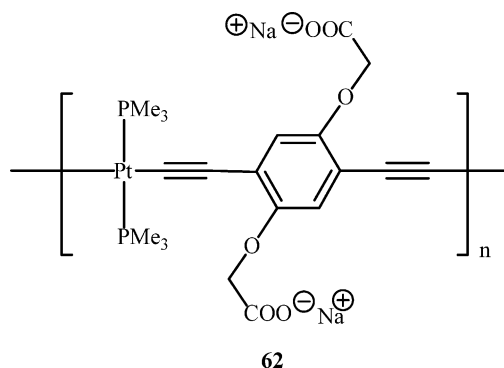
aided in elucidating the solid-state structure of polyyne (Fig. 12). Polymer **60** exhibits good thermal stability with decomposition commencing at 347 °C and decompose without melting. It was shown that introduction of the diphenylfluorene group has the added advantage of increasing the thermal stability of this class of metallopolymers. With reference to the energy gap law, it was shown that it is advantageous to work on polymers with high-energy triplets to avoid competition with nonradiative decay. The sp³-carbon site in diphenylfluorene is an effective conjugation-interrupter to limit the conjugation length in metal polyynes,

Fig. 11. Comparison of the optical-limiting response of **49** and its purely organic polyyne ($T=82\%$).Fig. 10. Z-scan results for **49**, **51** and **53** as compared to C₆₀ at the same linear transmittance (T) of 82%.Fig. 12. X-ray crystal structure of **61**.

leading to materials with high optical gaps and high-energy triplet states. At 11 K, there is virtually no fluorescence band but only the phosphorescence band associated with the organic chromophore in both **60** and **61**. The hindered conjugation with the use of diphenylfluorene unit in **60** shifts the phosphorescence to the blue by 0.45 eV as compared to **15**. It was found that the order of S_1 – T_1 crossover efficiency is $\mathbf{60} > \mathbf{15} \approx \mathbf{1}$. The $(k_r)_P$ and $(k_{nr})_P$ values for **60** were computed to be $(9.5 \pm 0.5) \times 10^4$ and $(2.5 \pm 0.5) \times 10^4 \text{ s}^{-1}$ for $(k_{nr})_P$ and $(k_r)_P$ at 20 K, respectively. The heavy-atom effect of Pt can increase the $(k_r)_P$ value for the triplet emission by 4 orders of magnitude and incorporation of the diphenylfluorene group in metal polyynes with larger T_1 – S_0 gaps can speed up the radiative decay as compared to **1** ($(k_r)_P = (6 \pm 4) \times 10^3 \text{ s}^{-1}$ at 20 K). Therefore, high-energy triplet states can lead to the more efficient phosphorescence in metal-containing aryleneethynyls.

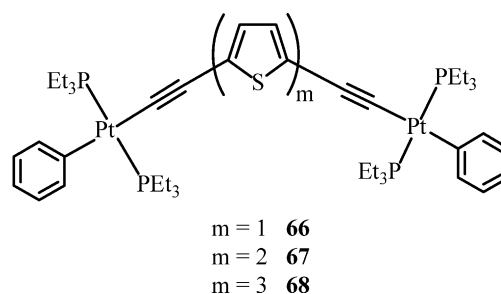
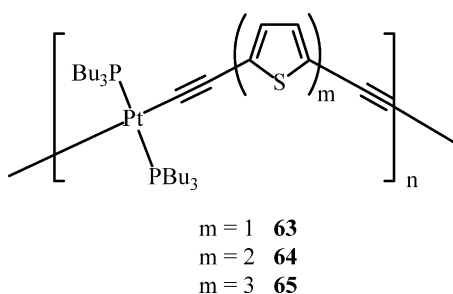


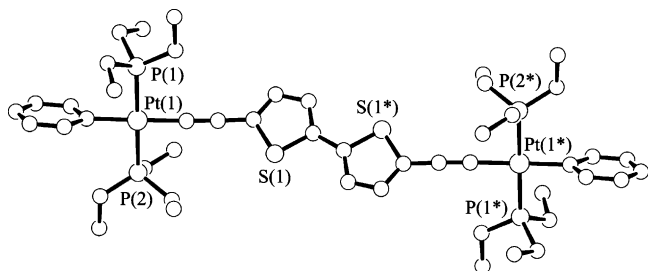
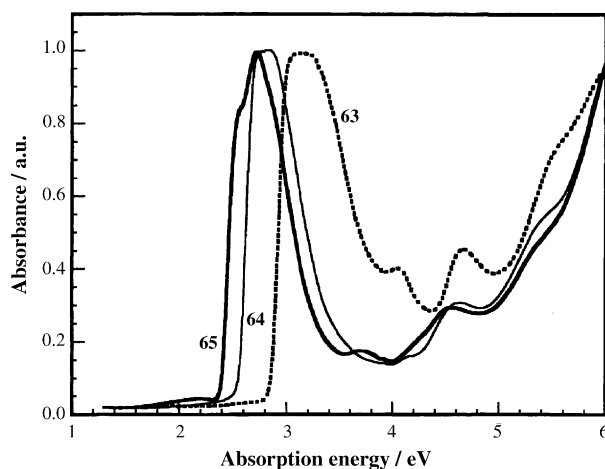
Recently, a water-soluble platinum(II) acetylide polyelectrolyte **62** was prepared and isolated which was shown to be phosphorescent at ambient temperature with the $^3(\pi\pi^*)$ character localized on the conjugated backbone [82]. The polymer chains tend to aggregate at low pH value in which the weakly acidic carboxyl groups can be protonated and the stacked aggregate structure leads to a marked blue-shift of its absorption band as well as the phosphorescence quenching effect. The triplet emission was shown to be quenched by various viologens and the quenching being dominated by a dynamic diffusional mechanism. The Stern–Volmer quenching properties of **62** was studied relative to those of the corresponding fluorescent organic polyelectrolytes and the results suggest that the amplified quenching effect does not play a key role in **62**.



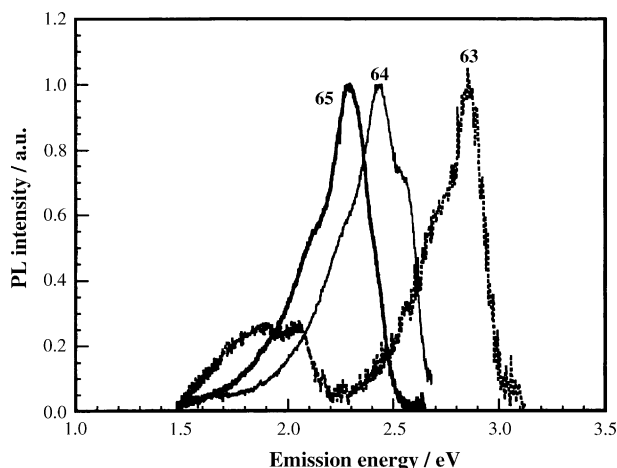
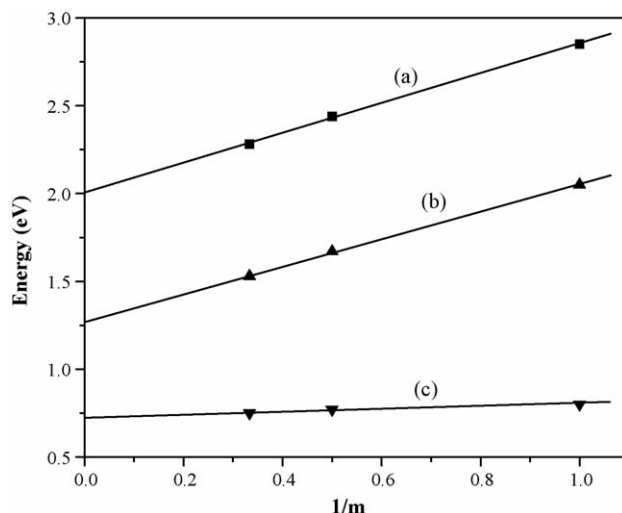
3.1.2. Compounds with heterocyclic spacers

A series of conjugated platinum(II) acetylide polymers containing oligothiophene groups **63**–**65** and their corresponding model complexes **66**–**68** were synthesized by the classical CuI-catalyzed dehydrohalogenation reactions [83,84]. The photophysical, redox and structural properties of these metallaynes were extensively studied in terms of the number of oligothiophenyl rings within the bridging ligand. The solid-state structures of **66** and **67** were established by X-ray crystallography in which they provided conclusive proof of the *trans* configuration at the metal center. Fig. 13 portrays the crystallographically determined structure for **67**.



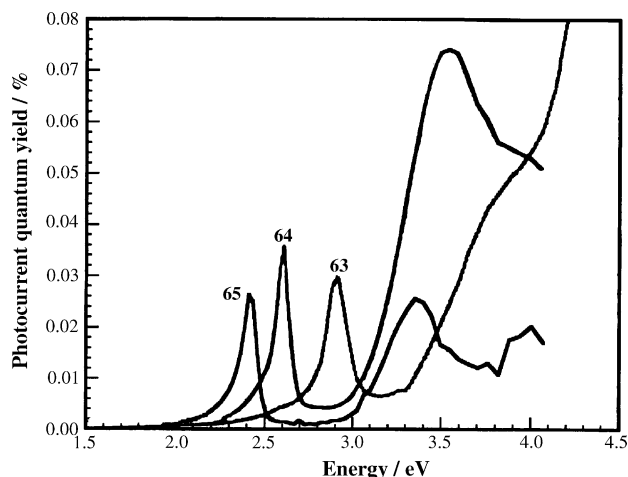
Fig. 13. X-ray crystal structure of **67**.Fig. 14. Solid-state absorption spectra of **63–65** at 290 K.

The absorption and PL spectra of **63–65** are shown in Figs. 14 and 15, respectively. The E_g values of **63–65** decrease with increasing m value, in line with an increased delocalization of π -electrons along the polymer chain. However, as the m value increases, the overall effect on E_g decreases, and this reduction tends to get saturated up to $m=3$. The transition energies of the platinum polyynes are lowered compared to the corresponding diynes, consistent with π -conjugation of the ligands through the metal group. The emission features are shifted to lower energy with an increase in chain length of the thiophene segment. The measured S_1 – T_1 separations lie essentially con-

Fig. 15. Thin-film PL spectra of **63–65** at 290 K.Fig. 16. Energy vs. chain length dependence of **63–65** for (a) S_1 – S_0 , (b) T_1 – S_0 and (c) S_1 – T_1 .

stant at 0.75–0.80 eV (Fig. 16). The intensity of triplet emission decreases rapidly with increasing m value. This finding is consistent with two lines of evidence. The higher m value in the ligand reduces the influence of the heavy metal center, which is mainly responsible for the ISC process. Next, ISC is reduced with increasing value of m in oligothiophene systems themselves, as the energy of the singlet excited state drops below the corresponding resonance state for ISC in those systems [85]. We also observe that the energy of the phosphorescence band shifts when adding more thiophene rings in the ligand (from 2.05 to 1.53 eV for **63–65**), suggesting that the triplet excited state should be extended over three or more thiophene rings in the present system. This shift of phosphorescence energy observed in **63–65** agrees with the calculations on the evolution of the triplet energy in organic oligothiophene systems [85,86]. Li and co-workers have recently extended the studies to the platinum polyynes and diynes functionalized with thienothiophene and dithienothiophene entities [87]. The design rationale lies in the fact that the self-rigidification of these cores due to the fused ring system and the delocalized π -systems extending over the fused rings confer them novel optoelectronic properties. They observed that the bandgap is more related to the conjugation length through the oligothiophene system instead of whether the thiophene is fused or not.

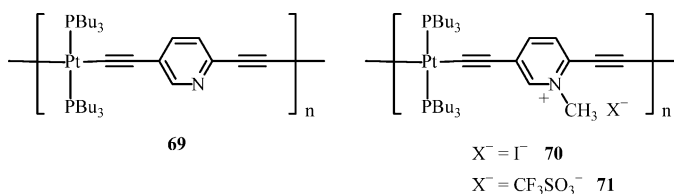
More interestingly, platinum polyynes **63–65** can behave as good photoconductors [83,88]. The photocurrent spectra of the Au/**63**/Al, ITO/**64**/Al and ITO/**65**/Al photocells display two peaks, one at the onset of absorption and one at higher photon energies (Fig. 17). The second photocurrent peaks were suggested to be caused by absorption into the higher-lying absorption bands. Polymers **63–65** show a short-circuit quantum efficiency of about 0.04% at the first photocurrent peak, a typical value for single-layer devices. No strong dependence of the quantum efficiency with variation of the thiophene content in these metallopolymer was observed. However, the quantum efficiency of the second peak is different among these three polymers and is very air-sensitive. The effect of air exposure on the

Fig. 17. Photocurrent spectra for **63–65**.

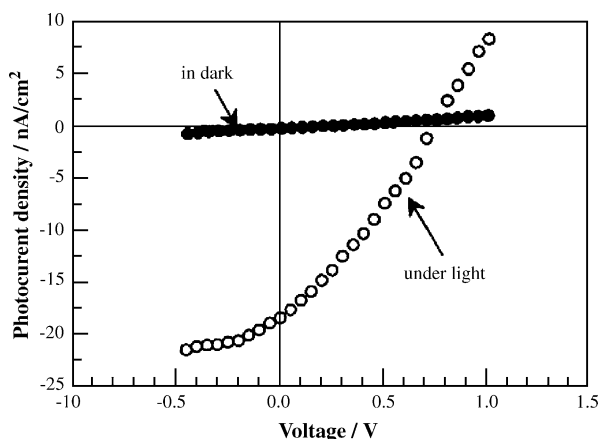
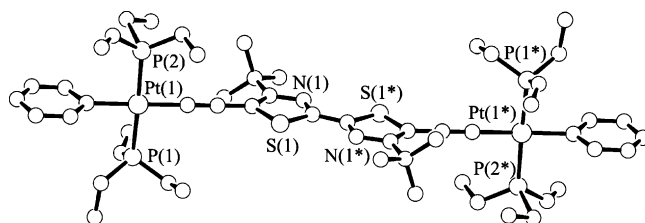
photocurrent in Au/**63**/Al was studied and it was shown that air can enhance exciton dissociation easily [88]. The overall photocurrent increases upon exposure to air and is reduced after annealing under vacuum. The enhancement of the photovoltaic response to air was found to be reversible after annealing under vacuum. The I – V characteristics at the first peak in the spectral response give open-circuit voltages of 0.47–0.75 and fill-factors of 0.30–0.35 for **63–65** and Fig. 18 shows the typical case for **64** under illumination at 480 nm.

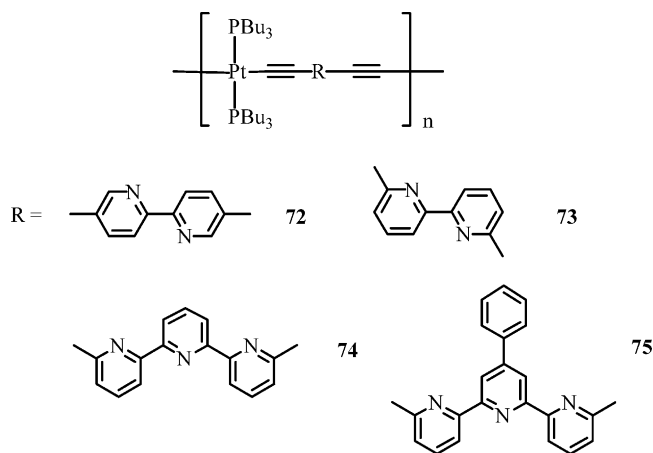
Kakkar and co-workers have developed the preparative routes to the Pt-acetylide polymer **69** with 2,5-diethynylpyridine moiety and its stable quaternized counterparts **70** and **71** [89]. Quaternization of pyridyl nitrogen was achieved by nucleophilic substitution of **69** with CH_3X which results in a strong bathochromic shift in the UV–vis absorption spectrum and an enhanced emission quantum yield. There is an improved π -electron delocalization along the backbone upon quaternization. Both polymers are basically insulators in the undoped state. Upon doping with iodine vapor, they become semiconducting and the conductivity of **70** ($3.4 \times 10^{-3} \text{ S cm}^{-1}$) was found to be higher than that for **69** ($2.5 \times 10^{-3} \text{ S cm}^{-1}$). The authors also

compared the results for **69–71** with their organic congeners [89,90].



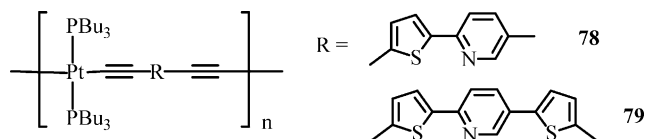
Researchers in Cambridge also discussed the dependence of intersystem crossing and the spatial extent of singlet and triplet excited states in **1**, **63** and **69** as a function of electron delocalization in the spacer group. From the optical absorption and photoluminescence data of these materials, conjugation is increased but ISC rate is reduced by the electron-rich thiophene ring, whereas the opposite trend prevails for the electron-deficient pyridine moiety as compared to the phenylene unit [91]. With the aid of steady-state photoinduced absorption spectra, an energy scheme for the lower-lying excitations has been constructed and discussed. In all the three cases, the T_1 triplet state remains strongly localized and the T_n triplet state remains strongly delocalized even more than the delocalized S_1 singlet state. It was shown that the extent of delocalization is larger for the electron-rich thiophene group. Later on, the same research groups further accomplished the synthesis, structural characterization and photophysical studies of a series of oligopyridine-linked platinum(II) polyynes **72–75** and diynes and the results were compared to those for **69** [92]. The more the number of pyridine units in the backbone, the less thermally stable the polymer is. For **72**, the inclusion of a second pyridine unit shifts the bandgap to the red relative to **69** by 0.1 eV, while for **73–75**, the bandgap is blue-shifted compared to **69** by 0.3 eV. This is in line with the fact that in **72**, the alkynyl groups are at the 5,5'-positions and the polymer is fully conjugated, whereas in **73–75**, the alkynyl units at the 6,6'- or 6,6''-positions can hinder conjugation between the pyridine rings. It appears that the phosphorescence spectra for **72–75** show some excimer formation at room temperature but only intrachain emission occurs at 10 K. In particular, the authors observed no fluorescence band but only the phosphorescence band at 10 K for the kinked bi- and terpyridine-containing compounds **73** and **74**. The reduced conjugation in **73** and **74** shifts the triplet emission peak to the blue by 0.3 eV compared to the linear bipyridine-containing analogue **72**. Polyynes **73** and **74** also constitute a class of materials with high-energy triplet states with lowered nonradiative decay rate constants from the T_1 state.

Fig. 18. I – V curve for the ITO/**64**/Al photocell.Fig. 19. X-ray crystal structure of **77**.

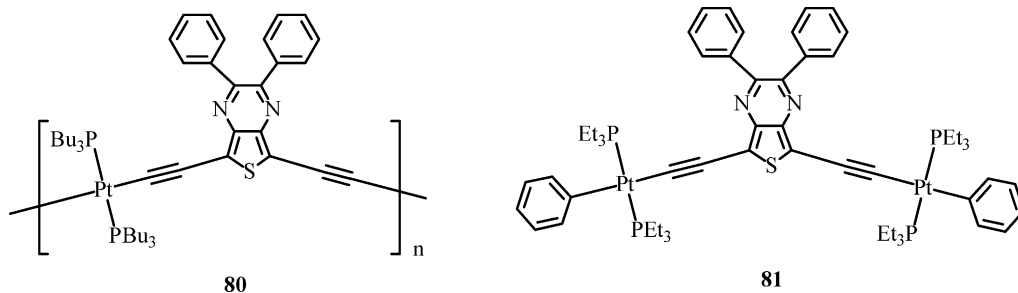


By virtue of the electron-donating and electron-accepting features of the thiazole ring as compared to the thienyl analogue, a luminescent bithiazole-bridged polyyne **76** was also made and the X-ray crystal structure of the model diplatinum complex **77** was established (Fig. 19) [93]. A thiazole unit can be considered as a hybrid of the thiophene and pyridine groups that can be a valuable spacer for controlling the bandgaps of these metallated materials. For **76** and **77**, the absorption peaks show a significant spectral red-shift as compared to their bithienyl

masses in the range 85,000–140,000. The optical energy gaps for **78** and **79** are 2.67 and 2.55 eV, respectively, which compare to the gaps of 2.55 and 2.40 eV found for **64** and **65** that contain bi and ter-thiophene linker units, and the blue-shifts of 0.12 and 0.15 eV are consistent with a reduction in the donor–acceptor interaction between the metal and the ligand. Again, both polymers exhibit interesting fluorescence and phosphorescence features in the emission profile at 10 K.

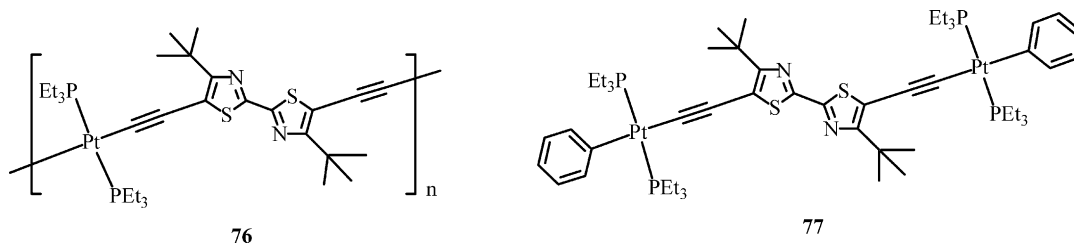


One of the most spectacular advance in the area of platinum polyynes is the report of the soluble blue materials containing the thieno[3,4-b]pyrazine spacer **80** and **81** [95]. The polymer was designed by using the concept of alternating donor and acceptor units, as has been successfully exploited for the production of low-bandgap organic polymers. Polymer **80** shows a bandgap of 1.77 eV, presumably caused by the push-pull interaction between the electron-donating metal acetylene group and the electron-withdrawing thieno[3,4-b]pyrazine unit. While this polymer is not phosphorescent, it exhibits an unusually high photocurrent efficiency of up to 1% at 400 nm for single-layer sandwich-type photovoltaic cells in air.



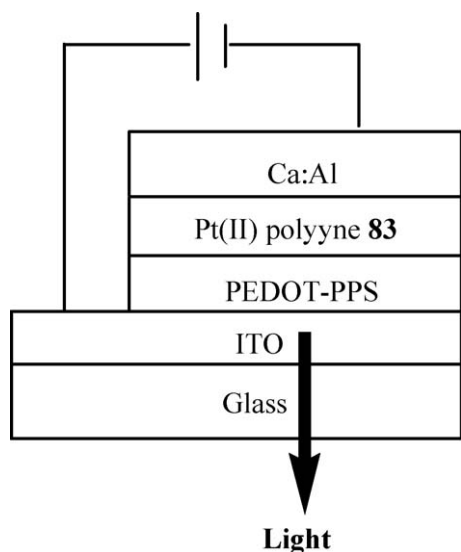
counterparts **64** and **67**, respectively, due to the electron-withdrawing effect of the imine nitrogen atoms. No phosphorescence band was detected for **76** even at low temperature. The potential of using polymer **76** as photoconductors was also investigated in a single-layer device [93]. Recent study also showed that polymer **76** can find appealing NLO applications. It displays a large optical-limiting response to a nanosecond laser pulse with satisfactory threshold value at 0.12 J/cm² and its behavior is superior to that for poly(4,4'-diethynyl-5,5'-bithiazole) organic polymer [79].

A series of platinum polyynes **82–84** and their metal diynes functionalized with quinoline, quinoxaline and benzothiadiazole units have been reported which provide an excellent system to study the evolution of the singlet and triplet excited states with electronegativity of the spacer groups [96]. The absorption spectra of **82–84** reveal substantial donor–acceptor interaction between the platinum center and the conjugated ligands. Both the singlet and triplet emissions as well as the absorption bands decrease in energy with increasing electronegativity of the spacers along the series from **82** to **84**. In other words,

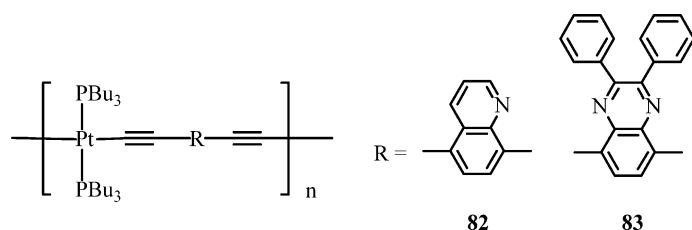


The synthesis and optical spectroscopy of two interesting Pt(II) polyynes that possess mixed heterocyclic groups consisting of both thienyl and pyridyl rings **78** and **79** were described [94]. They are high-molecular-weight polymers with molar

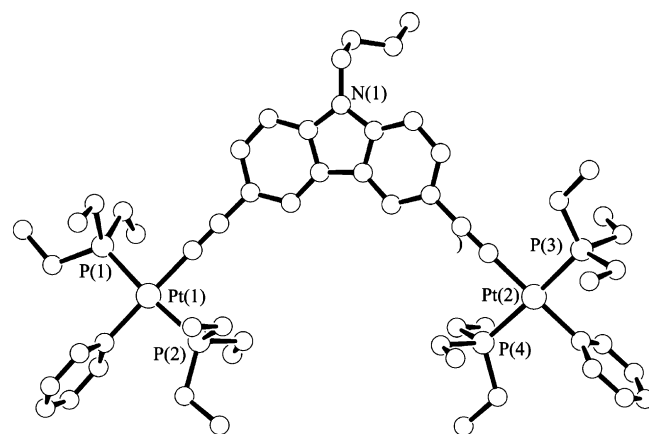
the more electron-withdrawing the spacer is, the lower is the E_g value between the S_0 ground state and S_1 first excited state. The same authors have also investigated extensively the triplet

Fig. 20. Polymer LED structure based on platinum(II) polyyn **83**.

excited state properties of a range of polyynes including polymers **1**, **44** and **82–84** by means of optical steady-state and time resolved spectroscopy as a function of optical gaps and they found that the S_1 – T_1 energy splitting is independent of the spacer such that the T_1 state is always 0.7 ± 0.1 eV below the S_1 state [97]. With decreasing optical gap, the lifetimes and intensities of phosphorescence are dramatically reduced. Based on these experimental results, the authors formulated for the first time a useful energy gap law for the triplet states in this class of Pt-containing conjugated polyyn polymers with tunable triplet energy level spanning from 1.3 to 2.5 eV and the $(k_{nr})_P$ value increases exponentially with decreasing T_1 – S_0 gap [98]. This suggests that future work should be more concentrated on soluble polymers with high-energy triplet states in order to attain the most efficient phosphorescence for practical applications.



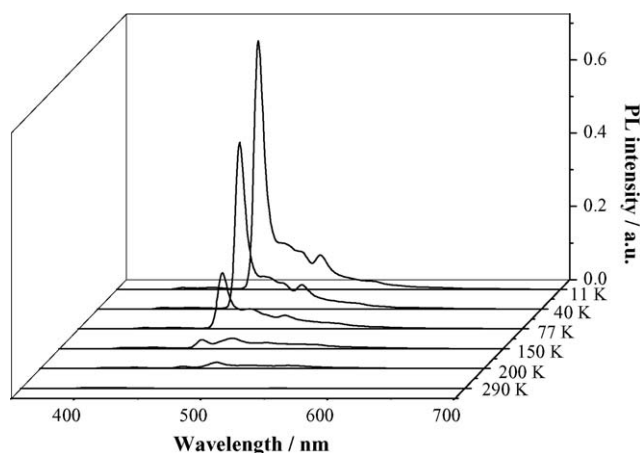
To realize the role of this class of Pt(II) polyyn materials in practical LED devices, Friend and co-workers have reported their seminal work on the spin-dependent exciton formation in the platinum polyyn **83**. Direct photoluminescence and electroluminescence emission from the triplet state can be observed and measured for a LED in a structure of ITO/PEDOT-PPS/**83**/Ca:Al (Fig. 20, PEDOT = poly(3,4-ethylenedioxythiophene); PSS = poly(styrenesulfonate)) [99]. The average singlet generation fraction of $57 \pm 4\%$ for **83** was determined, suggesting that a spin-dependent process, favoring singlet formation, is operative in the polymer film. The value is more than double the value expected from simple spin statistics and is above the lower limit for the singlet generation

Fig. 21. X-ray crystal structure of **86**.

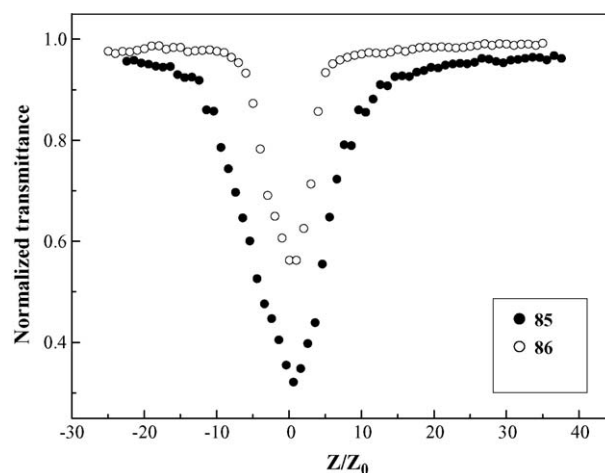
fraction of 0.35–0.5 measured for poly(*p*-phenylenevinylene) derivatives. The results demonstrate that singlets are favored over triplets and the probable processes responsible for this phenomenon have been discussed. The value for the corresponding diplatinum model complex is about $22 \pm 1\%$, which is close to 0.25 expected from simple spin statistics and in agreement with the value of 0.22 ± 0.03 measured for tris(8-hydroxyquinolinato)aluminium. This suggests that recombination of holes and electrons is spin-independent.

Among the heterocyclic derivatives, carbazole ring has emerged as an excellent building block in the synthesis of a variety of optoelectronic materials. However, to our knowledge, carbazole-containing metal alkynyl compounds are very rare in the literature. The first examples are the platinum(II) polyyn **85** and diyne **86** prepared through the CuI-catalyzed dehydrohalogenation between the platinum(II) chloride precursors and 9-butyl-3,6-diethynylcarbazole [77]. The regiochemical structure of polymer **85** has been ascertained by single-crystal

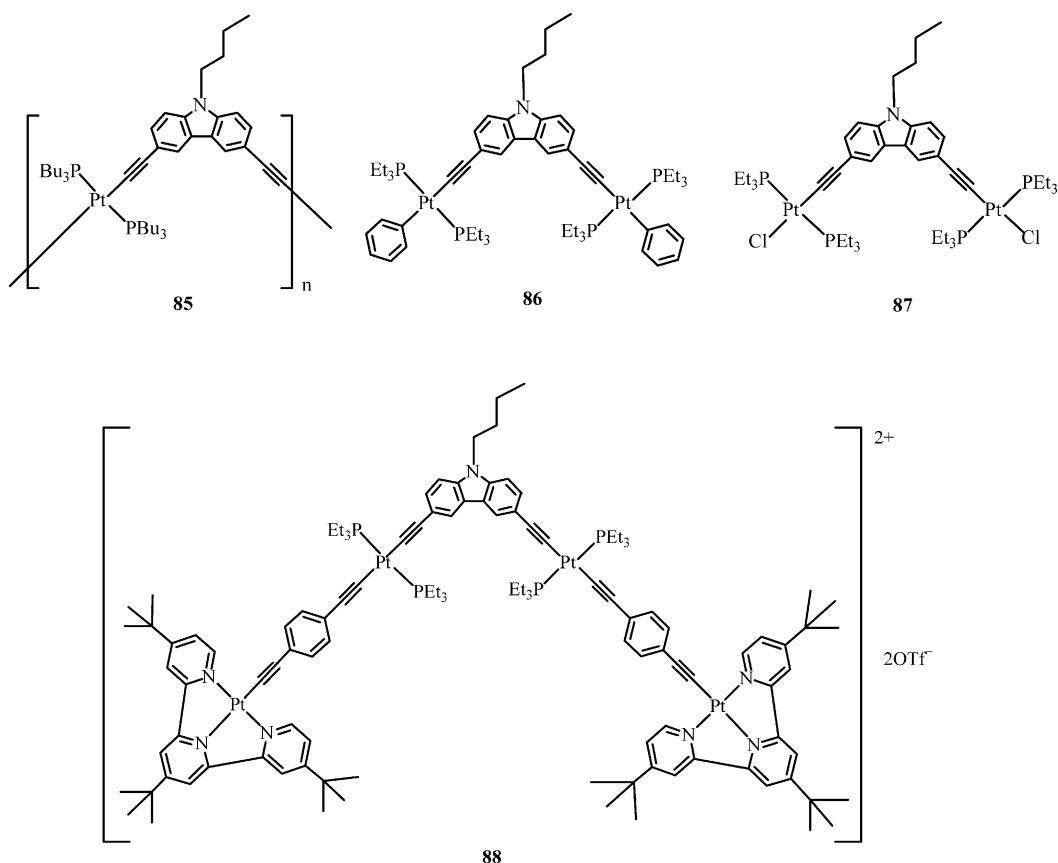
X-ray analysis on the model complex **86** (Fig. 21). Similar to other related systems, there is a red-shift in the absorption bands from the free alkyne to the platinum complexes and the transition energies of **85** are lowered with respect to **86**. It was shown that the S_1 state extends over more than a repeat unit while the T_1 state remains localized to less than one repeat unit. The bandgap measured is ca. 3.10 eV. The photoluminescence spectra of **85** and **86** show characteristic singlet emissions at ~ 425 nm and triplet emissions at ~ 460 nm, both of which are π – π^* ligand-centered (Fig. 22). The study indicates that the use of carbazole unit leads to high-energy triplet states and represents an effective approach in the enhancement of the ISC rate. Polymer **85** was also shown to be a photoconducting material in a single-layer

Fig. 22. Temperature dependence of the PL spectra of **85**.

architecture with a photocurrent quantum efficiency of $\sim 0.01\%$ in the forward bias mode. Moreover, polymer **85** is an effective optical limiter for nanosecond pulses of visible light and it is the triplet excited-state absorption that contributes to the optical-limiting action [79]. As depicted in Fig. 23, compound **85** is a better optical limiter than **86**, suggesting that the optical-limiting effect of the polyyne is contributed not only by the single repeating segment but the entity that is delocalized over more than one repeat unit. The organometallic polyyne **85** also gives better optical-limiting performance than the organic counterpart, viz.

Fig. 23. Comparison of the optical-limiting behavior of **85** and **86** ($T = 80\%$).

poly(9-buty1-3,6-diethynylcarbazole). More recently, Yam et al. have reported the synthesis, electrochemistry, luminescence studies and structural characterization of **87**. This complex, with two terminal chloro ligands, can serve as versatile building block for the assembly of a charged oligomeric complex **88** [100]. The emission of **88** probably arises from an excited state of mixed ${}^3\text{MLCT}/{}^3\text{LLCT}$ character, involving a charge transfer from the platinum diethynylcarbazole unit to the terpyridyl part of the molecule and this was supported by cyclic voltammetric measurements.

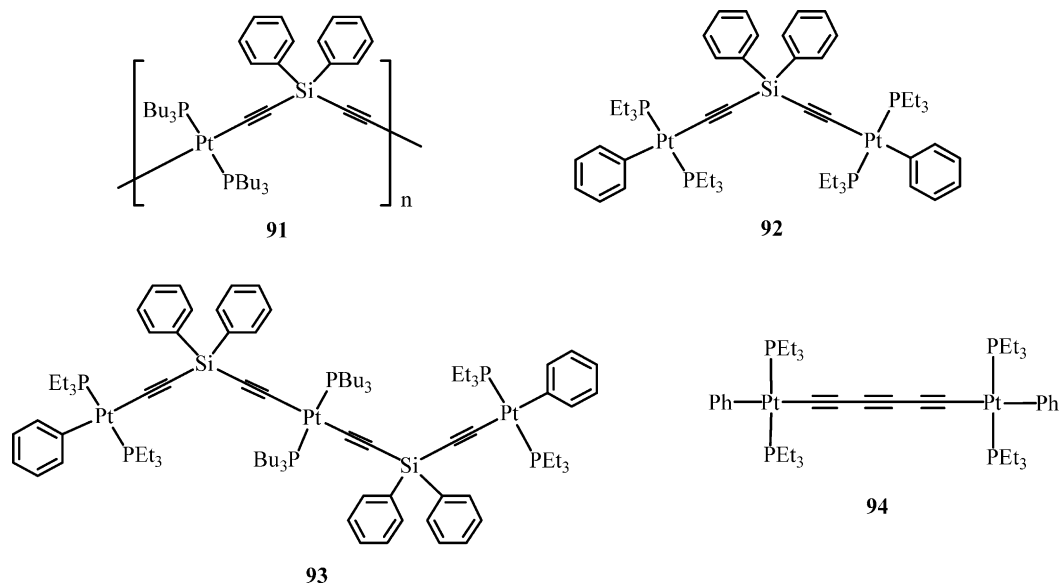


3.1.3. Compounds with main group elements

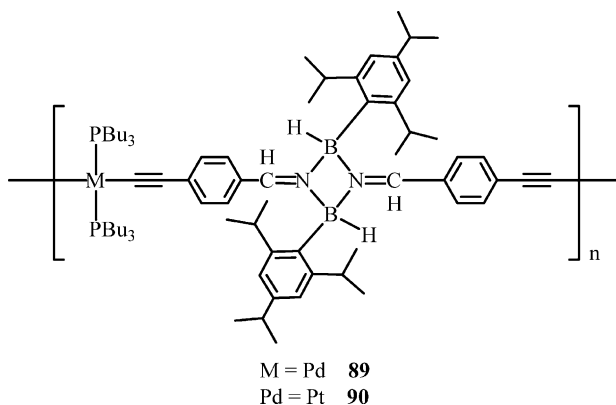
The majority of work in the metal polyyne area has mainly concentrated on the chemistry of such polymers with (hetero)aromatic or carbon-rich spacer unit, however, much less is known for systems involving main group elements and little research in this important area has been carried out. The progress in the polymetallayne area was recently spurred by the search for new materials with high-energy triplet levels. In view of this, efforts were devoted to the exploitation of some main group elements as the spacer units in the buildup of polymetallaynes. The main group elements studied so far are mostly group 13, 14 and 16 elements.

Two poly(cyclodiborazane) polymers containing group 10 transition metal-acetylide groups **89** and **90** were prepared by Chujo et al. and represent a new kind of organometallic acetylide polymers functionalized with group 13 boron elements in the main chain [101]. The structures of **89** and **90** were confirmed by IR and NMR (^1H , ^{31}P and ^{11}B) spectra. The optical

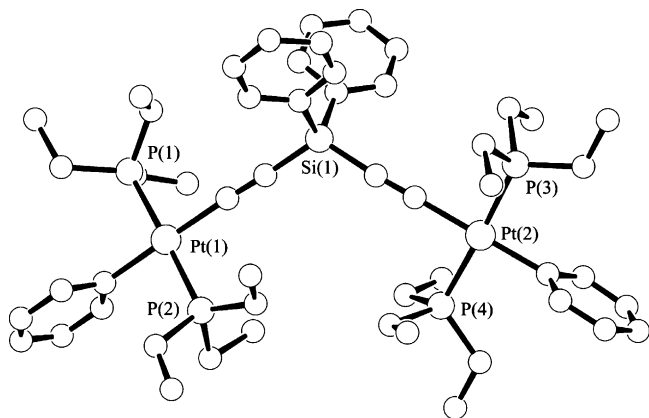
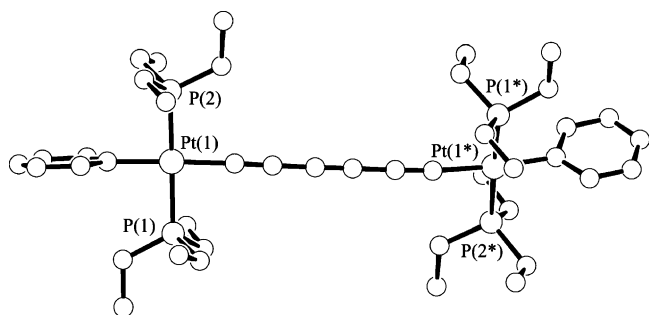
It was envisaged that the lower ionization energy (IE) of the silicon atom compared with carbon can enhance the through-bond interaction of ethynyl units along the backbone [102]. π -Conjugated organosilicon systems incorporating aromatic units were widely studied regarding their applications to optoelectronic devices [103–105]. Along these lines, the first synthesis, characterization and luminescence behavior of a series of novel platinum-containing oligo- and poly(silylacetylene)s **91–93** were described [106]. Complexes **92** and **93** provide the best finite models for the polymeric analogue **91**. These new compounds were prepared using the dehydrohalogenating route and isolated as off-white to light yellow solids by preparative TLC plates or column chromatography on silica. In the same study, an unexpected carbon-rich diplatinum triacetylenic complex **94** was also obtained as the unexpected product from the oxidative coupling of $\text{trans}[\text{Ph}(\text{Et}_3\text{P})_2\text{PtC}\equiv\text{CSiPh}_2\text{C}\equiv\text{CH}]$ in $\text{Cu}(\text{OAc})_2/\text{O}_2/\text{pyridine}$ whose molecular structure together with that for **92** were determined by X-ray crystallography (Figs. 24 and 25).



properties were studied by UV–vis absorption and emission measurements. It was shown that these polymers display extended π -conjugation length via transition metal and boron atom with enhanced air- and moisture stability.

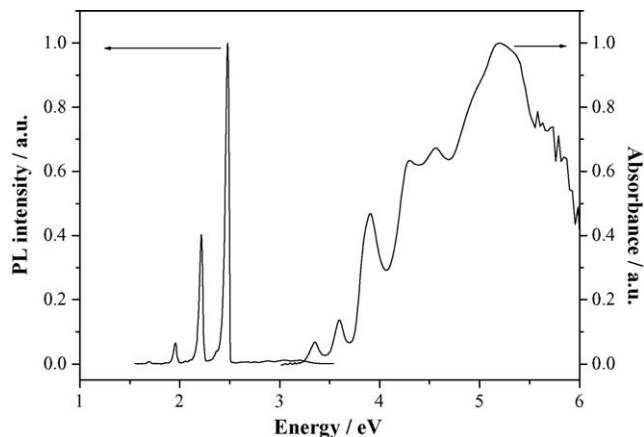
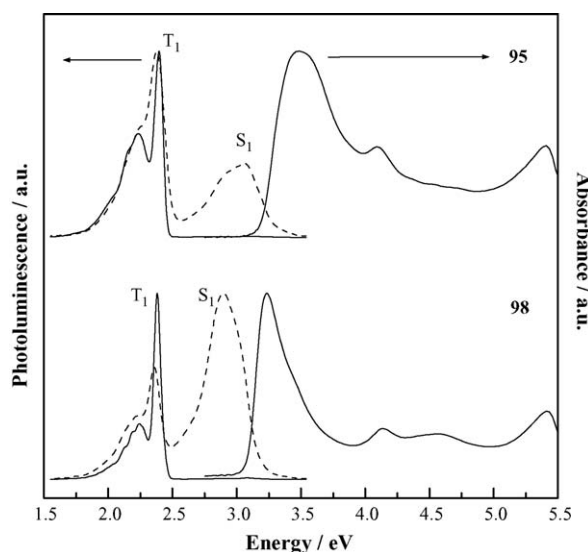


All these Si-bridged platinum complexes are air-stable and have good solubility in common organic solvents. The ^{29}Si NMR chemical shifts for each of them ($\delta = -57.50$ to -58.10) appear at more downfield positions in comparison to $\text{Ph}_2\text{Si}(\text{C}\equiv\text{CH})_2$ ($\delta = -48.42$) and do not differ significantly from those for related polymers comprising silylacetylene and π -conjugated organic groups [107]. Polymer **91** is thermally stable up to $\sim 380^\circ\text{C}$ with the onset decomposition temperature higher than those in **1**, **48**, **63** and **69**, revealing the role played by the SiPh_2 unit in increasing the thermal stability of Pt(II) polyyynes. The degree of electronic conjugation roughly follows the order $\text{C}\equiv\text{C} \geq 2,5\text{-thienyl} > p\text{-C}_6\text{H}_4 > 2,5\text{-pyridyl} > \text{SiPh}_2$ (Fig. 26), implying that acetylene and thiophene units are best suited for transmitting electron flow. But, the silyl moiety tends to interrupt electron movement and the energy of the S_1 state is highest for **91**. At 11 K, the principal emissive peak occurs at ca. 508 nm for **91**. The emission lifetimes of 11.0 μs at 290 K and 40.2 μs at 11 K for **91** (versus $\tau_{\text{P}} = 30 \mu\text{s}$ at 10 K for **1**) support the $^3(\pi\pi^*)$ character of the phosphorescent state. The hindered conjugation in

Fig. 24. X-ray crystal structure of **92**.Fig. 25. X-ray crystal structure of **94**.

91 shifts the phosphorescence to the blue by 0.06 and 0.38 eV, respectively as compared to **1** and **63**. The authors also recorded a blue-shift of the triplet emission band in **91** after the acetylene unit in **4**, which phosphoresces at 1.88, 2.09 and 2.37 eV [108,109], was replaced by the silyl group. Oligomers **92** and **93** showed analogous PL characteristics as **91** while the metallatriyne **94** is emissive both at 290 and 11 K with sharp vibronically structured emissions that can be assigned to the lowest-energy $^3(\pi\pi^*)$ excited states of the $(C\equiv C)_3^{2-}$ chain (see Fig. 27).

Synthetic extension to new silylacetylene derivatives with additional aromatic chromophore is equally interesting, and new Pt(II) polyynes **95** and oligoynes **96** and **97** were successfully isolated [110]. Polymer **98** was prepared as a structural analogue to **95** to evaluate the effect of $SiPh_2$ in such system. The ^{29}Si

Fig. 27. Absorption (290 K) and PL (11 K) spectra of **94**.Fig. 28. Solid-state absorption and PL (11 K) spectra of **95** and **98** (solid line). The PL spectrum in CH_2Cl_2 solution at room temperature is represented by the dashed line.

NMR chemical shifts of **95–97** ($\delta = -48.16$ to -49.32) remain relatively unshifted as compared to the free alkyne ($\delta = -48.49$). It is also experimentally evident that addition of $SiPh_2$ units in **95** can enhance the thermal stability of polyplatinaynes.

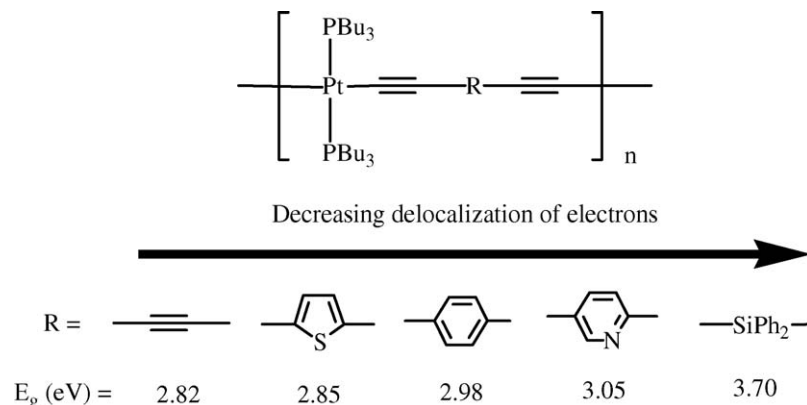
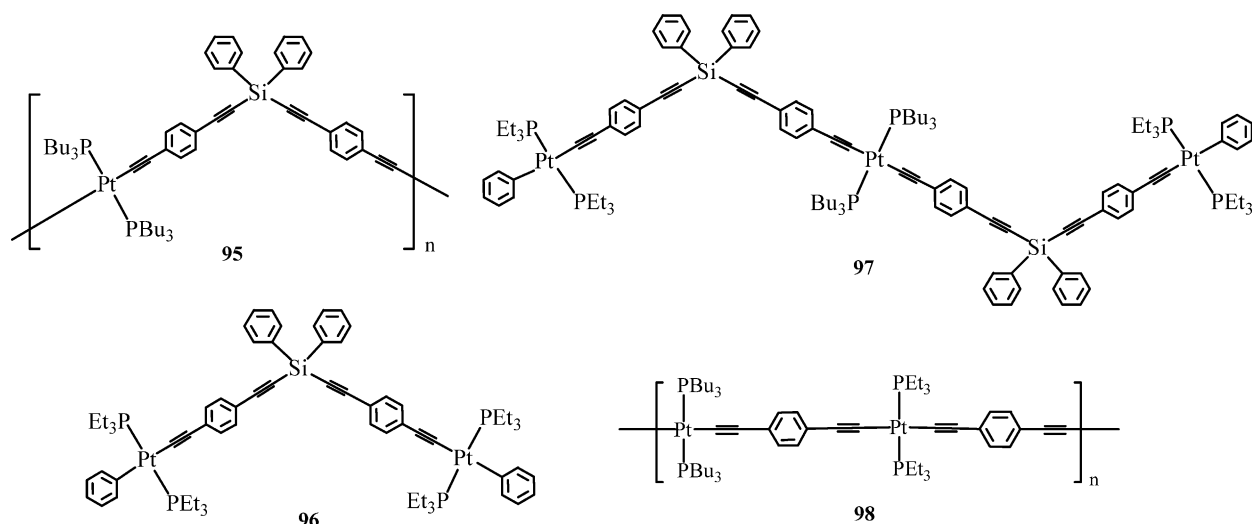


Fig. 26. Optical bandgaps for platinum polyynes with different spacer groups.



From the absorption data, it was shown that SiPh_2 is less effective than the *p*-phenylene and metal-phosphine units in electronic conjugation. Moreover, it was found that the E_g values gradually decrease in the order $96 > 97 > 95$ with increasing chain length. In general, characteristic fluorescence and phosphorescence emission bands were observed at 11 K for **95** and **98**. The ISC rate is much stronger in polymer **95** than in the corresponding oligomers **96** and **97**. We note a very high efficiency of triplet emission for **95**, and the order of S_1 – T_1 crossover efficiency is $95 > 98$. As observed in Fig. 28, the ratio of integrated intensities of phosphorescence to fluorescence is greater than unity for **95** but is less than unity for **98**. The use of conjugation-interrupting silyl segment in such metal polyynes can thus fine-tune the effective conjugation length and gives rise to efficient crossover between S_1 and T_1 states. The S_1 – T_1 energy gap for **95** was found to lie within the constant range of 0.7 ± 0.1 eV.

The photoconductivity of polymer **95** was also examined, and a photocell in a single-layer structure of ITO/**95**/Al was fabricated. The quantum efficiency detected was moderate at 0.01%. Alternate substitution of $\text{Pt}(\text{PBu}_3)_2$ units in **1** by SiPh_2 does not affect significantly the photoconducting behavior of this class of platinum polyynes [110].

Being prompted by the propitious results for the silyl-tethered systems, work has then proliferated on the metalopolynes with heavier group 14 germanium element of even lower I.E. (first IE: Si 791; Ge 762 kJ mol^{-1}). The first examples of thermostable Ge-bridged Pt(II) metalopolymers **99–104**, derived from oligo(fluorenyleneethynylene)germylene)s, were reported recently which can display very fast phosphorescence decay rate [111]. This is the first organogermanium material of this kind to exhibit these properties and this work represents a significant step forward in the development of triplet-emitting materials for organic LEDs. Inclusion of the group 14 atoms into the organic bridge as conjugation interruptors can limit the effective conjugation length and trigger the triplet light emission by taking advantage of the heavy-atom effect of Ge atoms. The onset decomposition temperatures are almost invariant of the chain length and the R substituent

group. While polymer **49** commences decomposition at 349°C [77], addition of GeR_2 unit into the aryl-acetylene segment in **99–104** notably increases the thermal stability of these Pt(II) polyynes.

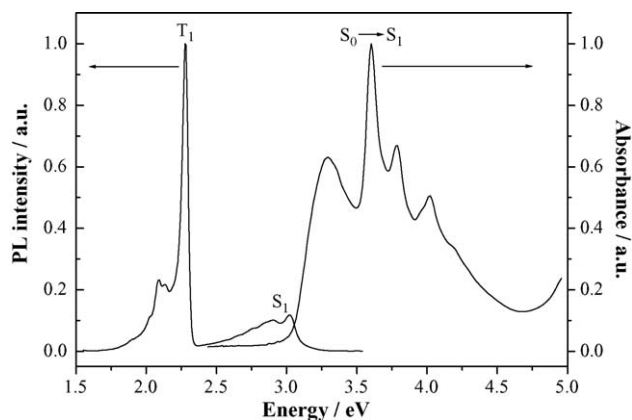


Fig. 29. Optical absorption and PL spectra (11 K) of **101**.

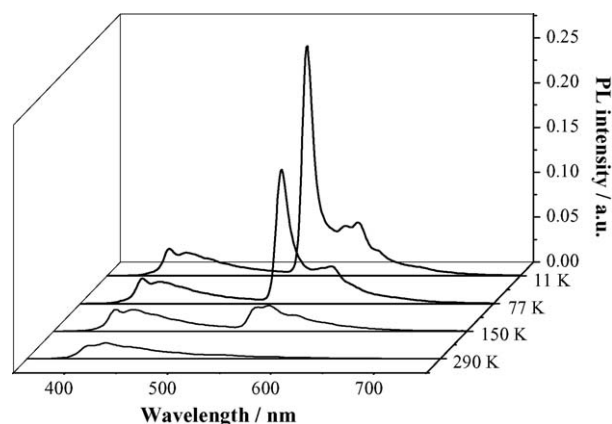
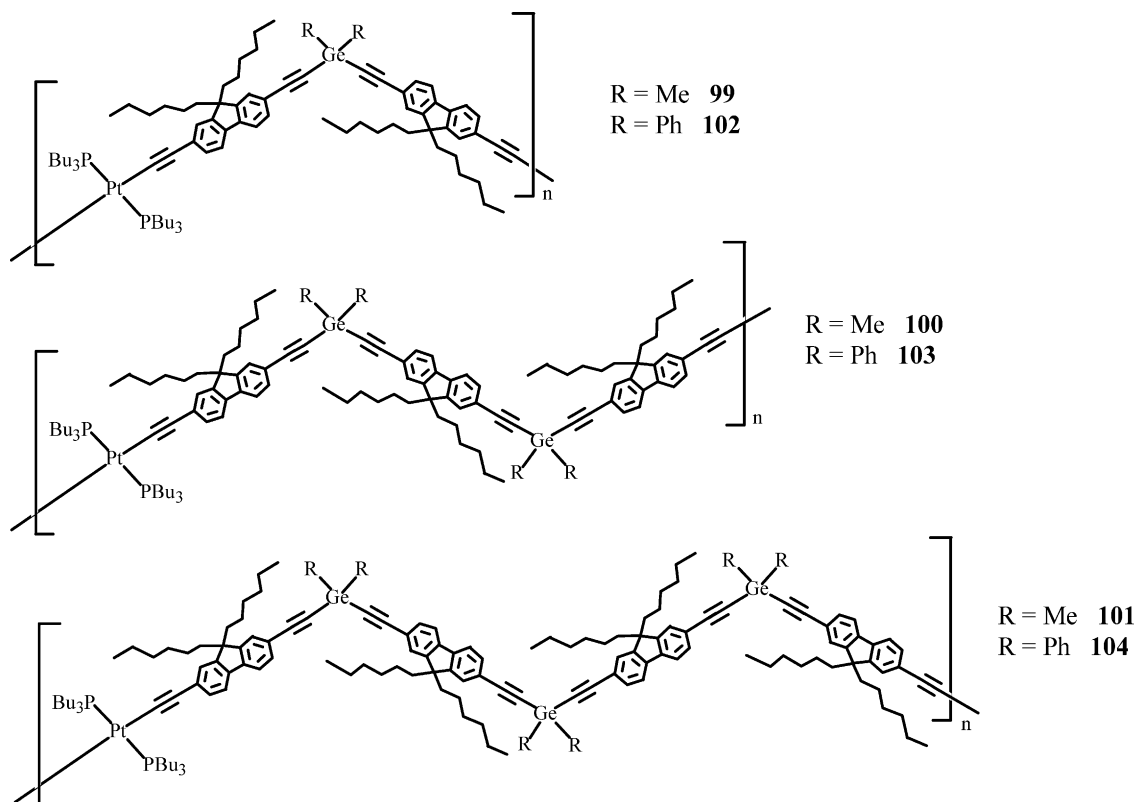


Fig. 30. Temperature dependence of the PL spectra of **101**.



For **99–104**, both fluorescent and phosphorescent emissions arise from ligand-centered $^1(\pi\pi^*)$ transitions. Fig. 29 illustrates the absorption and emission spectra for **101** and the observed large Stokes shift between the absorption and low-energy emission bands confirms the $^3(\pi\pi^*)$ state of the PL peak at 544 nm. The phosphorescence was also identified by the strong temperature dependence of its intensity (Fig. 30). The triplet energy does not vary much with the oligomer chain length, i.e. the lowest T_1 state is confined to a single repeat unit. Variation of the R group does not seem to change this strong confinement. Insertion of conjugation hindered GeR_2 group in these polymers shifts the phosphorescence bands to the blue relative to **49**. Values of the S_0 – T_1 energy gap were found to be ca. 2.27–2.28 eV for both series and the S_1 level is ca. 0.7 eV above the T_1 state within experimental errors.

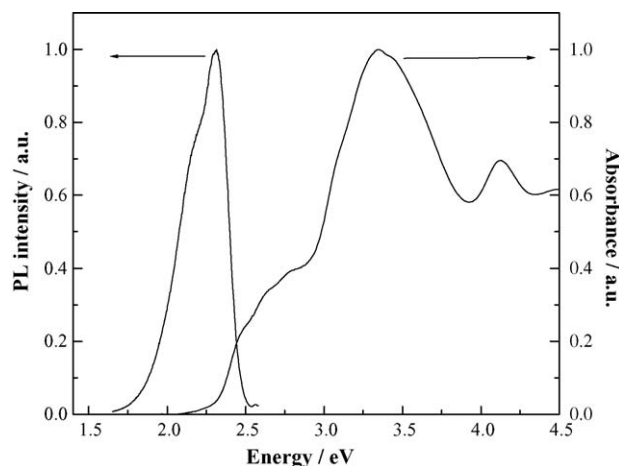
Table 2
Photophysical data of high-energy triplet-emitting polyplatinaynes at 20 K

Polymer	τ_P (μs)	Φ_P	$(k_{nr})_P$ (s^{-1})	$(k_r)_P$ (s^{-1})
99	1.27	0.45	4.3×10^5	3.5×10^5
100	2.08	0.43	2.7×10^5	2.1×10^5
101	1.41	0.45	3.9×10^5	3.2×10^5
102	1.32	0.17	6.3×10^5	1.3×10^5
103	1.21	0.18	6.8×10^5	1.5×10^5
104	1.16	0.20	6.9×10^5	1.7×10^5
108	6.38	0.46	8.5×10^4	7.2×10^4
109	6.02	0.49	8.5×10^4	8.1×10^4
110	7.27	0.51	6.7×10^4	7.1×10^4
111	8.57	0.46	6.3×10^4	5.4×10^4

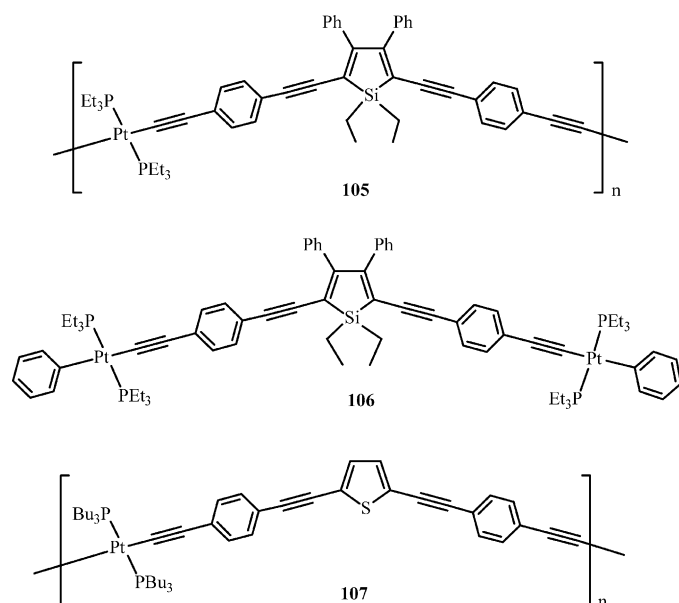
$$(k_{nr})_P = (1 - \Phi_P)/\tau_P \text{ and } (k_r)_P = \Phi_P/\tau_P.$$

Table 2 collects $(k_r)_P$ and $(k_{nr})_P$ values together with the phosphorescence lifetimes, τ_P , and quantum yields, Φ_P , at 20 K for **99–104** [111]. While the measured Φ_P values were found to be relatively insensitive to the oligomer chain length, they vary with the ER_2 group ($\text{E} = \text{Si}, \text{Ge}$). The GeMe_2 systems give more efficient phosphorescence than the GePh_2 congeners by over two times. However, the heavy-atom effect associated with the Ge atoms in **102–104** can almost double Φ_P as compared to the SiPh_2 congeners ($\Phi_P \sim 10$ – 13%). The $(k_r)_P$ values at 20 K are $(2.1$ – $3.5) \times 10^5 \text{ s}^{-1}$ for **99–101** and $(1.3$ – $1.7) \times 10^5 \text{ s}^{-1}$ for **102–104**. Relative to **49** ($(k_r)_P \sim 4.4 \times 10^4 \text{ s}^{-1}$), insertion of the germylene component can increase $(k_r)_P$ by about 1 order of magnitude. It is impressive to get comparable orders of magnitude for $(k_{nr})_P$ and $(k_r)_P$ in **99–101**. Hence, heavy-atom derivatization using Pt and Ge atoms in conjunction with conjugation interruption by the latter can greatly boost $(k_r)_P$ values by ca. 5 orders of magnitude.

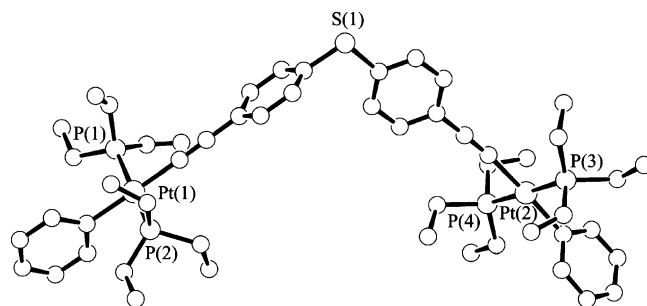
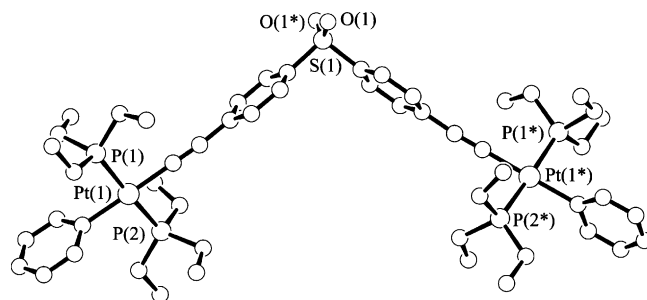
Very recently, we have also accomplished the synthesis of a soluble silole-containing polyplatina-yne **105** and its model compound **106** [112]. The UV–vis absorption spectra of both compounds in CH_2Cl_2 exhibit intense π – π^* transitions in the near UV region and relatively low-energy shoulder bands in the visible range that tail off between 570 and 590 nm. As compared to 2,5-dibromo-1,1-diethylsilole ($\lambda_{\text{max}} = 326 \text{ nm}$), the positions of the low-lying shoulder bands ($\lambda_{\text{max}} = 504$ (**105**) and 470 (**106**) nm) are remarkably red-shifted by ca. 178 and 144 nm for **105** and **106**, respectively, after the inclusion of heavy transition metal chromophores. This is likely due to the intramolecular donor–acceptor interaction between metal ethynyl units and silole rings. The E_g value is 2.10 eV for

Fig. 31. Absorption and PL spectra of **105** in CH₂Cl₂ at 290 K.

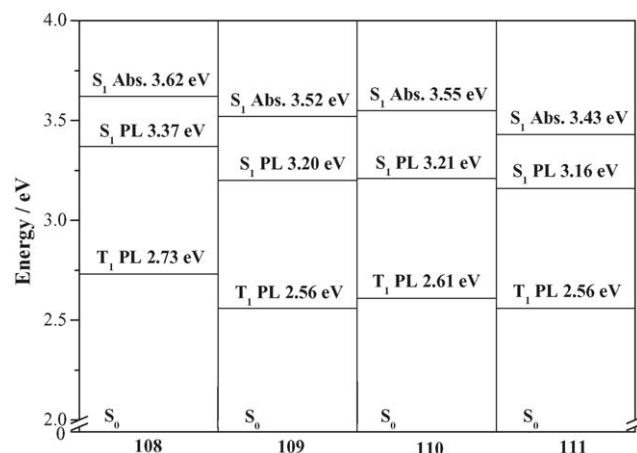
105 and it is significantly lowered by ca. 0.6–1.0 eV relative to the electron-rich thienyl-bridged (**107**, 2.70 eV) [113] and silyl-bridged (**95**, 3.10 eV) counterparts [110]. The incorporation of electron-accepting silole unit in the metallopolymer main chain creates a new narrow bandgap π -conjugated system with a unique donor–acceptor characteristics [114]. Compounds **105** and **106** are photoluminescent with the singlet emission bands at 537 and 525 nm, respectively (Fig. 31). No room temperature emission from the T₁ state was detected over the measured spectral range. The HOMO and LUMO levels of **105** were estimated to be –5.62 and –3.52 eV, respectively, signalling its good electron-transporting and hole-blocking ability for polymeric LEDs.



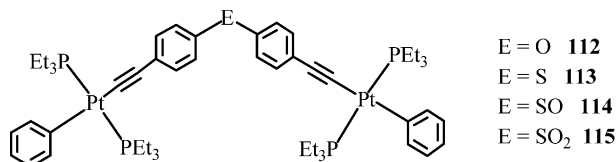
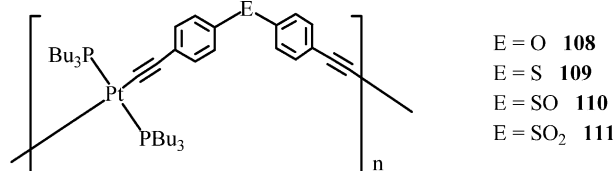
For the same reasoning as the group 14 elements, a novel approach based on conjugation interruption was developed by Wong and co-workers for the first time for a series of luminescent and thermally stable group 16 chalcogen-bridged platinum(II) polyyne polymers **108–111** [115]. However, attempts to make the corresponding mercury-based polyyne only resulted in insoluble substances. The authors reported in depth studies of the photophysical properties of these group 10 polymetallayne

Fig. 32. X-ray crystal structure of **113**.Fig. 33. X-ray crystal structure of **115**.

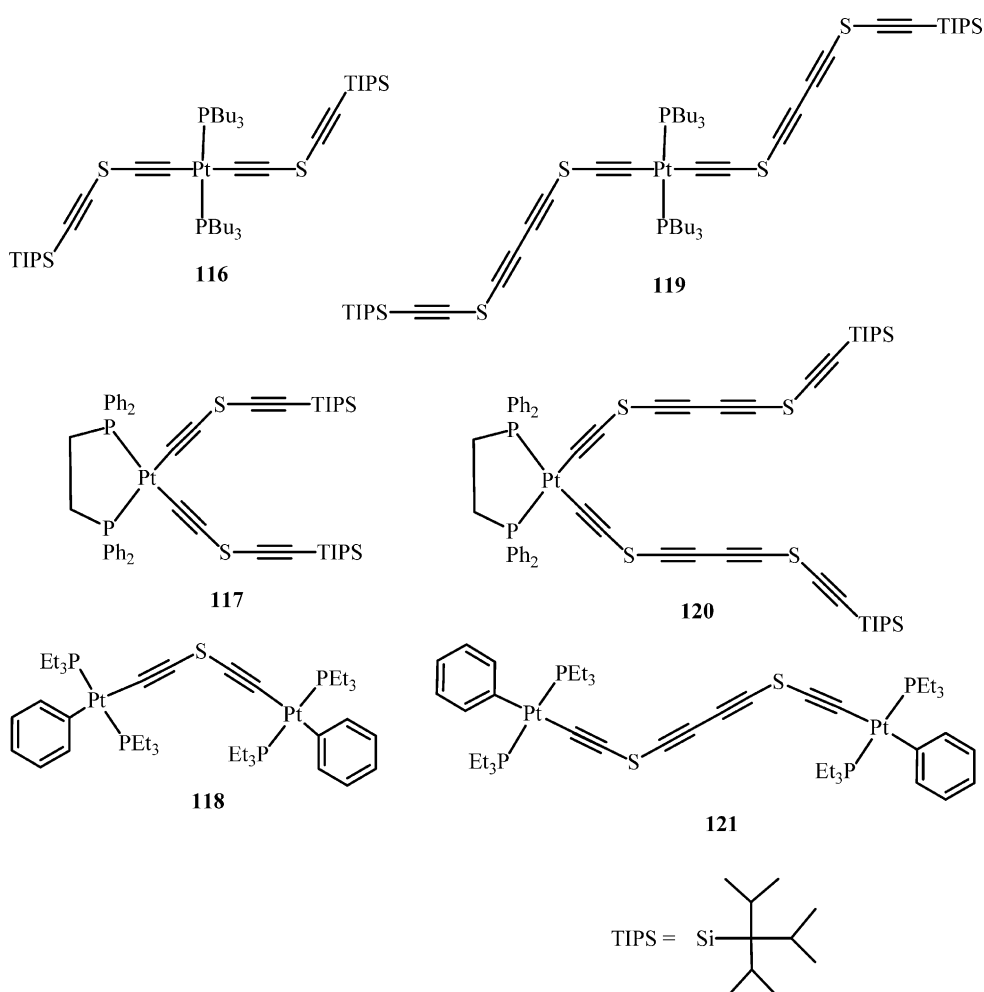
materials in which the conjugation path is controlled by the presence of an insulating spacer. Comparison was made to their diplatinum model complexes **112–115** and their group 11 gold(I) and group 12 mercury(II) closest neighbors. The regiochemical structures of these angular-shaped molecules were studied by NMR spectroscopy and single-crystal X-ray structural analyses (Figs. 32 and 33). Harvesting of organic triplet emissions harnessed through the heavy-atom effects of groups 10–12 transition metals was systematically studied. These metal-containing aryleneethynylenes spaced by chalcogen units were found to have large E_g values and high-energy T₁ states. The influence of metal and chalcogen-based conjugation-interruptors on the intersystem crossing rate and the spatial extent of the lowest singlet and triplet excitons was fully elucidated (see Fig. 34). While it appears that chalcogenide centers do not show coordinating ability, they play more than spectator's role in being a good conjugation-interruptor. A salient feature is that the use of

Fig. 34. Energy level diagram showing the S₁ and T₁ states for **108–111**.

chalcogen units greatly boosts the phosphorescence decay and one could readily observe room-temperature phosphorescence for **108–111** (Fig. 35). The results are remarkable in regard to achieving comparable orders of magnitude for $(k_{nr})_P$ and $(k_r)_P$ which are rarely the case for polymetallaynes (Table 2).



In a related context, a series of platinum(II) acetylide complexes of oligoacetylenic sulfides of various chain lengths **116–121** have been prepared as molecular models for their long chain organometallic polymers [116]. The crystal structures of **117** and **118** were determined and that for **118** is depicted in Fig. 36. Compounds **116–118** with monoacetylenic sulfide units were shown to be air-stable in the solid state, but the oily diacetylenic sulfide species **119–121** turned dark within several days when exposed to light and kept at room temperature under air. The optical properties of these molecules were briefly examined and will likely act as a benchmark for future polymer characterization. Compounds **119** and **120** possessing a diacetylenic unit show significant red shifts in the emission wavelengths with respect to the monoacetylenic counterparts **116** and **117**, respectively.



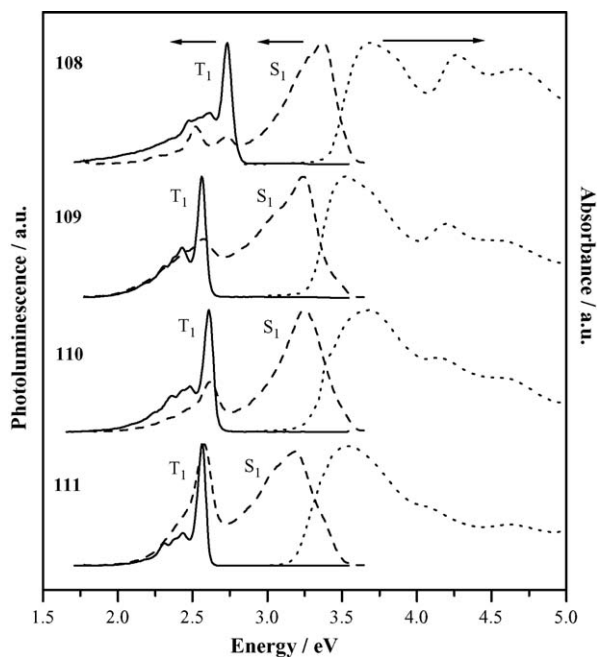


Fig. 35. The absorption and PL spectra of **108–111**. The absorption spectra are the higher energy dotted lines measured at 290 K. PL spectra were taken at both 290 K (dashed lines, in CH_2Cl_2) and 20 K (solid lines, as thin films).

3.1.4. Compounds with metalloligand components

A novel heterobimetallic platinum acetylide polymer of ferrocenylfluorene **122** was reported and spectroscopically characterized [117]. The crystal structure of its binuclear model complex **123** was determined (Fig. 37). The presence of

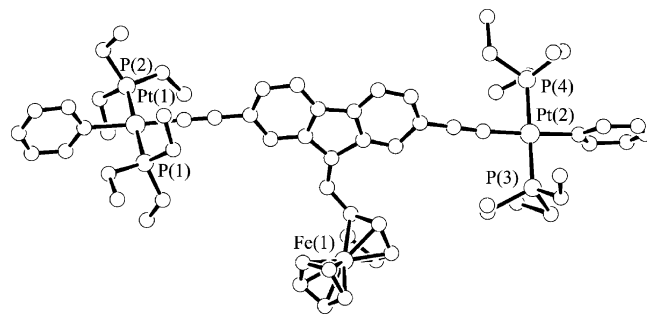


Fig. 37. X-ray crystal structure of **123**.

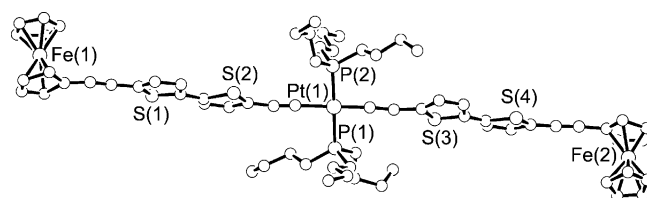


Fig. 38. X-ray crystal structure of **122**.

significant donor–acceptor interaction leads to a narrow bandgap value of 2.10 eV for this Pt–Fe mixed material, which is much lower than that for the parent polymer **48**. The polymer is electroactive with the half-wave potential of the ferrocene moiety slightly more anodic in **122** than in the diethynyl ligand precursor, in line with the transfer of electron density from the ferrocenyl donor unit to the electron-accepting Pt center through the acetylide linkage.

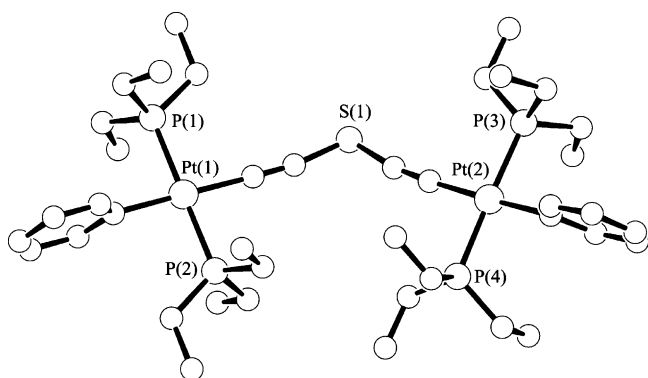
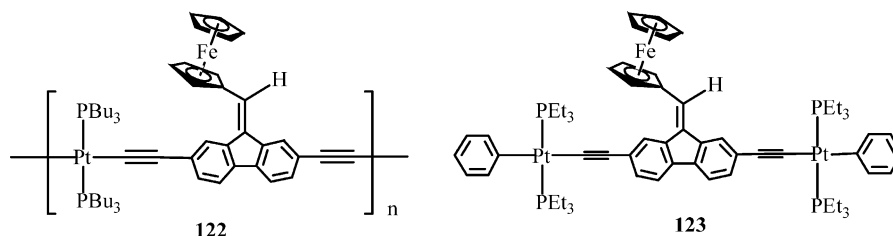
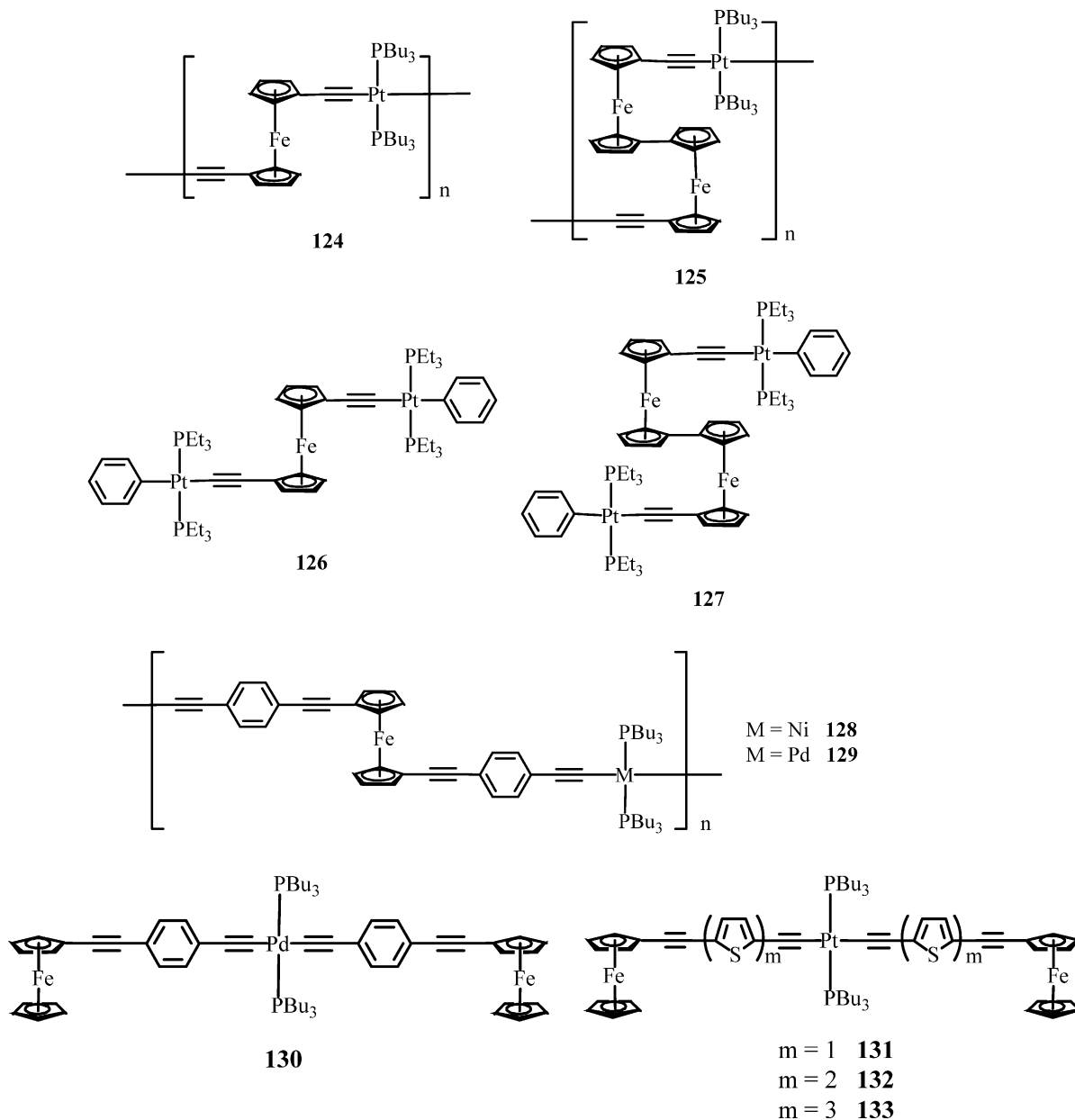


Fig. 36. X-ray crystal structure of **118**.

Long and co-workers have incorporated disubstituted alkynylferrocenyl and -biferrocenyl ligands into the main chain of rigid-rod Pt-acetylide molecules to furnish di- and polymeric platinum-based alkynyl compounds **124–127** [118]. Characterization of these molecules was accomplished by optical spectroscopy and X-ray crystallography. GPC measurements revealed the formation of different sized oligomers for **124**. The insolubility of these oligomeric substances and the low-yielding reaction itself both appear to prevent the formation of polymer. Likewise, compound **125** exists as an oligomeric species of up to 12 repeat units. The greater stability of the biferrocenyl ligands compared to that of the monoferrocenyl analogue results in a higher reaction yield for **125** than **124**. Electrochemical data and extended Hückel theoretical calculations suggest no ferrocene–ferrocene interaction through the Pt-alkynyl bridges. The preparation of the more extended heterobimetallic Fe–Ni and Fe–Pd macromolecules **128** and **129** has also been described

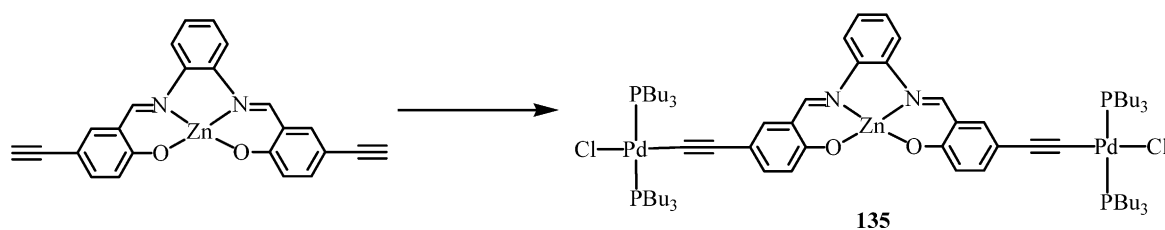
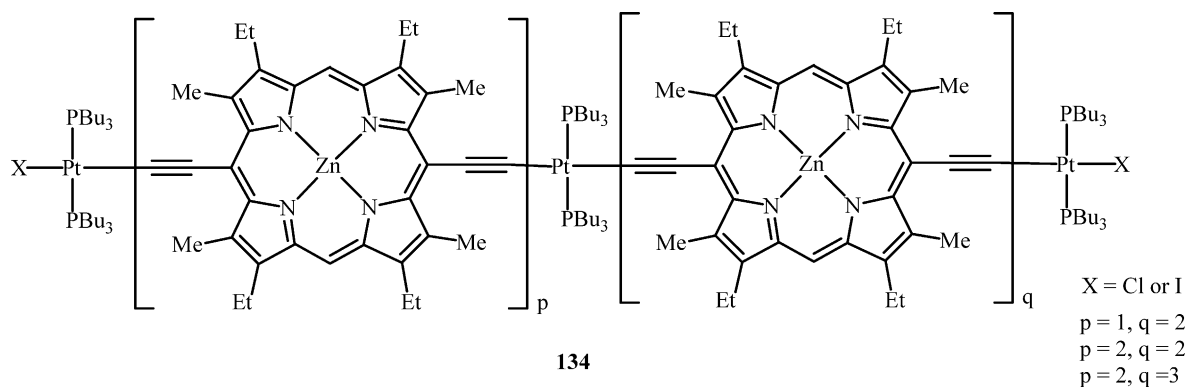
[119]. The related Fe–Pd model complex **130** and the Fe–Pt oligomers **131–133** were also isolated in the hope of gaining further insights on the degree of π -electron delocalization within the system. Fig. 38 illustrates the solid-state structure established for the long-chain oligomer **132** in which the Fe···Fe through-space separation of 32.29 Å was observed [120].

mers that may be suitable for applications in various optical devices [121]. The oligomeric structure was identified by matrix assisted laser desorption ionization (MALDI) mass spectrometry. While the use of PBu_3 ligands can afford stable, isolable and characterizable compounds, it appears that it was not the case when PPh_3 ligands were used. On the other hand,



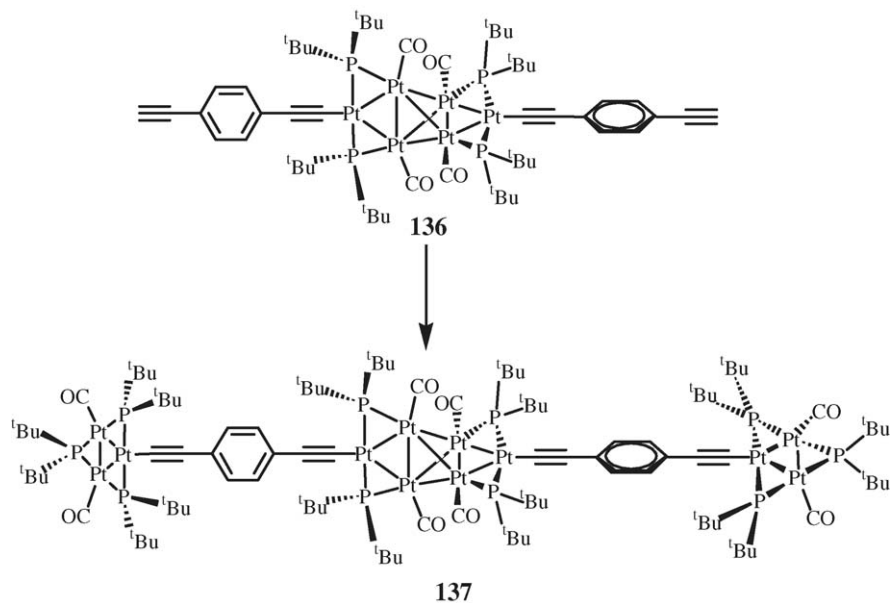
The use of platinum(II)-ethyne entity in the construction of new heterometallic Pt–Zn complexes was known for some zinc porphyrins and Schiff bases. The synthesis and characterization of some oligomeric Pt–Zn porphyrinate molecules **134** were reported and they can act as useful models for the extended π -conjugated low bandgap organometallic poly-

a trinuclear heterometallic complex **135** was isolated upon the reaction of diethynyl-derivatized Zn(II) Schiff base with *trans*-[Pd(PBu₃)₂Cl₂] in the presence of CuI in Et₂NH at room temperature but surprisingly, the diethynyl-substituted Zn(II) precursor is handicapped for the polymerization reaction and no expected Pt(II) polyyne polymers can be isolated [122].



The hexaplatinum-linked diethynyl precursor **136** was used to furnish an interesting Pt₃–Pt₆–Pt₃ linear oligomer of polynuclear platinum clusters bridged by 1,4-diethynylbenzene linking moiety **137** [123]. Compound **137** was characterized by spectroscopic methods and it can potentially act as a building structural motif for the construction of one-dimensional polymetallic platinum-containing polyynes. This model complex was identified by ³¹P{¹H} NMR and IR spectroscopies, MALDI-TOF mass spectrometry and analytical data.

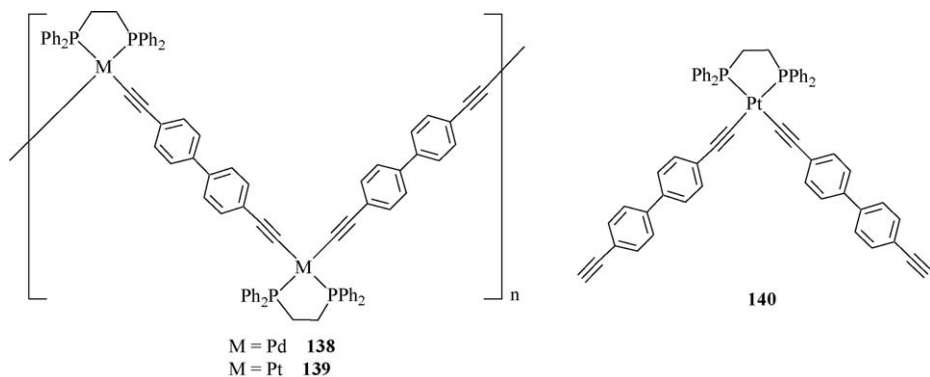
design of polymetallaynes. Group 10 metal complexes containing chelating diphosphine ligand such as *cis*-[M(dppe)Cl₂] (M = Pd, Pt; dppe = bis(diphenylphosphino)ethane) have been employed, via reaction with 4,4'-diethynylbiphenyl, to yield zig-zag organometallic chains **138** and **139** with the metal groups blocked in the *cis* geometry. For **138**, a polymeric material was obtained but only an oligomer can be isolated for **139** [124]. The chemical structures of these materials were also studied using



4. Effect of auxiliary co-ligands on the metal group

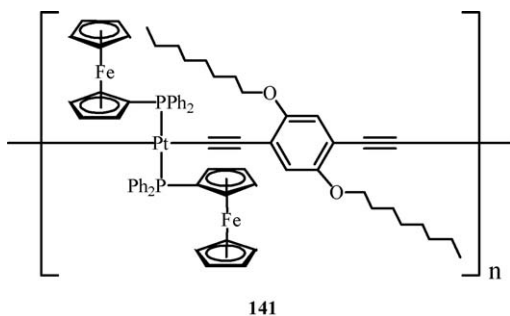
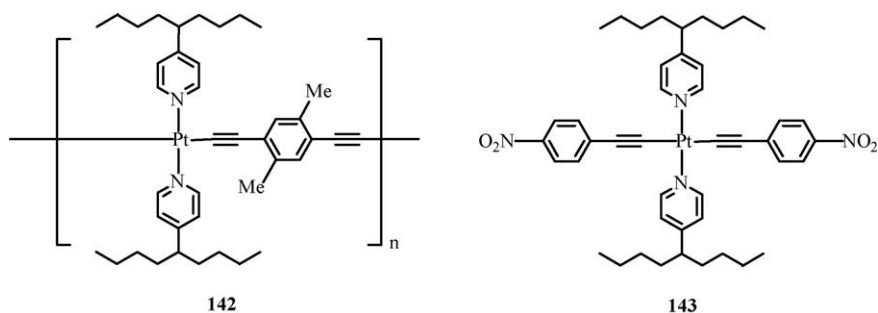
In the past few years, only a few reports are available for the variation of auxiliary ligands on the metal center in the

XPS spectroscopy. Very recently, the corresponding monomer model complex *cis*-[Pt(dppe)(C≡C-*p*-C₆H₄-*p*-C₆H₄-C≡CH)₂] **140** and its derivatives were synthesized and their optical and structural properties have been thoroughly examined [125].



Instead of the widely used trialkylphosphine auxiliary ligands on the group 10 metals, the synthesis of a new platinum(II) complex *trans*-[Pt(PPh₂Fc)₂Cl₂] (Fc = ferrocenyl) was established which can then afford a soluble pale-yellow platinum polyyn **141** through the Sonogashira-type reaction with 1,4-diethynyl-2,5-dioctyloxybenzene [126]. GPC data on **141** show a high degree of polymerization with an average molecular weight of ca. 88,000.

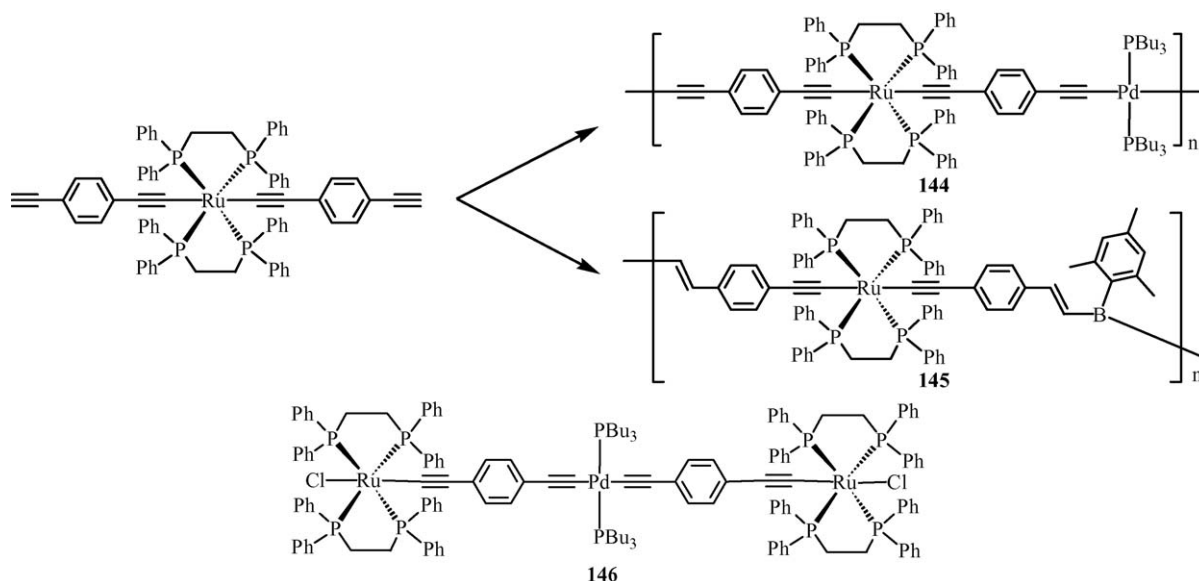
class of ligands has been extensively used in ruthenium(II) chemistry. Adams and others have successfully prepared for the first time a novel platinum(II) alkynyl polymers stabilized by 4-(1-butylpentyl)pyridine ligands **142** in which the long alkyl chain can act as the solubilizing group [128]. The crystal structure determined for the mononuclear Pt(II) model complex **143** ascertains the rod-like skeleton of the as-prepared polymer.



Almost without exception the polymers synthesized so far have auxiliary phosphine or arsine ligands associated with them. Analogous group 10 polymeric materials containing nitrogen donor ligands in a *trans* geometry are extremely rare in the literature which are probably caused by the insolubility of these materials. Earlier work has shown that bipyridyl ligands offer the opportunity for the auxiliary ligands to act as electron sinks in redox processes [127]. Indeed, this

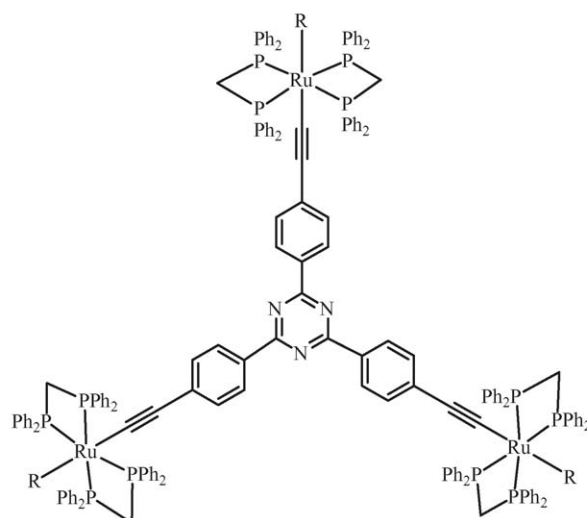
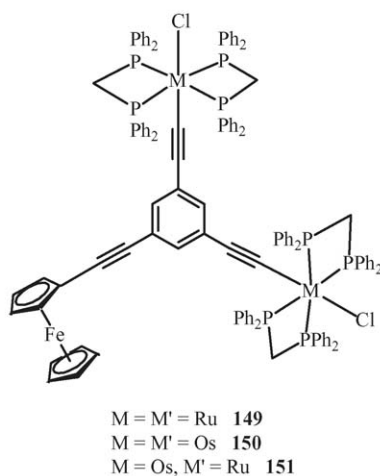
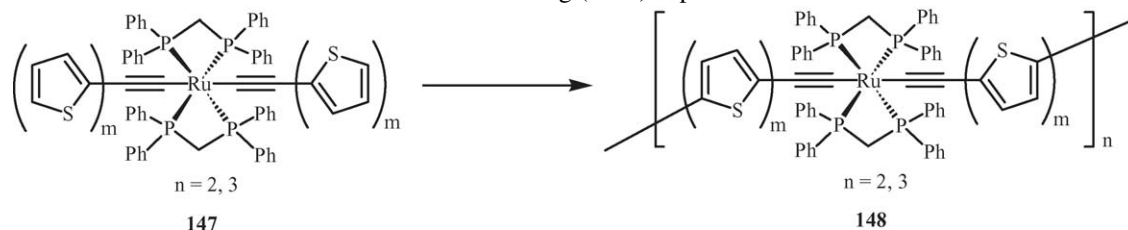
5. Effect of metal centers

In the past 5 years, the diversity of polymetallaynes was extended to include other transition metals. An efficient synthetic access to an organometallic Ru(II) tetrayne complex *trans*-[Ru(dppe)₂(C≡C-*p*-C₆H₄-C≡CH)₂] was developed which can be utilized to copolymerize with *trans*-[Pd(PBu₃)₂Cl₂] or mesitylborane to form a d⁶/d⁸ Ru–Pd mixed-metal polymer **144** [119] and a novel organoboron π-conjugated Ru-containing polymer **145** [129], respectively. Compound **144** represents the first Ru–Pd polymetallayne to be isolated in the literature and its trimetallic model compound **146** was also prepared [130]. For **145**, the absorption maximum of the MLCT band experiences a large red-shift of 141 nm relative to the Ru(II) monomer since the push-pull effect between the electron-rich Ru group and the electron-deficient organoboron unit might facilitate the dπ–pπ* transition in such rigid-rod polymers.



Wolf et al. also reported that the group 8 ruthenium-oligothienylacetylide precursor complex **147** can undergo electropolymerization on an electrode surface to generate new polymetallayne hybrid materials **148** [131]. A series of unsymmetrical group 8 oligoynes bearing a 1,3,5-triethynylbenzene unit **149–151** were reported by Long et al. and their electrochemical behavior were discussed in relation to the electronic interaction among the metal groups [132].

More recently, some trinuclear ruthenium acetylide complexes **152–154** with an electron-accepting 1,3,5-triazine structural core have been isolated. The redox and photophysical properties of these symmetrical molecules were investigated and the X-ray structure of **152** was determined [133]. Complexes **152–154** are essentially nonemissive at room temperature and the first hyperpolarizability values were measured by hyper-Rayleigh scattering (HRS) experiments at 1064 nm.



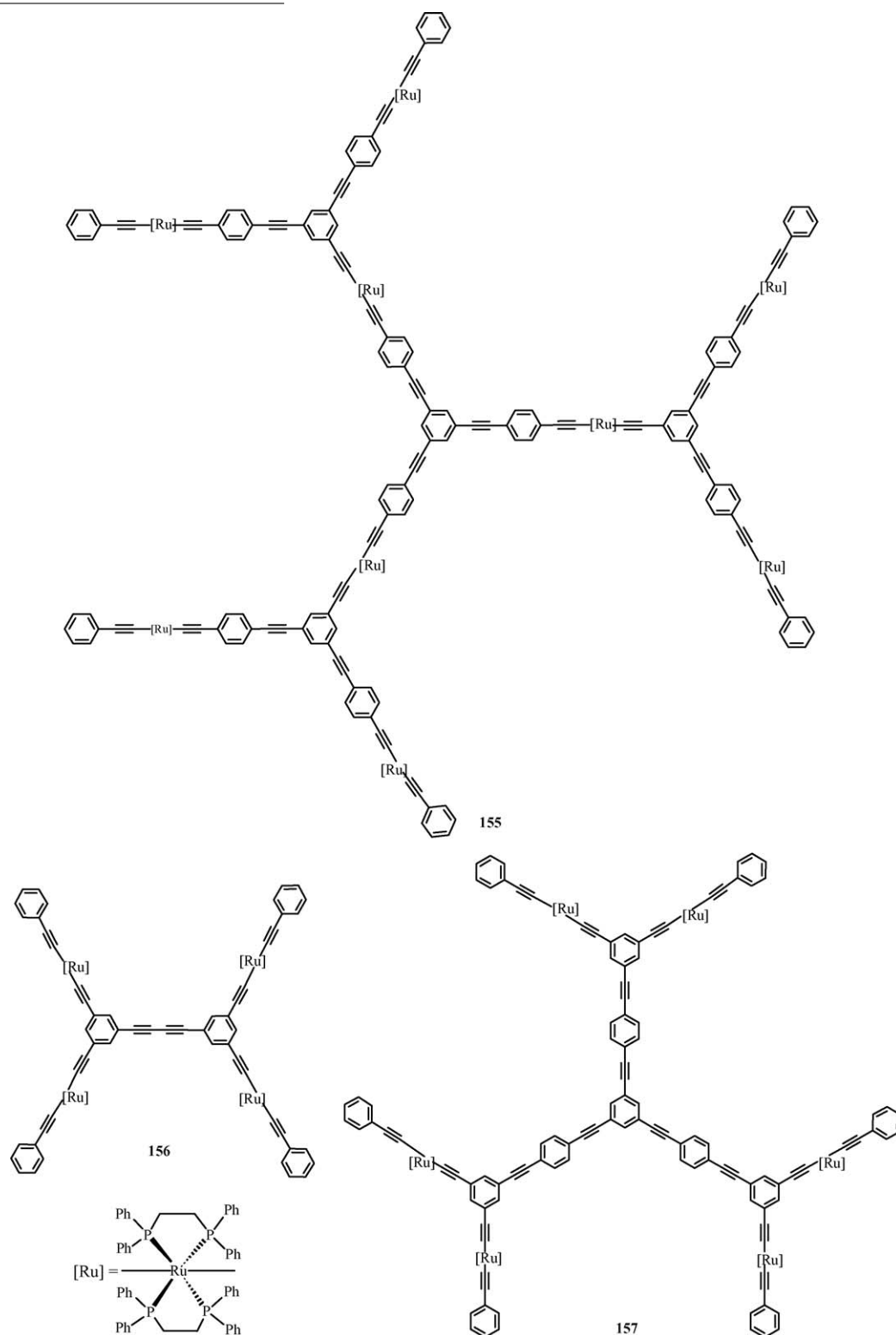
R = Cl **152**

R = **153**

R = **154**

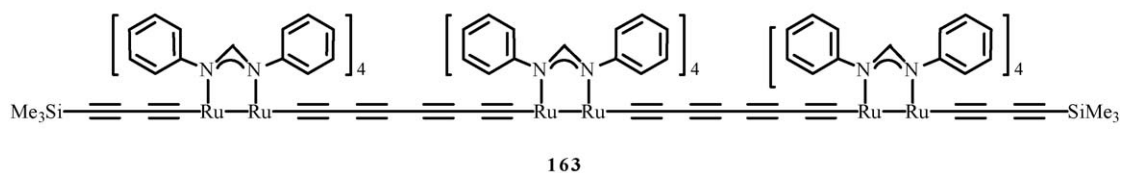
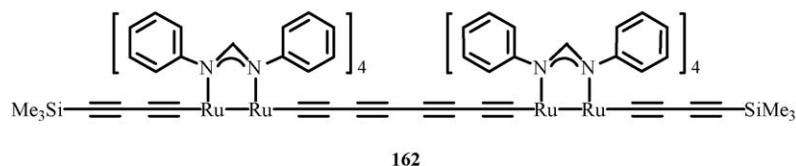
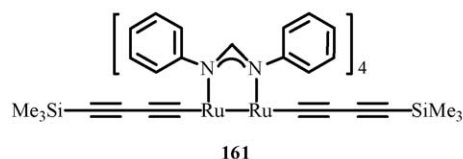
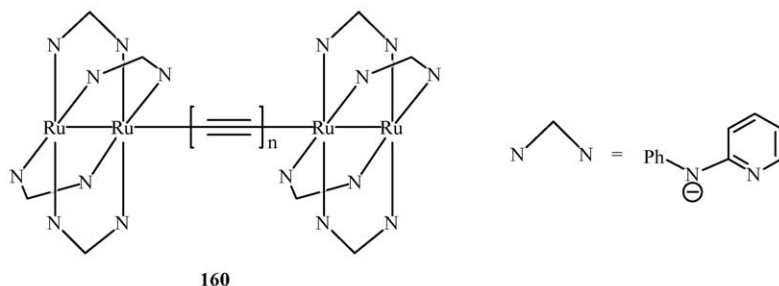
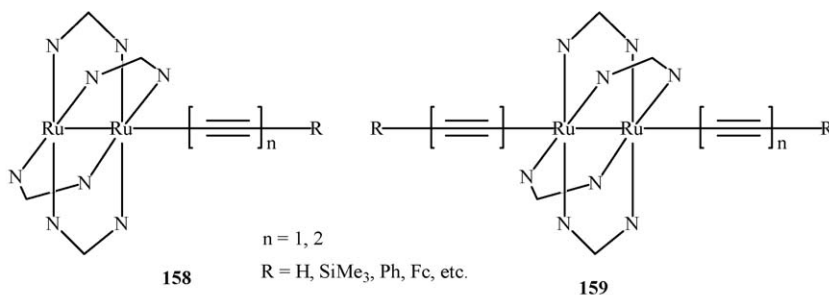
Facile synthetic routes to a series of Ru(dppe)₂-linked organometallic dendrimers were developed by Humphrey and co-workers using a convergent approach. A thermally stable and soluble alkynylruthenium(II) dendrimer containing a large two-dimensional π -delocalized system **155** was isolated successfully [134]. Its third-order NLO properties, and in particular, its two-photon absorption (TPA) properties were studied. The third-order NLO measurements for **155** indicate a marked

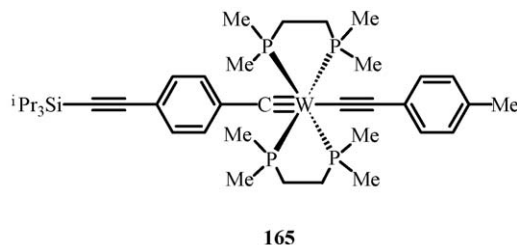
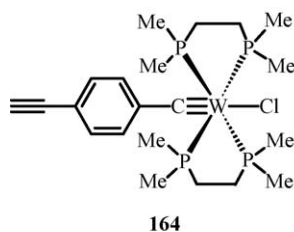
enhancement of TPA from the fragment molecules to the dendritic compound. Nanometer-sized π -delocalized quadrupolar and octopolar dendrons **156** and **157** were also prepared and electrochemical data show comproportionation constants typical of weakly interacting Robin and Day Class II behavior for these molecules [135]. The dimensions of **156** and **157** were also examined by transmission electron microscopy (TEM).



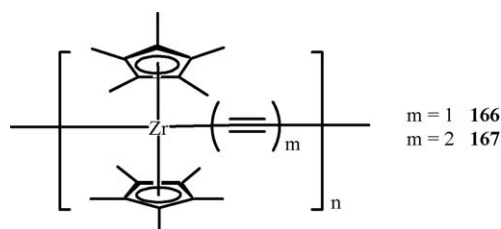
The chemistry of σ -alkynyl compounds derived from diruthenium core of various types **158–160** was comprehensively summarized in an excellent review by Ren recently [136] and full details will not be included here [137–140]. Development of synthetic routes to these organometallic oligoynyl and polyynyl species and studies of their redox behavior were highlighted. A novel type of carbon-rich organometallic molecular wires connected by redox-active Ru_2 units **161–163** having 2–6 ruthenium centers and 4–12 triple bonds along the chain was described. The crystal structure of **162** was determined which reveals a total chain length in the nanoscale of up to ca. 3.5 nm [141].

The metallo-diethynylbenzene precursor **164** was prepared and shown to be a useful building block leading in a facile way to redox-active metal-containing poly(*p*-phenyleneethynylene)s based on the alkyne-metathesis approach. Compound **164** can be easily incorporated into extended unsaturated organic frameworks by further functionalization at both the tungsten center and the $\text{C}\equiv\text{CH}$ headgroup to afford, for example, alkylidyne-containing oligoyne **165** [142]. Electronic spectra of both **164** and **165** are dominated by characteristic bands assignable to the $[n \rightarrow \pi^*(\text{W}\equiv\text{CR})]$ transitions and the data suggest extensive π -electron delocalization along the chain.



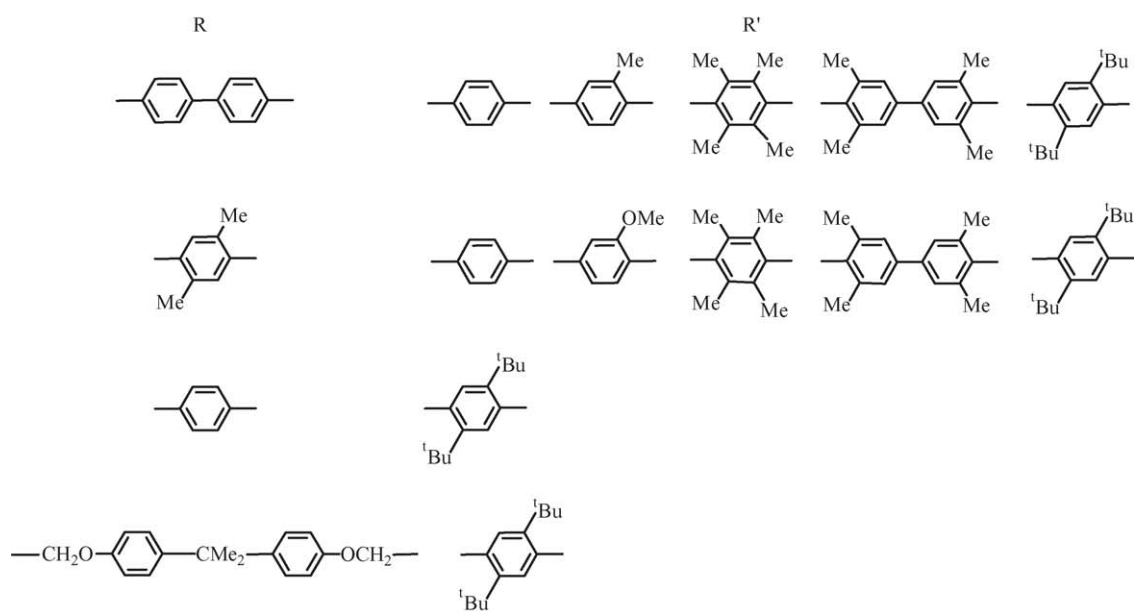
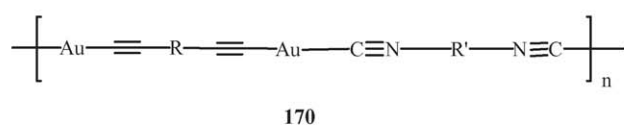
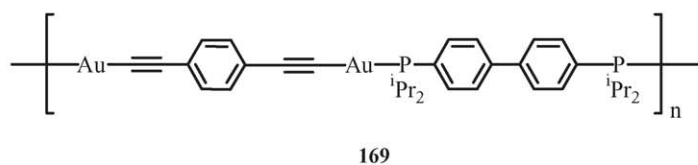
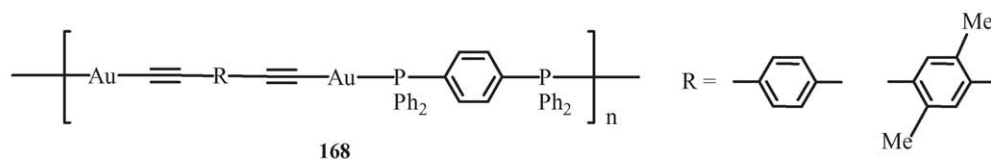


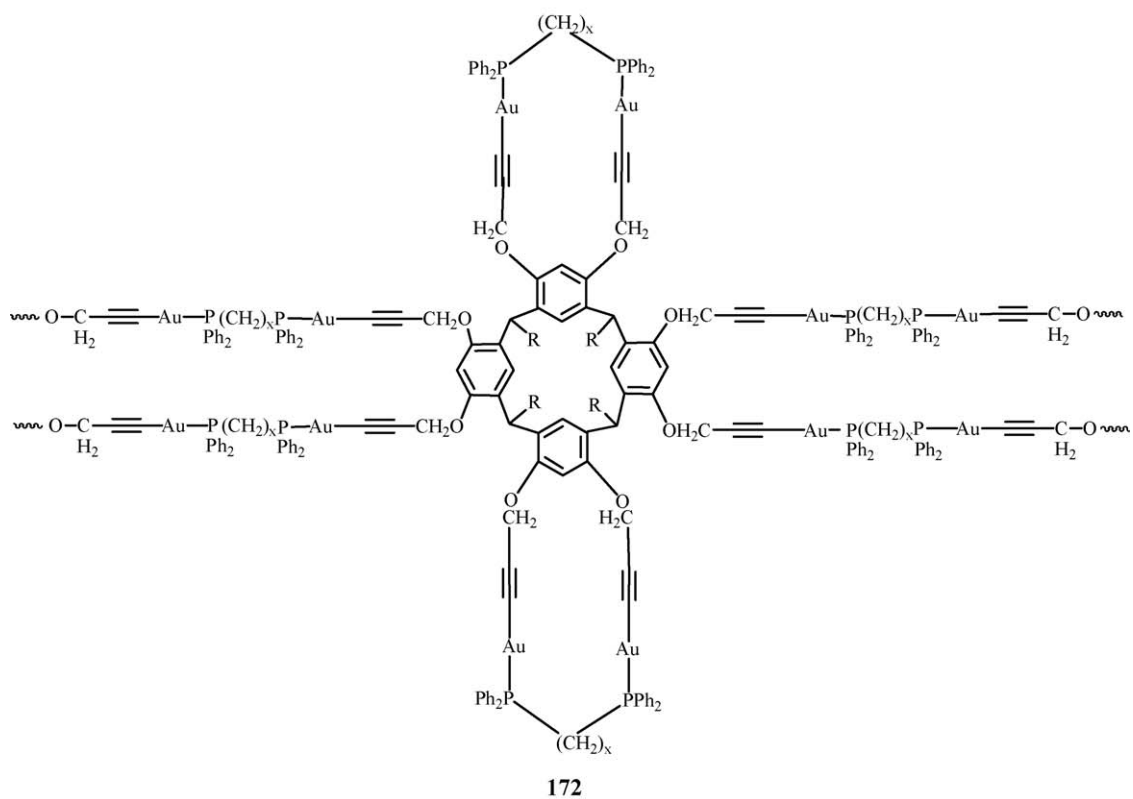
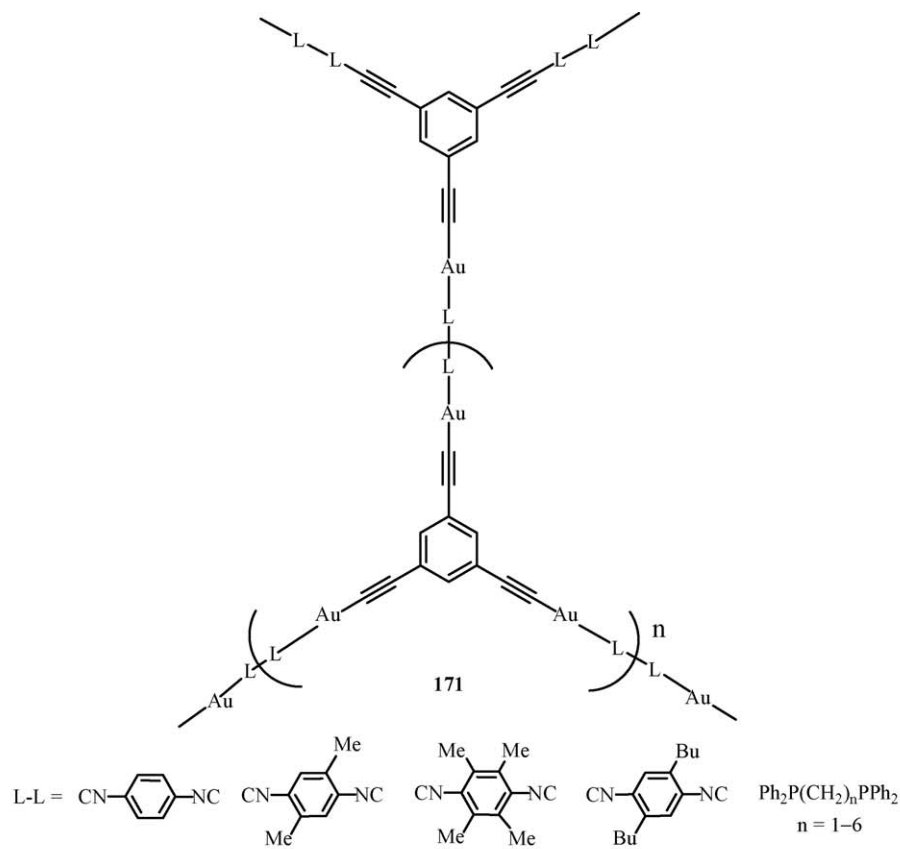
Two conjugated zirconocene–acetylene and zirconocene–diacetylene polymers of group 4 metals **166** and **167** were synthesized in a single step from the reactions of $[\text{Zr}(\text{Cp}^*)_2\text{Cl}_2]$ (Cp^* = bis(pentamethylcyclopentadienyl)) with $\text{Li}(\text{C}\equiv\text{C})_m\text{Li}$ ($m = 1, 2$). Both polymers display limited solubility in common organic solvents and are thermally stable [143].

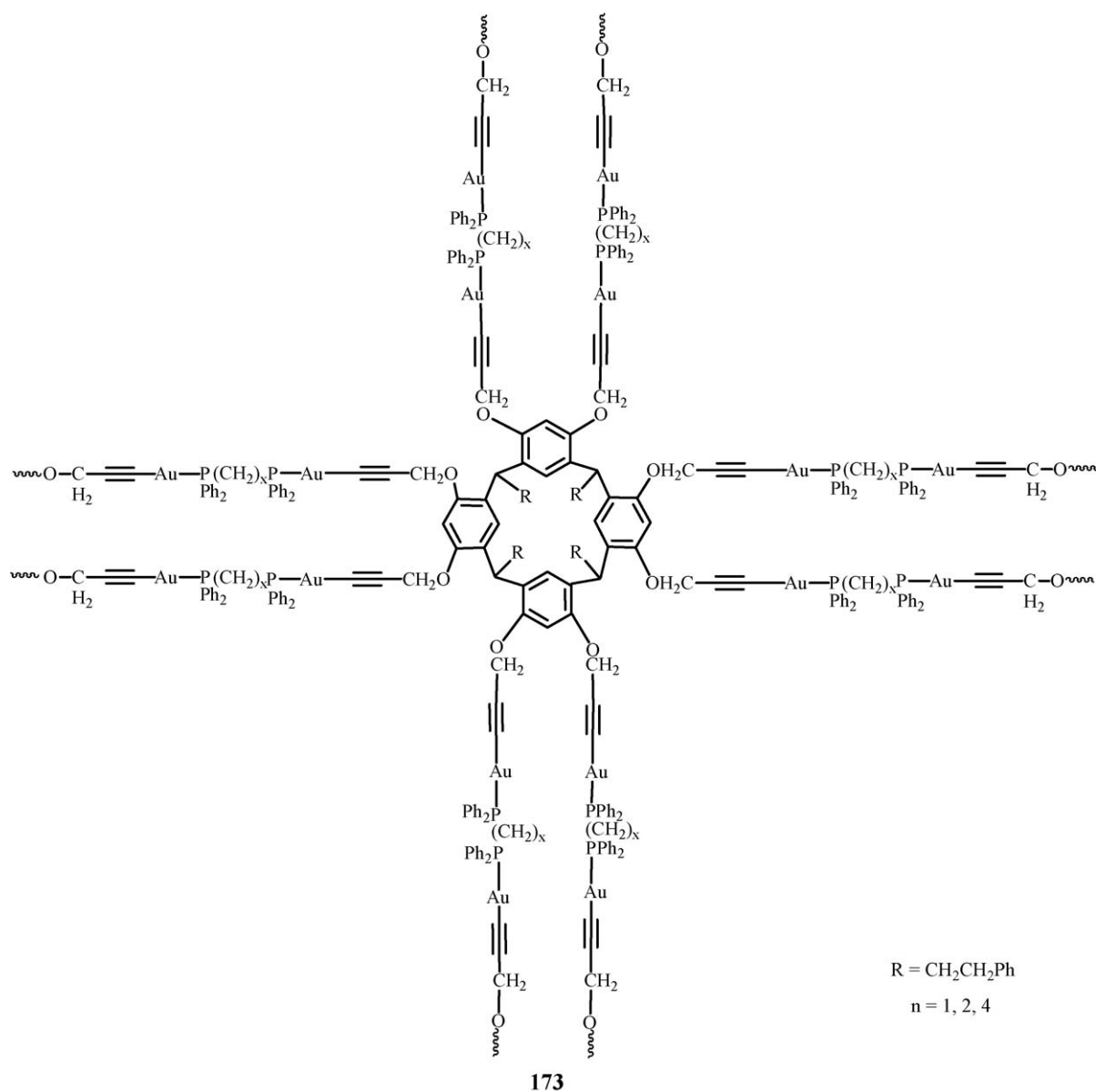


Although the organometallic chemistry of the group 11 metals with σ -alkynyl ligands to produce luminescent complexes can be dated back to nearly four decades ago [144–146], there is still much interest in pursuing research on gold(I) acetylide oligomers and polymers. Gold(I) ion tends to possess a coordination number of two with linear stereochemistry, so it is well suited for forming rigid-rod polymers. Puddephatt et al. have reported on the synthesis, structural and luminescent properties of a novel family of rigid-rod alkynylgold(I) polymers bridged by alternating diacetylide and diphosphine ligands **168** and **169**. These polymers are organic-insoluble solids, which could only be characterized in the solid state [147]. Their photophysical properties were compared to those for the analogous mononu-

clear and binuclear alkynylgold(I) model compounds. The role of aurophilicity in the solid-state packing was discussed. As an extension of the work in such area, the same research group explored the use of diisocyanide ligands in the formation of new organometallic acetylide polymers of gold(I) **170**. Polymers **170** can be obtained by reacting the linear digold compounds $[\text{AuC}\equiv\text{CRC}\equiv\text{CAu}]_n$ ($\text{R} = p\text{-C}_6\text{H}_4$, $p\text{-C}_6\text{H}_4\text{-}p\text{-C}_6\text{H}_4$, $p\text{-C}_6\text{H}_2\text{Me}_2$ and $\text{CH}_2\text{O-}p\text{-C}_6\text{H}_4\text{-}p\text{-C}(\text{Me})_2\text{-}p\text{-C}_6\text{H}_4\text{OCH}_2$) with a range of *para*-substituted diisocynoarenes and they are found to be insoluble in common organic solvents. All attempts to introduce organic solubilizing substituents such as *tert*-butyl groups to enhance polymer solubility failed, which were believed to be partly due to the crosslinking effect caused by interchain $\text{Au}\cdots\text{Au}$ bonding interactions [148]. Characterization of the polymers was achieved using elemental analysis, IR and XPS methods, and the results conform to the fact that they consist of the same backbone as the digold model compounds. Furthermore, new routes to covalently bridged network polymers of gold(I) **171** were developed from $[\text{C}_6\text{H}_3(\text{C}\equiv\text{CAu})_3]$ and some neutral bidentate ligands [149]. Polymers **171** appear as pale yellow insoluble solids and their formulations compare very well to the corresponding model compounds based on the IR and XPS data. Resorcinarene-functionalized alkynylgold(I) polymers were obtained by Puddephatt et al. as insoluble materials and they proposed two possible formulations **172** and **173** for the substances. The composition and identity of the polymers were rarely studied by IR and microanalytical data [150].

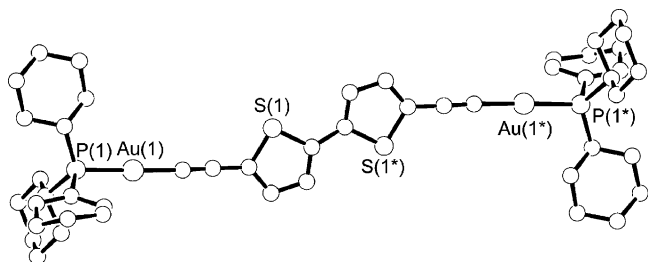




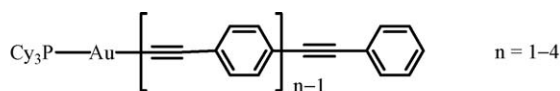
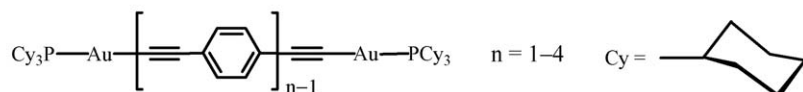
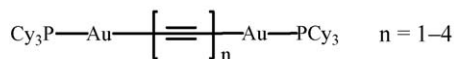
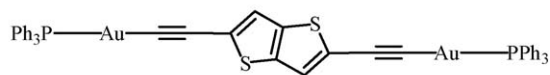
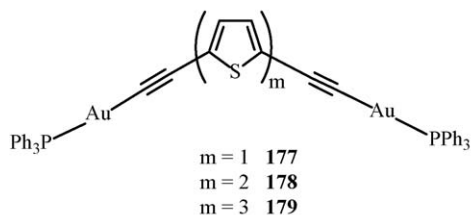
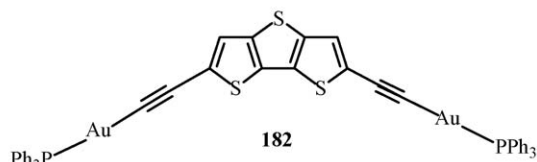
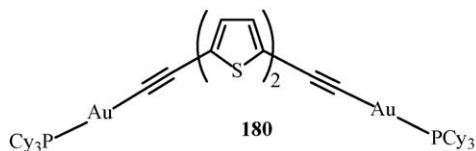
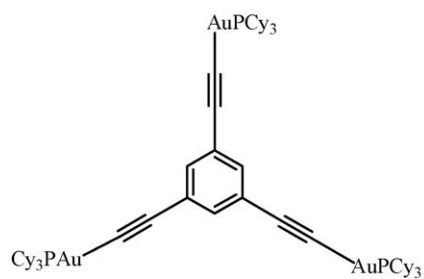
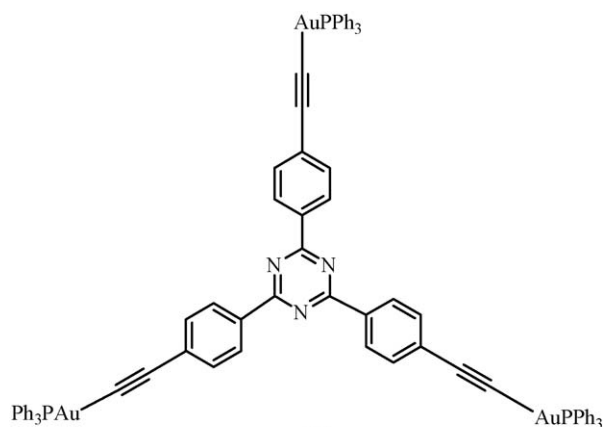


In order to gain useful information on the photophysical nature of $[-C\equiv C-Ar-C\equiv C-]_n$, two homologous series of gold(I)-derived oligo(aryleneethynylene)s **174** and **175** and oligoynes **176** were prepared by Che et al., and their detailed steady-state emission spectroscopy, electrochemistry and photoredox properties were discussed [151–153]. The advantage of exploiting tricyclohexylphosphine (PCy₃) ligand in the study is that it has no low-lying ligand-localized excited states and its bulkiness precludes metal–metal and π – π oligomerization. The organic triplet emissions of arylacetylide groups can be easily harvested at room temperature by ligation to the $[Au(PCy_3)]^+$ unit. The intensity of phosphorescence relative to fluorescence decreases when the arylacetylide chain is extended in length, in accordance with the established energy gap law. The structure–property relationship between the phosphorescent emission energy and arylacetylide chain length was investigated in detail. The limiting value for the

energy gap S_0-T_1 was estimated to be 1.98 and 2.04 eV for **174** and **175**, respectively. The values compare well with the observed S_0-T_1 gaps of 1.90–2.08 eV for the phosphorescence bands of poly(*p*-phenylene) derivatives. The S_1-T_1 splitting for $n = \infty$ was estimated to be ~ 0.8 eV, which corresponds well with the corresponding energy gap of 0.7 ± 0.1 eV reported for a series of polymeric Pt(II) arylacetylide compounds. The limiting λ_{0-0} value for the phosphorescence of **176** was estimated to be 1.36 eV with the singlet–triplet splitting of the $(C\equiv C)_n^{2-}$ chain of about 0.87 eV. A large series of digold(I) bis(alkynyl) compounds incorporating oligothiophenes **177–180**, thienothiophene **181** and dithienothiophene **182** were also reported [87,154]. The crystal structure of **180** is shown in Fig. 39. These classes of compounds can serve as the molecular precursors for their corresponding polyynes.

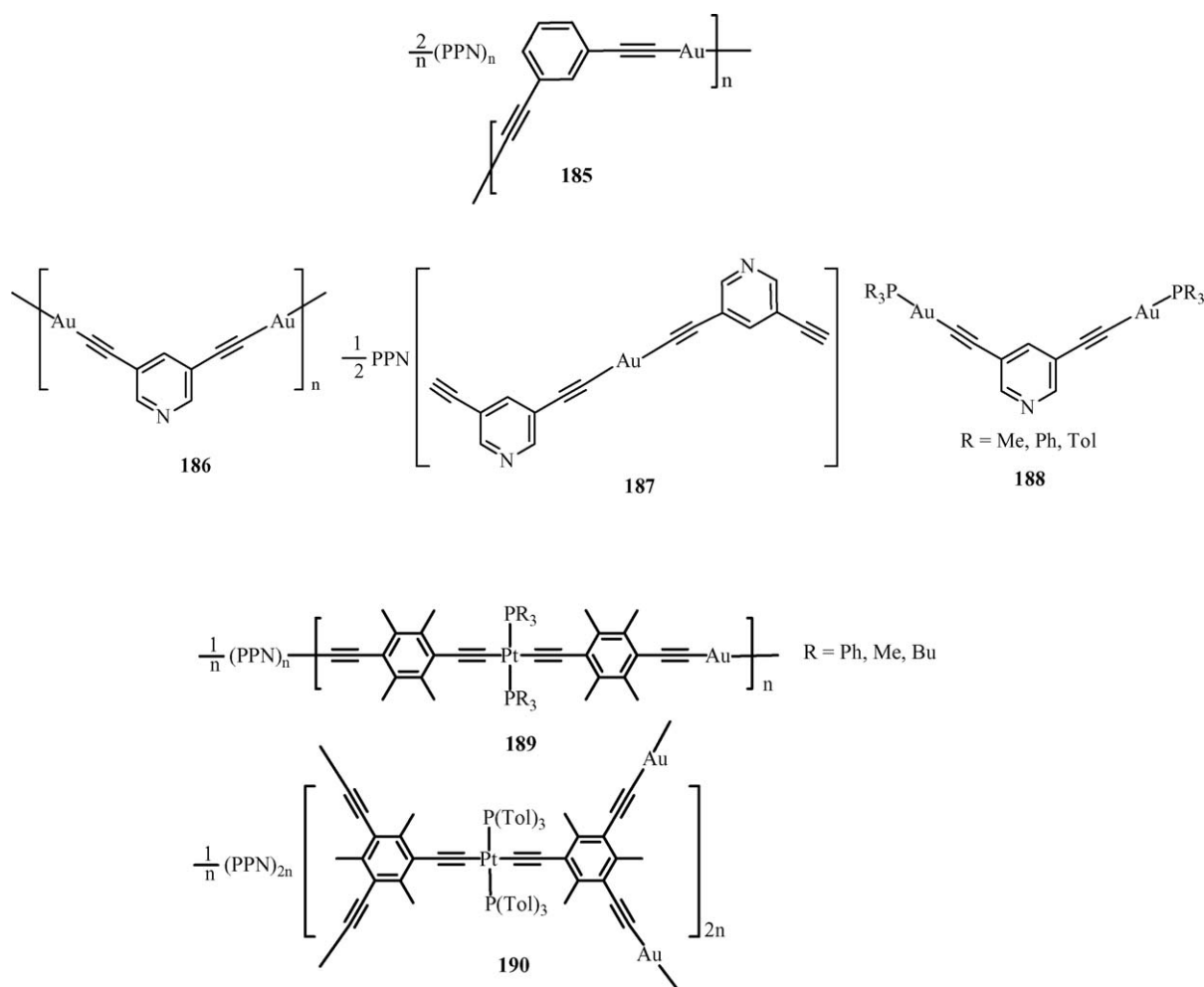
Fig. 39. X-ray crystal structure of **180**.

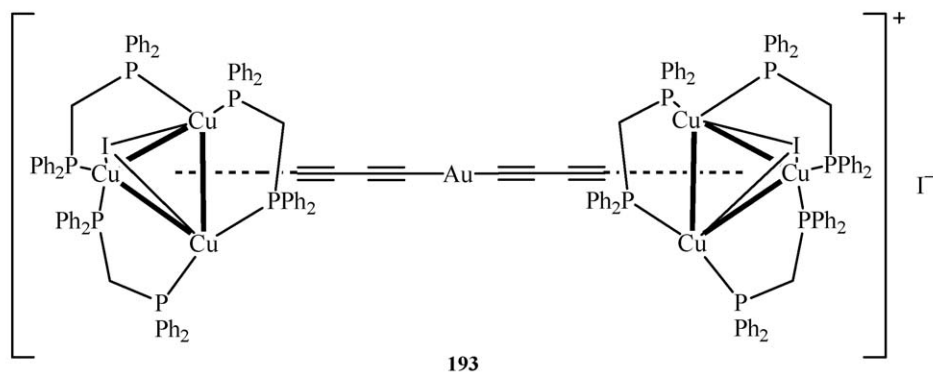
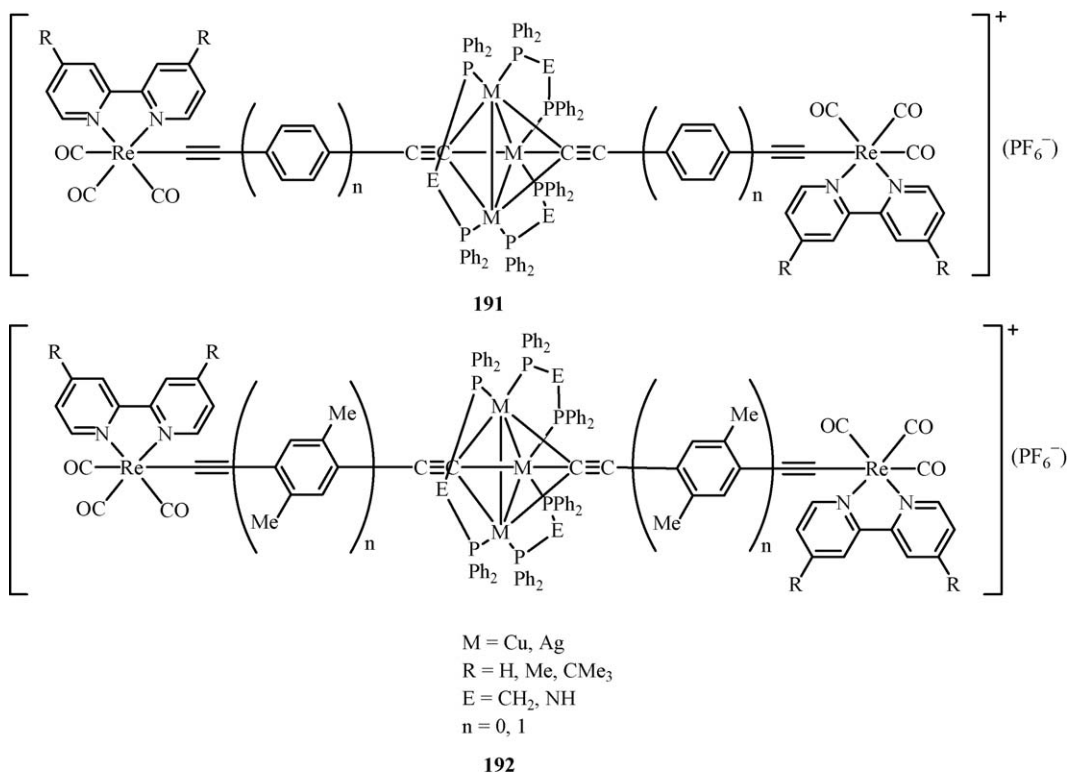
Carbon-rich starburst gold(I) alkynyl compounds **183** and **184** were also successfully synthesized and photophysically characterized [133,155]. Complex **183** is phosphorescent with the emission band at 479 nm whereas compound **184** emits at 401 nm. These trinuclear complexes can be potential building blocks for the design of metallodendrimers.

**174****175****176****181****182****180****183****184**

The first anionic polymetallayne of gold(I) **185** was prepared in moderate yield (36%) from the reaction of $\text{PPN}[\text{Au}(\text{acac})_2]$ with 1,3-diethynylbenzene in a 1:1 stoichiometric ratio [156]. It was characterized by IR and ^1H NMR spectroscopies. The preparation of gold(I) alkynyl polymer **186** and their model complexes **187** and **188** containing 3,5-diethynylpyridine was described [157]. The crystal structure of **188** represents the first structurally characterized example of this type and the presence of intermolecular aurophilic contacts between adjacent molecules gives rise to infinite polymer chains of digold(I) molecules in the solid state. The metal coordinating ability of **188** towards mononuclear metal complexes was studied but there is no mention of their photophysical properties. More interestingly, efforts were made to make two novel anionic heteronuclear Pt(II)–Au(I) σ -acetylide polymers exhibiting both the linear (**189**) and branched (**190**) forms and these polymers possess very poor solubility in all common organic solvents [158].

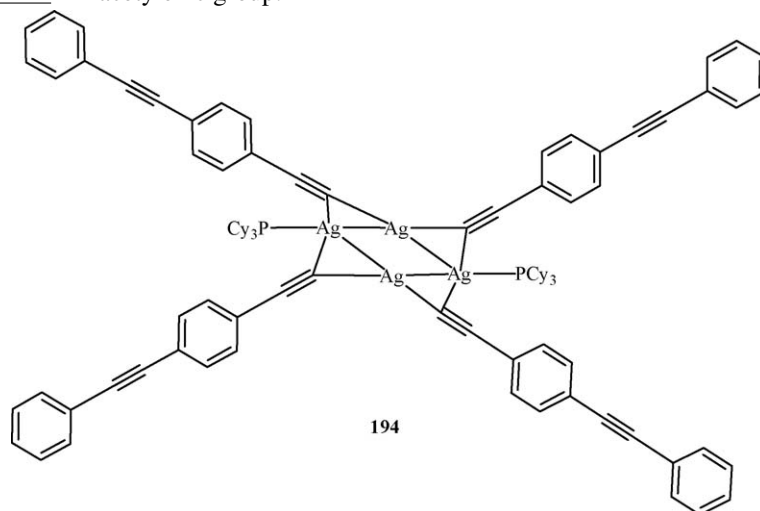
A series of luminescent mixed-metal carbon-rich molecular rods of rhenium-copper and rhenium-silver alkynyls **191** and **192** were synthesized and the photophysical properties of these molecules can be modified by varying the nature of the central trinuclear metal core, the alkynyl ligands and the diimine ligands on the terminal rhenium center. The bonding geometry was studied by X-ray crystallography in several cases [159]. Bruce et al. also reported a molecular dumbbell complex **193** which consists of two $\{\text{Cu}_3(\mu_3\text{-I})(\mu\text{-dppm})_3\}$ units connected by a linear $\text{C}\equiv\text{CC}\equiv\text{CAu}\text{C}\equiv\text{CC}\equiv\text{C}$ chain bonding in a μ_3 fashion. Highly metalated complex **193** showed a peak at $m/z = 3232$ in its electrospray mass spectrum due to $[M + \text{H}]^+$ [160].



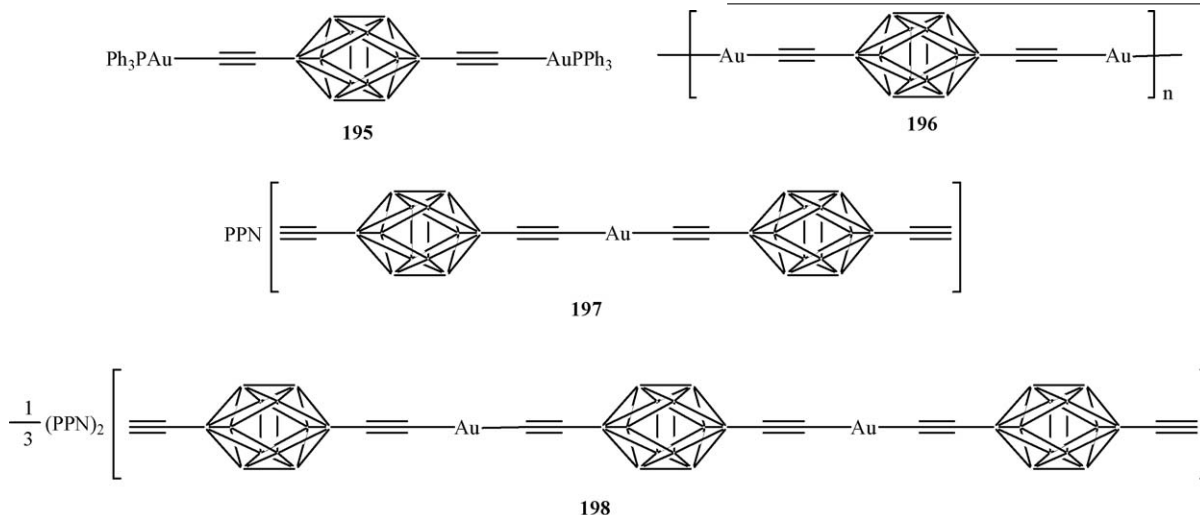


An interesting tetranuclear silver(I) oligo(aryleneethynylene)s **194** was reported by Che and co-workers. The crystal structure and photophysical characterization of **194** were described [161]. Intramolecular argentophilic

interactions between Ag(I) centers were clearly observed. This complex emits weakly in CH₂Cl₂ at 510 nm, which is attributable to the ³(ππ*) excited state localized on the acetylenic group.



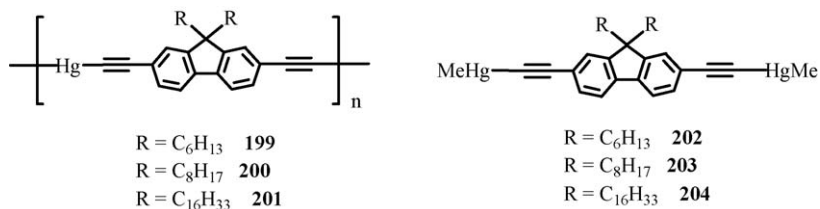
Rigid-rod alkynylgold(I) compounds of various dimensions **195–198** were isolated based on 1,12-bis(ethynyl)-1,12-dicarbocloso-dodecaborane(12) [162]. The X-ray structures of **195** and **197** were established to confirm the dicoordination at gold. The authors claimed that oligomeric complexes **197** and **198** exist as a mixture, which can hardly be separated.



While metal-alkynyls of group 12 elements have been known for many years [163,164], the designed synthesis and chemistry of mercury-alkynyl compounds, however, has not been so thoroughly studied with regard to photophysical characterization. Low solubility of compounds is a major difficulty associated with the preparation of conjugated mercury(II) σ -acetylide polymers. Although linear polymeric copper and mercury acetylides of the form $[-MC\equiv C(p-C_6H_4)C\equiv C-]_n$ were reported as early as 1960 [164], these materials were often shown to be insoluble and intractable which hampered their purification and spectroscopic characterization. Wong et al. reported the first examples of a novel series of soluble well-defined high-molecular-weight d^{10} mercury(II) polyyne polymers with 9,9-dialkylfluorene spacers, which could render ligand-localized phosphorescence through efficient ISC by ligation to the Hg(II) center [165]. The synthesis of Hg(II) polyyne polymers **199–201** involves room-temperature mercuration reaction of

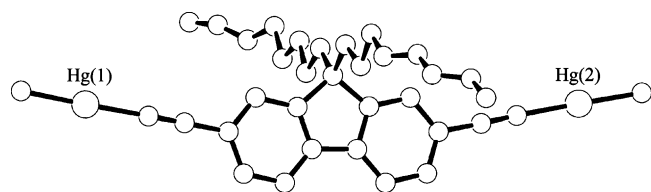
their macromolecular nature. Similar synthetic route using 2,7-diethynylfluorene only gave an intractable off-white solid, suggesting that the long alkyl chains are essential as solubilizing groups to produce these soluble organometallic mercury(II) polyyne polymers. The symmetrical nature and high structural regularity of the polymers were confirmed by NMR

studies. In attempts to model the polymers and gain added insight, complexes **202–204** were also prepared, in which one coordination site on Hg(II) is capped by a Me group [166]. The X-ray crystal structure of **203** (Fig. 40) also helped to establish polymer structures in the solid state and to correlate the photophysical properties with the structural data. Another point worth addressing is the observation of solid-state aggregates in thin films for the polymers as evidenced by the development of a new absorption band at around 365 nm as a nonsolvent is continuously being added to the polymer solution in $CHCl_3$ [167]. The lattice structure is characterized by the presence of weak intermolecular mercuriophilic interactions (3.738 and 4.183 Å) [168–170], linking the individual molecules together to afford a loose polymeric aggregate in a three-dimensional network. Polymers **199–201** show decomposition temperatures in excess of 200 °C. They exhibit increasing decomposition temperatures as the chain length of R groups decreases.



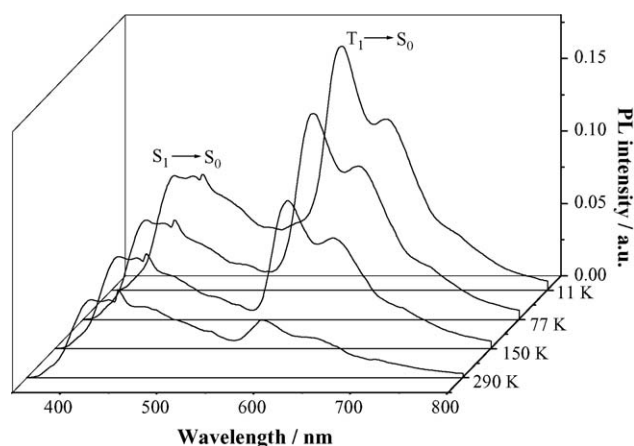
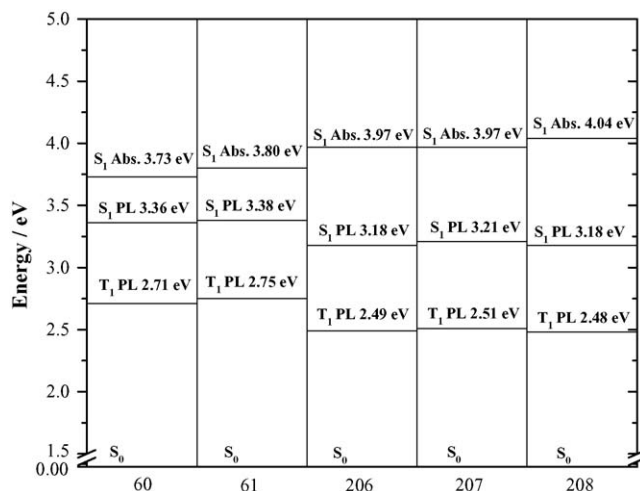
9,9-dialkyl-2,7-diethynylfluorenes with $HgCl_2$ in the presence of methanolic NaOH. They exhibit excellent film-forming properties and their good solubilities in CH_2Cl_2 and $CHCl_3$ make them readily solution-processable for further optical characterization. The degree of polymerization is very high in these polyyne polymers from GPC experiments and the absence of end group NMR resonances also supports

Compounds **199–201** all show similar structured absorption bands in the near UV region, which are mainly due to organic $^1(\pi\pi^*)$ transitions, possibly with some admixture of metal orbitals. We note a red-shift of absorption and emission bands in **199–201** after the inclusion of Hg(II) center which indicates an increase in π -conjugation. The absorption energies and E_g values are insensitive to the nature of R groups on the fluorene ring for these polymers. The transition energies of **199–201** are

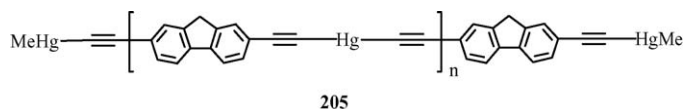
Fig. 40. X-ray crystal structure of **203**.

lowered with respect to those of **202–204**, which indicates a well-extended singlet excited state in the polymers. Both absorption and X-ray structural studies confirm the presence of solid-state aggregates in polymer thin films. The PL spectra also display a red-shift on going from binuclear to polynuclear structures. At 11 K, strong triplet emissions appear at ~ 570 – 590 nm for **199–201** and the large Stokes shifts of these peaks from the dipole-allowed absorptions (ca. 1.2–1.3 eV), plus the long emission lifetimes in the microsecond regime at 11 K suggests the $^3(\pi\pi^*)$ excited states of the parent organic chromophores. The intensity of the phosphorescence relative to fluorescence tends to increase as the alkyl chain length increases from **199** to **201**. Typical of many Pt(II) polyynes, the phosphorescence spectra display a strong temperature (Fig. 41). The S_1 – T_1 crossover efficiency follows the order **201** > **200** > **199**. Values of the energy gap between S_0 and T_1 levels were found to be 2.10–2.23 eV for **199–201**. The S_1 – T_1 gaps lie within the range of 0.73–0.79 eV which match well the S_1 – T_1 separation of 0.7 ± 0.1 eV for similar π -conjugated Pt(II) and Au(I) polyynes, and are also close to the gaps estimated for a series of related organic-based polymers [171,172].

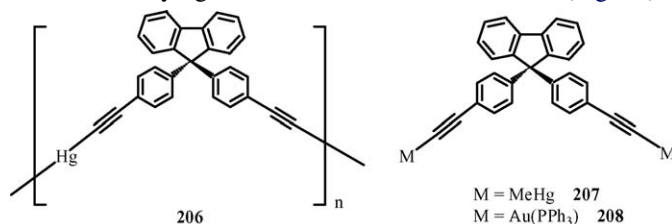
Following the first report on the mercury(II)-containing poly(fluorenyleneethynylene) copolymers, Feng and co-workers have performed detailed theoretical investigations using Hartree–Fock and density functional theory calculations on a series of d^{10} mercury-based diethynylfluorene monomer, oligomer and polymer **205** in order to establish their structure–property relationships [173]. The results show that there is a weak electronic interaction between the metal-based fragment and the π -conjugated organic groups, and thus the photophysical properties are mainly based on the diethynylfluorene

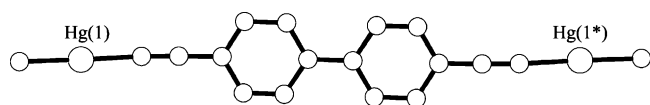
Fig. 41. Temperature dependence of the PL spectra of **201**.Fig. 42. Electronic energy level diagram of **60**, **61** and **206–208**.

π -conjugated segment with relatively little contribution from the metal center. The role of the metal center can be described as weak delocalization coupled with strong localization along the organometallic polymer main chain. Both singlet and triplet excited states of the polymer are localized principally on the conjugated ligand group. From the chain length dependence of emission energies, a limiting value for the emission peak at 385 nm was estimated for the polymer, which is comparable to the experimentally value of 382 nm from the solution phase PL spectrum [117].

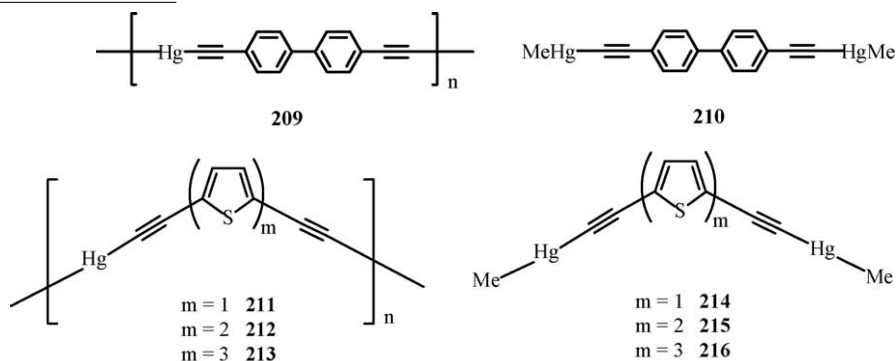


As a continuation of this new area of research, the team led by Wong also reported a high-yield synthetic access to another mercury polyyne **206** prepared from the direct base-catalyzed mercuration of HgCl_2 with 9,9-bis(4-ethynylphenyl)fluorene [81]. Dimerccury(II) complex **207**, as a model of **206**, was also synthesized. However, only the lower molecular weight oligomeric fraction of **206** can dissolve in CH_2Cl_2 and CHCl_3 . Systematic investigations of the photoluminescence properties for **206** and **207** and its Pt(II) (**60** and **61**) and isoelectronic Au(I) (**208**) congeners were made. According to the type of the metal groups, the E_g values of the polyynes follow the experimental order **206** > **60** and those of the monomers **207** > **208** > **61**. All three metals (viz. Pt, Au and Hg) can exert heavy-atom effects in the enhancement of ISC rate, and the effect is most significant for Pt(II) possessing the highest T_1 energy state. The spatial extent of the S_1 and T_1 excitons was evaluated and the detailed energy level diagram for the lower-lying excitations has been constructed (Fig. 42).



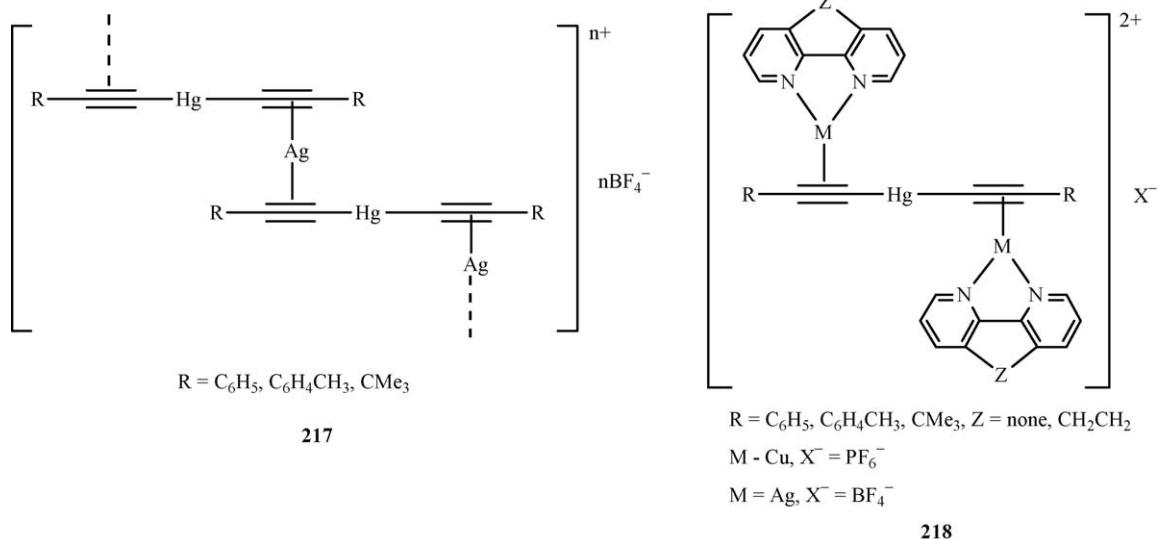
Fig. 43. X-ray crystal structure of **210**.

Similarly, the evolution of lowest S_1 and T_1 states with the type of metal center was examined for biphenyl-bridged metal-aynes **15** and **16** and their mercury(II) analogues **209** and **210**



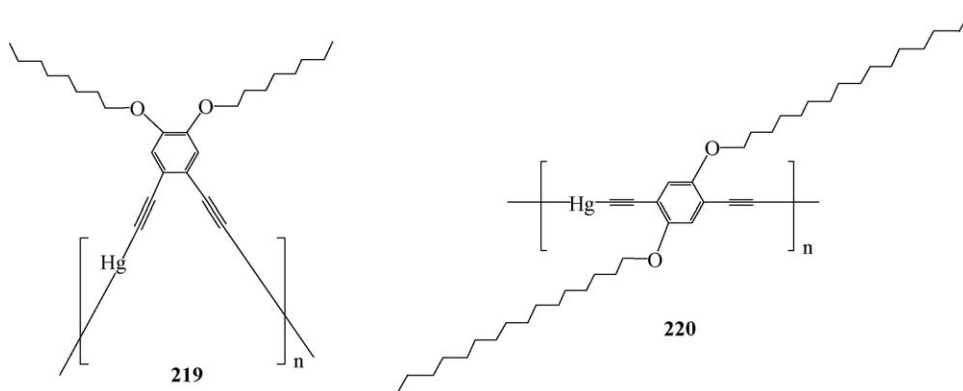
[53]. Since only the low-molecular-weight oligomer of **209** was found to be soluble in chlorinated solvents, its photophysical properties was studied instead. On the structural aspect, the rod-like geometry of **210** was identified from its crystallographic

The use of mercury(II) bis(alkynyl) compounds $(RC\equiv C)_2Hg$ in the generation of novel metal-organic polymeric assemblies **217** and their molecular models **218** has been discussed by Mingos and co-workers [175,176]. Group 11 metals such as Cu(I) and Ag(I) were found to bond to the alkynyl units via π -coordination. Interesting supramolecular interactions were observed in the solid-state structures of these molecules.



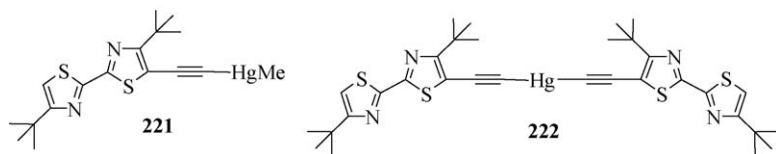
study (Fig. 43) and it is interesting to note the observation of a polymeric mercury(II) acetylide system in the solid state aggregated through $Hg \cdots Hg$ secondary interactions [174], which is also reflected by the presence of a broad aggregate band in its PL spectrum. The work has also been extended to the oligothiophenyl spacers in the polyyne **211–213** and diynyl systems **214–216**.

Wong et al. also recently described the synthesis and spectral and optical characterization of two organomercury(II) acetylide polymers containing dialkoxy-substituted benzene spacers **219** and **220** [177]. These polymers possess M_n values of 44760 and 35630, respectively, corresponding to 75 and 44 in DP. There is a noticeable difference in the emission features and thermal stability of these metallopolymers that contain substituents on the phenyl ring in a different relative position.



Recent exploitation of some luminescent derivatives of inorganic mercury and methylmercury bearing 4,4'-di(*tert*-butyl)-5-ethynyl-2,2'-bithiazole ligand **221** and **222** in the development of a simple procedure for the speciation of mercury(II) by HPLC analysis with UV detection was presented. Such analytical protocol offers a new approach for the simultaneous determination of inorganic Hg(II) and MeHg(II) in aqueous solutions, which will be beneficial to analytical green chemistry in the long run [178].

The efforts by various researchers have circumvented the problem of the triplet exciton being nonemissive by using a model system consisting of d^8 platinum-containing polyyne polymers of the form *trans*-[Pt(PBu₃)₂C≡CRC≡C-]_n for which the spin-forbidden long-lived phosphorescence can be observed and insights on the triplet energies can be acquired directly.



6. Summary and outlook

The past decade has realized great advances in the syntheses, properties, structures and applications of organometallic polymers constructed from metal alkynyl structural motifs. These polymetallaynes are of interest not only as an academic curiosity but also as a commercial reality and they hold a fascination for practitioners in the area of conjugated organic polymers, organometallic chemists, and workers in the field of metal-containing polymers. This article provides a comprehensive review of the syntheses, optical, structural and thermal properties (Table 3) and applications of metal-derived polyyne polymers in the last 10 years which have seen an ever-increasing interest in these compounds, especially in light of their important optoelectronic and photonic properties. The vast body of synthetic methodologies combined with their remarkable applications are the main reasons for the rapid developments in this field. The plenty of examples covered in this contribution highlight the richness and diversity in such research platform.

Currently, compounds with phosphorescent properties have fascinated several groups of scientists and are still attracting considerable attention both experimentally and theoretically.

Over the past 5 years, impressive progress has been made in this area. The triplet energy level can be tuned over a wide spectral range by varying the spacer functionality where a list of aromatic and heterocyclic rings as well as some inorganic and organometallic units were explored. This provides us an opportunity to study the relationship between triplet energy and the rate of nonradiative decay for this class of conjugated polymers. The evolution of singlet and triplet excited states with chemical and electronic structures can be systematically probed and the results contribute to our understanding of the structure–property relationship in this class of organometallic acetylide polymers. Such research topic can lead to a number of technological developments within the realm of molecular electronics and materials science. For instance, the use of platinum-containing polyyne both as semiconductor and as triplet emitters was demonstrated. While considerable reports are available for groups 8 and 10 metal alkynyl systems of various kinds (**I–III**), similar research work has recently been extended to their closest groups 11 and 12 d^{10} gold(I) and mercury(II) neighbors (**IV**), in which both organometallic building blocks adopt a linear two-coordinate configuration to provide a rigid-rod framework.

Table 3
Structural, thermal stability and optical data for polymetallaynes

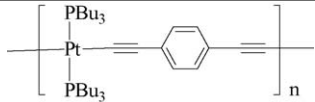
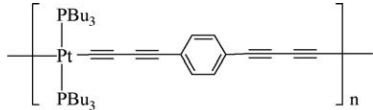
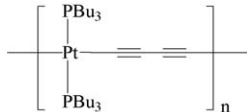
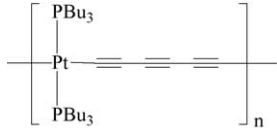
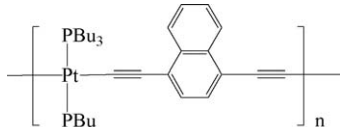
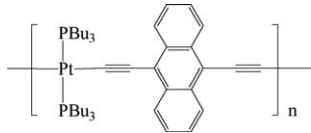
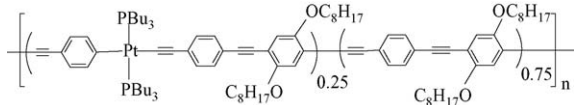
Polymer	Polymer structure	M_w^a	M_n^b	$T_{decomp} (^{\circ}C)^c$	E_g (eV) ^d	Solid film UV (nm)	Solution UV (nm)	Film PL (nm)	Solution PL (nm)	Film or frozen PL (<100 K) (nm) ^e	XR ^f	References
1		96000		302	2.98	380	380		516	405 (S ₁), 521 (T ₁)	Yes	[46]
2		175000			2.60		396			569 (T ₁)	No	[44,109]
3		130000		350	2.88		384			475 (T ₁), 530, 599	No	[108,109]
4		160000			2.63		397			523 (T ₁), 593, 659	Yes	[108,109]
6		78000	41020	308	2.80	404				443 (S ₁), 633 (T ₁)	Yes	[46]
7		50500	28000	315	2.35	459, 502				564 (S ₁)	No	[46]
10		281045	140982				421			451 (S ₁), 628 (T ₁)	No	[51]

Table 3 (Continued)

Polymer	Polymer structure	M_w^a	M_n^b	T_{decomp} ($^{\circ}C$) ^c	E_g (eV) ^d	Solid film UV (nm)	Solution UV (nm)	Film PL (nm)	Solution PL (nm)	Film or frozen PL (<100 K) (nm) ^e	XR ^f	References
11		32152	11453				404			447 (S ₁), 612 (T ₁)	No	[51]
12		79605	16300				414			450 (S ₁), 611 (T ₁)	No	[51]
13		5850	4350			345	342	492	562 (T ₁)		Yes	[52]
15		14770	13060	297	3.10	362, 374	304, 372		369, 409, 556	418 (S ₁), 549 (T ₁), 592	Yes	[53]
25		6000	2610	210			330, 390, 420		520		No	[59]
26		14600	6080	267			360, 390, 420		520		No	[59]

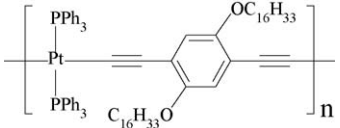
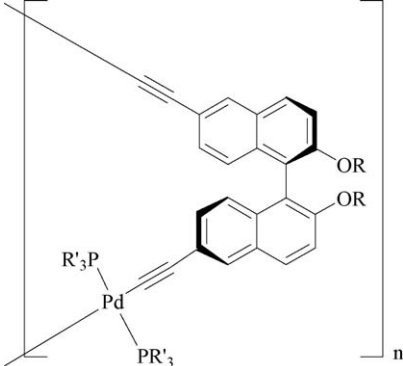
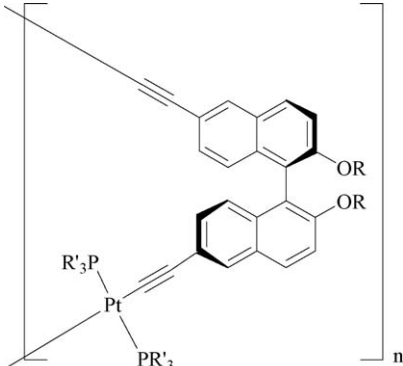
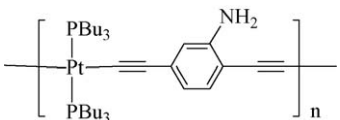
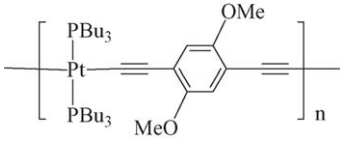
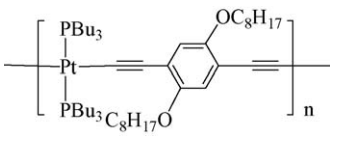
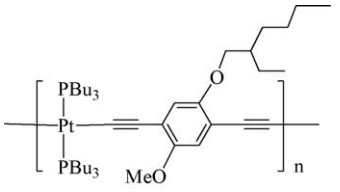
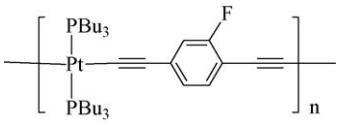
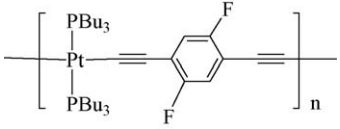
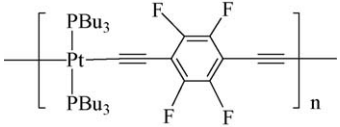
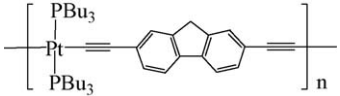
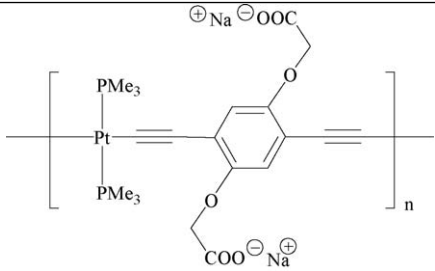
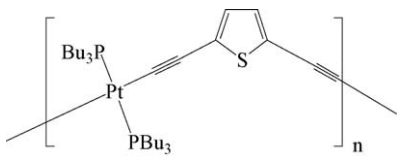
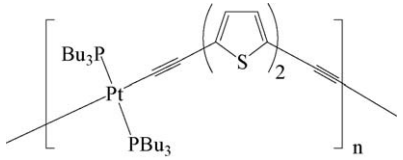
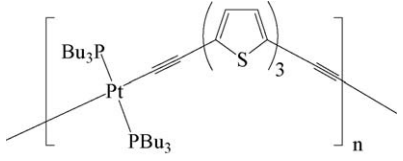
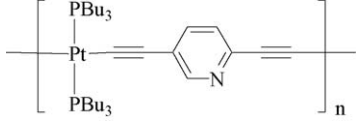
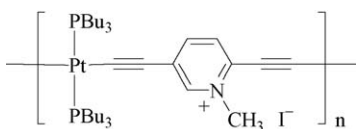
29		26700	15800			No	[60]
33		5400–12000	3375–6316			No	[64]
34		12000–100000	4444–25000			No	[64]
41		151500	94700	248	381	428 (S ₁), 528 (T ₁)	No [68]

Table 3 (Continued)

Polymer	Polymer structure	M_w^a	M_n^b	$T_{decomp} (^{\circ}C)^c$	E_g (eV) ^d	Solid film UV (nm)	Solution UV (nm)	Film PL (nm)	Solution PL (nm)	Film or frozen PL (<100 K) (nm) ^e	XR ^f	References
42		111200	74100	254		403	400			435 (S ₁), 551 (T ₁)	No	[68]
43		151750	94850	310							No	[68]
44		210110	156870			400			551	415 (S ₁), 551 (T ₁)	No	[97]
45		160900	94650	300			386				No	[68]
46		158810	88230	304							No	[68]
47		156770	82500	312		390				539 (T ₁)	No	[68]
48		38960	21410	295	2.90	380	394	427		427 (S ₁), 549 (T ₁)	Yes	[69,117]

49		28900	16900	349	2.92	309, 404	307, 399	432, 552	421, 555	416, 433 (S ₁), 554 (T ₁), 589, 606	No	[77]
50		82745	43550		2.92	391				428 (S ₁), 551 (T ₁)	Yes	[78]
51		64810	29920	310	2.17		392, 467 sh		588	530 (S ₁)	Yes	[79]
52		76460	38820	294	2.10	503	382, 506	641	646	646 (S ₁)	No	[69]
53		116910	101600	352	1.58		303, 348, 393, 660		421, 680, 698		Yes	[80]
60		45700	43410	347	3.38	270, 290, 332	267, 291, 331, 342	459, 512, 547	369, 419, 456, 509	458 (T ₁), 478, 490, 505	Yes	[81]

Table 3 (Continued)

Polymer	Polymer structure	M_w^a	M_n^b	T_{decomp} (°C) ^c	E_g (eV) ^d	Solid film UV (nm)	Solution UV (nm)	Film PL (nm)	Solution PL (nm)	Film or frozen PL (<100 K) (nm) ^e	XR ^f	References
62		36600	23100				398		548 (T ₁)		No	[82]
63		219940			2.80	224, 264, 308, 407	416			435 (S ₁), 605 (T ₁)	Yes	[83]
64		181900	56180	278	2.55	230, 268, 301, 446	458			508 (S ₁), 742 (T ₁)	Yes	[83]
65		82860	64560	290	2.40	233, 272, 334, 457, 484	470			544 (S ₁), 810 (T ₁)	No	[83]
69		80000	48000	320	3.00	378	382			387 (S ₁), 523 (T ₁)	No	[89,91]
70		576000	18000	250			440				No	[89,91]

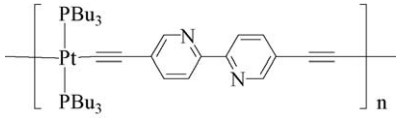
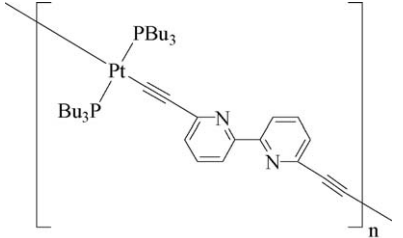
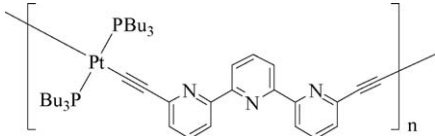
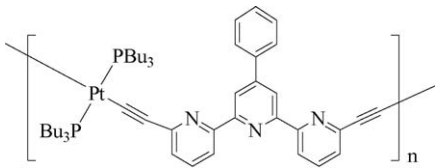
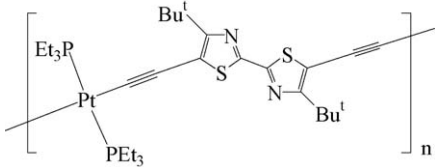
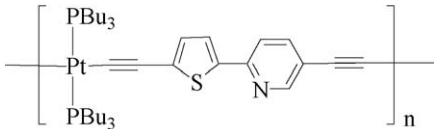
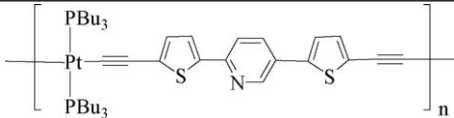
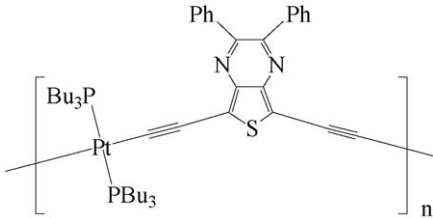
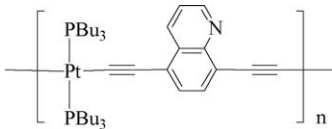
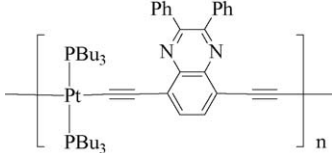
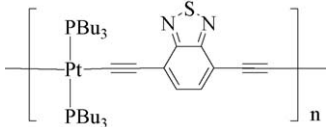
72		89570	68900	274	2.90	394			426 (S ₁), 569 (T ₁)	No	[92]
73		102170	60100	287	3.30	344			463 (T ₁)	Yes	[92]
74		129780	72100	169	3.30	344			461 (T ₁)	No	[92]
75		156240	86800		3.30	344				No	[92]
76		47500	40390	321	2.35	436, 460	439, 464	539	539 (S ₁), 562 sh	Yes	[93]
78		85420			2.67	430, 455		460	460 (S ₁), 646 (T ₁)	No	[94]

Table 3 (Continued)

Polymer	Polymer structure	M_w^a	M_n^b	$T_{\text{decomp}} (^{\circ}\text{C})^c$	E_g (eV) ^d	Solid film UV (nm)	Solution UV (nm)	Film PL (nm)	Solution PL (nm)	Film or frozen PL (<100 K) (nm) ^e	XR ^f	References
79		141467			2.55	405, 430	453	485		485 (S ₁), 691 (T ₁)	No	[94]
80		14006			1.77	650	627	715 (S ₁)			No	[95]
82		169700	114660		2.60	428				470 (S ₁), 667 (T ₁)	Yes	[96,97]
83		150900	96230		2.25	506				556 (S ₁), 747 (T ₁)	Yes	[96,97]
84		150910	113640		2.20	528				577 (S ₁), 832 (T ₁)	Yes	[96,97]

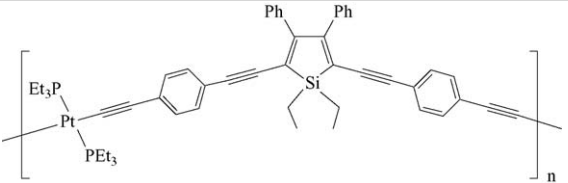
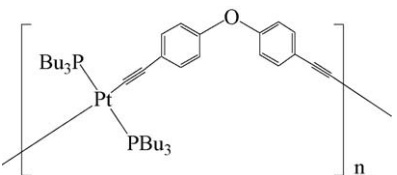
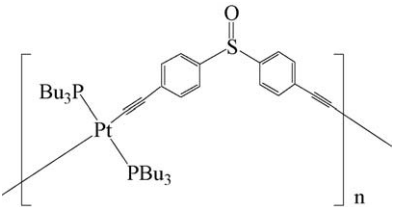
85		19100	8920	315	3.10	261, 304, 347	258, 301, 344	404, 427	412, 428	403 (S ₁), 426, 462 (T ₁), 497, 511	Yes	[77]
89		10400	6000				319		460 (S ₁), 530		No	[101]
90		9700	6300				352		460 (S ₁)		No	[101]
91		78700	52000	381	3.70	261, 278, 314	261, 277, 312	418, 510		419 (S ₁), 508 (T ₁)	Yes	[106]

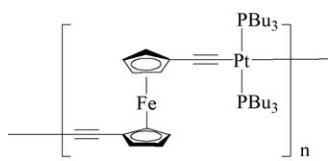
Table 3 (Continued)

Polymer	Polymer structure	M_w^a	M_n^b	$T_{decomp} (^{\circ}C)^c$	$E_g (eV)^d$	Solid film UV (nm)	Solution UV (nm)	Film PL (nm)	Solution PL (nm)	Film or frozen PL (<100 K) (nm) ^e	XR ^f	References
95		146000	82700	366	3.10	304, 360	303, 355	394, 513, 575	404, 520	394 (S ₁), 423, 512 (T ₁), 555, 575	No	[110]
98		102200	89400	357	3.05	272, 300, 384	271, 299, 383	402, 522	428, 525	402 (S ₁), 520 (T ₁), 552, 565, 581	No	[110]
99		42970	13580	410	3.05	309, 365, 374	309, 379		364, 413	412 (S ₁), 433, 547 (T ₁), 583, 597, 613	No	[111]
100		22950	11150	414	3.04	309, 328, 345, 365, 374	308, 327, 343, 378		371, 409, 421, 541	411 (S ₁), 428, 451, 544 (T ₁), 584, 594, 612	No	[111]

101		22790	16150	407	3.04	307, 328, 347, 374	308, 327, 344, 376	371, 409, 421, 541	410 (S ₁), 427, 544 (T ₁), 581, 593, 612	No	[111]
102		23970	10400	404	3.00	307, 366, 378	309, 382	366, 419, 436, 548	395, 414 (S ₁), 444, 507, 548 (T ₁), 585	No	[111]
103		28350	12830	407	3.00	310, 330, 347, 376	309, 329, 346, 380	358, 372, 413, 545	411 (S ₁), 545 (T ₁), 593	No	[111]
104		22600	17530	418	3.00	310, 331, 348, 376	309, 329, 346, 380	356, 373, 408	411 (S ₁), 433, 545 (T ₁), 582, 594	No	[111]

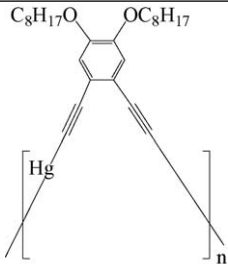
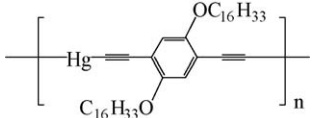
Table 3 (Continued)

Polymer	Polymer structure	M_w^a	M_n^b	$T_{decomp} (^{\circ}C)^c$	E_g (eV) ^d	Solid film UV (nm)	Solution UV (nm)	Film PL (nm)	Solution PL (nm)	Film or frozen PL (<100 K) (nm) ^e	XR ^f	References
105		17530	9930	348	2.10		275, 300, 370, 446, 472, 504		537 (S ₁), 565 sh		No	[112]
107		22545			2.70	380					No	[113]
108		37390	12750	363	3.40	266, 291, 337	267, 292, 343		368, 492	454 (T ₁), 475, 488	No	[115]
109		11430	7020	361	3.26	294, 344	269, 296, 352		382, 482	484 (T ₁), 510, 522, 537	Yes	[115]
110		11100	6550	354	3.28	266, 299, 337	272, 299, 349		382, 474	475 (T ₁), 501, 527	Yes	[115]

111		15480	7930	335	3.18	268, 301, 350	270, 301, 361	389, 481	484 (T ₁), 509, 536	Yes	[115]
122		34540	17970	250	2.10			437		Yes	[117]
124		4600	2800							Yes	[118]
125		11800	2640							Yes	[118]
128		26100	11600							No	[119]

167		68000		224								No	[143]
199		28720	27100	282	3.32	316, 345, 365	313, 341, 355	475	381, 406	427 (S ₁), 570 (T ₁), 610	No	[165]	
200		18320	15090	220	3.31	316, 345, 364	313, 340, 355	478	382, 406	426 (S ₁), 583 (T ₁), 630	Yes	[165]	
201		38650	36250	200	3.32	316, 345, 364	313, 338, 355	478	385, 409	429 (S ₁), 590 (T ₁), 634	No	[165]	
206		8900	8590	292	3.80	263, 278, 298, 312	260, 275, 289, 309	470	374, 390	473 (T ₁), 498, 523	No	[81]	
209		2390	2200	330	3.27	308	310	371		405 br (S ₁), 523 (T ₁), 551	Yes	[53]	

Table 3 (Continued)

Polymer	Polymer structure	M_w^a	M_n^b	T_{decomp} ($^{\circ}C$) ^c	E_g (eV) ^d	Solid film UV (nm)	Solution UV (nm)	Film PL (nm)	Solution PL (nm)	Film or frozen PL (<100 K) (nm) ^e	XR ^f	References
219		67390	44760	306			257, 306, 326		369, 404, 417	500, 523, 541	No	[177]
220		46460	35630	232			262, 271, 337		367, 395	413, 460, 512, 550	No	[177]

^a Weight-average molecular weight.

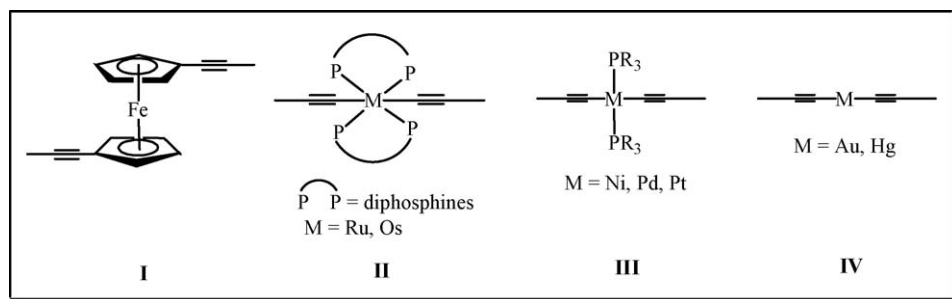
^b Number-average molecular weight.

^c Onset decomposition temperature.

^d Optical bandgap as estimated from the onset wavelength of solid-state optical absorption.

^e Parentheses show the lowest excited state from which emission arises.

^f X-ray crystal structure of the corresponding model complex was determined; sh = shoulder peak; br = broad peak.



From a synthetic point of view, polymetallaynes are available in a never-ending variety of different chemical structures and topologies. Several research groups have lately turned their attention to the use of other third-row transition metal groups including gold(I) and mercury(II) centers in the molecular design of new polymetallaynes and the properties of these molecules are eagerly awaited. While there is continued interest in these metallated materials, we believe that future research in this area should elucidate a direct evaluation of the role of different metal centers on the properties of conjugated compounds and the in-depth exploration of these functional polymers in optoelectronic work and applications. If they can be further activated to be multifunctional, it would also bring this class of polymeric materials to a higher platform. Investigations pertaining to the phosphorescent polymetallaynes are desirable for applications that harvest the T_1 state for light emission through light-harvesting techniques. Further research study and refinement along this direction could broaden the scope to other metal-organic triplet-emitting systems. While the multidisciplinary nature of this field of molecular science continues to attract an abundance of high quality research, it seems likely that more fascinating chemistry and advanced applications can be eventually developed. The extensive spectroscopic characterization of these metal-containing polyynes also renders them a suitable model system to probe theoretical calculations. The analysis of the optical response of metal-containing polyynes should also provide useful insight into the characteristics of the electronic excitations in the related conjugated systems. In this way, valuable insight into the photophysical nature of $(-C\equiv C-Ar-C\equiv C-)_n$ conjugated materials can be obtained. It is likely that the more general features of these results might also apply to conjugated hydrocarbon polymers such as PPV and polyfluorenes, which are investigated as suitable materials for light-emitting diodes and polymer-based lasers [179].

Acknowledgements

The authors gratefully acknowledge financial support from the Research Grants Council of the Hong Kong SAR (HKBU 2022/03P) and the Hong Kong Baptist University. W.-Y. Wong is also indebted to all his postgraduate students and postdoctoral associates for their hard research work cited in the references of this review.

References

- [1] I. Manners, *Synthetic Metal-containing Polymers*, Wiley-VCH, Weinheim, 2004, p. 153 (Chapter 5).
- [2] P. Nguyen, P. Gómez-Elipe, I. Manners, *Chem. Rev.* 99 (1999) 1515.
- [3] I. Manners, *Angew. Chem. Int. Ed. Engl.* 35 (1996) 1602.
- [4] A.S. Abd-El-Aziz, *Macromol. Rapid Commun.* 23 (2002) 995.
- [5] R.P. Kingsborough, T.M. Swager, *Prog. Inorg. Chem.* 48 (1999) 123.
- [6] N.J. Long, C.K. Williams, *Angew. Chem. Int. Ed.* 42 (2003) 2586.
- [7] W.-Y. Wong, *J. Inorg. Organomet. Polym. Mater.* 15 (2005) 197.
- [8] W.-Y. Wong, *Comm. Inorg. Chem.* 26 (2005) 39.
- [9] Y. Fujikura, K. Sonogashira, N. Hagihara, *Chem. Lett.* (1975) 1067.
- [10] K. Sonogashira, S. Takahashi, N. Hagihara, *Macromolecules* 10 (1977) 879.
- [11] S. Takahashi, M. Kariya, T. Yatake, K. Sonogashira, N. Hagihara, *Macromolecules* 11 (1978) 1063.
- [12] K. Sonogashira, S. Kataoka, S. Takahashi, N. Hagihara, *J. Organomet. Chem.* 160 (1978) 319.
- [13] S.J. Davies, B.F.G. Johnson, M.S. Khan, J. Lewis, *J. Chem. Soc. Chem. Commun.* (1991) 187.
- [14] Z. Atherton, C.W. Faulkner, S.L. Ingham, A.K. Kakkar, M.S. Khan, J. Lewis, N.J. Long, P.R. Raithby, *J. Organomet. Chem.* 462 (1993) 265.
- [15] B.F.G. Johnson, A.K. Kakkar, M.S. Khan, J. Lewis, *J. Organomet. Chem.* 409 (1991) C12.
- [16] S.J. Davies, B.F.G. Johnson, J. Lewis, P.R. Raithby, *J. Organomet. Chem.* 414 (1991) C51.
- [17] J.L. Brédas, R.R. Chance (Eds.), *Conjugated Polymeric Materials: Opportunities in Electronics, Optoelectronics and Molecular Electronics*, Kluwer Academic Publishers, Dordrecht, 1990.
- [18] M.A. Baldo, M.E. Thompson, S.R. Forrest, *Pure Appl. Chem.* 71 (1999) 2095.
- [19] W. Lu, B.-X. Mi, M.C.W. Chan, Z. Hui, C.-M. Che, N. Zhu, S.-T. Lee, *J. Am. Chem. Soc.* 126 (2004) 4958.
- [20] Y.-Y. Lin, S.-C. Chan, M.C.W. Chan, Y.-J. Hou, N. Zhu, C.-M. Che, Y. Liu, Y. Wang, *Chem. Eur. J.* 9 (2003) 1264.
- [21] J.M. Bedlek-Anslow, J.P. Hubner, B.F. Carroll, K.S. Schanze, *Langmuir* 16 (2000) 9137.
- [22] U.H.F. Bunz, *Chem. Rev.* 100 (2000) 1605.
- [23] J.L. Brédas, J. Cornil, A.J. Heeger, *Adv. Mater.* 8 (1996) 447.
- [24] N.S. Sariciftci (Ed.), *Primary Photoexcitations in Conjugated Polymers: Molecular Exciton vs. Semiconductor Band Model*, World Scientific, Singapore, 1997.
- [25] T.A. Skotheim, J.R. Reynolds, R.L. Elsenbaumer (Eds.), *Handbook of Conducting Polymers*, 2nd ed., Marcel Dekker, New York, 1998.
- [26] R.H. Friend, R.W. Gymer, A.B. Holmes, J.H. Burroughes, R.N. Marks, C. Taliani, D.D.C. Bradley, D.A. Dos Santos, J.L. Brédas, M. Lögdlund, W.R. Salaneck, *Nature (London)* 397 (1999) 121.
- [27] J.S. Wilson, A.S. Dhoot, A.J.A.B. Seeley, M.S. Khan, A. Köhler, R.H. Friend, *Nature (London)* 413 (2001) 828.
- [28] A. Köhler, J.S. Wilson, R.H. Friend, *Adv. Mater.* 14 (2002) 701.
- [29] C. Adachi, M.A. Baldo, M.E. Thompson, S.R. Forrest, *J. Appl. Lett.* 90 (2001) 5048.
- [30] J.M. Lupton, A. Pogantsch, T. Piok, E.J.W. List, S. Patil, U. Scherf, *Phys. Rev. Lett.* 89 (2002) 167401.
- [31] Y.V. Romanovskii, A. Gerhard, B. Schweitzer, U. Scherf, R.I. Personov, H. Bässler, *Phys. Rev. Lett.* 84 (2000) 1027.
- [32] X. Gong, J.C. Ostrowski, G.C. Bazan, D. Moses, A.J. Heeger, M.S. Liu, A.K.-Y. Jen, *Adv. Mater.* 15 (2003) 45.

- [33] A.S. Dhoot, N.C. Greenham, *Adv. Mater.* 14 (2002) 1834.
- [34] P.K.H. Ho, J.S. Kim, J.H. Burroughes, H. Becker, S.F.Y. Li, T.M. Brown, F. Cacialli, R.H. Friend, *Nature (London)* 404 (2000) 481.
- [35] Y. Cao, I.D. Parker, G. Yu, C. Zhang, A.J. Heeger, *Nature (London)* 397 (1999) 414.
- [36] V. Cleave, G. Yahiolglu, P. Le Barny, R.H. Friend, N. Tessler, *Adv. Mater.* 11 (1999) 285.
- [37] M.A. Baldo, D.F. O'Brien, Y. You, A. Shoustikov, S. Sibley, M.E. Thompson, S.R. Forrest, *Nature (London)* 395 (1998) 151.
- [38] M.A. Baldo, M.E. Thompson, S.R. Forrest, *Nature (London)* 403 (2000) 750.
- [39] M. Pope, C.E. Swenberg, *Electronic Processes in Organic Crystals and Polymers*, 2nd ed., Oxford Science Publications, Oxford, 1999.
- [40] S. Szafert, J.A. Gladysz, *Chem. Rev.* 103 (2003) 4175.
- [41] U.H.F. Bunz, *Angew. Chem. Int. Ed. Engl.* 35 (1996) 969.
- [42] H. Lang, *Angew. Chem. Int. Ed. Engl.* 33 (1994) 547.
- [43] V.W.-W. Yam, *Acc. Chem. Res.* 35 (2002) 555.
- [44] R.D. Markwell, I.S. Butler, A.K. Kakkar, M.S. Khan, Z.H. Al-Zakwani, J. Lewis, *Organometallics* 15 (1996) 2331.
- [45] D. Beljonne, H.F. Wittmann, A. Köhler, S. Graham, M. Younus, J. Lewis, P.R. Raithby, M.S. Khan, R.H. Friend, J.L. Brédas, *J. Chem. Phys.* 9 (1996) 105.
- [46] M.S. Khan, M.R.A. Al-Mandhary, M.K. Al-Suti, F.R. Al-Battashi, S. Al-Saadi, B. Ahrens, J.K. Bjernemose, M.F. Mahon, P.R. Raithby, M. Younus, N. Chawdhury, A. Köhler, E.A. Marseglia, E. Tedesco, N. Feeder, S.J. Teat, *Dalton Trans.* (2004) 2377.
- [47] E.E. Silverman, T. Cardolaccia, X. Zhao, K.Y. Kim, K. Haskins-Glusac, K.S. Schanze, *Coord. Chem. Rev.* 249 (2005) 1491.
- [48] Y. Liu, S. Jiang, K. Glusac, D.H. Powell, D.F. Anderson, K.S. Schanze, *J. Am. Chem. Soc.* 124 (2002) 12412.
- [49] A. Onipko, Y. Klymenko, L. Malysheva, *J. Chem. Phys.* 107 (1997) 7331.
- [50] I.N. Levine, *Quantum Chemistry*, 4th ed., Prentice-Hall, New Jersey, 1991, p. 545 (Chapter 16).
- [51] K.S. Schanze, E.E. Silverman, X. Zhao, *J. Phys. Chem. B* 109 (2005) 18451.
- [52] X. Zhao, T. Cardolaccia, R.T. Farley, K.A. Abboud, K.S. Schanze, *Inorg. Chem.* 44 (2005) 2619.
- [53] L. Liu, S.-Y. Poon, W.-Y. Wong, *J. Organomet. Chem.* 690 (2005) 5036.
- [54] M.V. Russo, C.L. Sterzo, P. Franceschini, G. Biagini, A. Furlani, *J. Organomet. Chem.* 619 (2001) 49.
- [55] T.M. Cooper, D.G. McLean, J.E. Rogers, *Chem. Phys. Lett.* 349 (2001) 31.
- [56] J.E. Rogers, T.M. Cooper, P.A. Fleitz, D.J. Glass, D.G. McLean, *J. Phys. Chem. A* 106 (2002) 10108.
- [57] T.M. Cooper, B.C. Hall, A.R. Burke, J.E. Rogers, D.G. McLean, J.E. Slagle, P.A. Fleitz, *Chem. Mater.* 16 (2004) 3215.
- [58] K. Haskins-Glusac, I. Ghiviriga, K.A. Abboud, K.S. Schanze, *J. Phys. Chem. B* 108 (2004) 4969.
- [59] R. D'Amato, I. Fratoddi, A. Cappotto, P. Altamura, M. Delfini, C. Bianchetti, A. Bolasco, G. Polzonetti, M.V. Russo, *Organometallics* 23 (2004) 2860.
- [60] C. Caliendo, I. Fratoddi, M.V. Russo, C.L. Sterzo, *J. Appl. Phys.* 93 (2003) 10071.
- [61] M.J. Irwin, G. Jia, J.J. Vittal, R.J. Puddephatt, *Organometallics* 15 (1996) 5321.
- [62] V.W.-W. Yam, C.-K. Hui, K.M.-C. Wong, N. Zhu, K.-K. Cheung, *Organometallics* 21 (2002) 4326.
- [63] C.-K. Hui, B.W.-K. Chu, N. Zhu, V.W.-W. Yam, *Inorg. Chem.* 41 (2002) 6178.
- [64] K. Onitsuka, Y. Harada, F. Takei, S. Takahashi, *Chem. Commun.* (1998) 643.
- [65] K. Onitsuka, A. Shimizu, S. Takahashi, *Chem. Commun.* (2003) 280.
- [66] C.-H. Tao, N. Zhu, V.W.-W. Yam, *Chem. Eur. J.* 11 (2005) 1647.
- [67] V.W.-W. Yam, C.-H. Tao, L. Zhang, K.M.-C. Wong, K.-K. Cheung, *Organometallics* 20 (2001) 453.
- [68] M.S. Muhammad, M.R.A. Al-Mandhary, M.K. Al-Suti, T.C. Corcoran, Y. Al-Mahrooqi, J.P. Attfield, N. Feeder, W.I.F. David, K. Shankland, R.H. Friend, A. Köhler, E.A. Marseglia, E. Tedesco, C.C. Tang, P.R. Raithby, J.C. Collings, K.P. Roscoe, A.S. Batsanov, L.M. Stimson, T.B. Marder, *New J. Chem.* 27 (2003) 140.
- [69] J. Lewis, P.R. Raithby, W.-Y. Wong, *J. Organomet. Chem.* 556 (1998) 219.
- [70] W.-Y. Wong, *Coord. Chem. Rev.* 249 (2005) 971.
- [71] D. Neher, *Macromol. Rapid Commun.* 22 (2001) 1365.
- [72] B. Tsuie, J.L. Reddinger, G.A. Sotzing, J. Soloducho, A.R. Katritzky, J.R. Reynolds, *J. Mater. Chem.* 9 (1999) 2189.
- [73] K.-T. Wong, Y.-Y. Chien, R.-T. Chen, C.-F. Wang, Y.-T. Lin, H.-H. Chiang, P.-Y. Hsieh, C.-C. Wu, C.-H. Chou, Y.O. Su, *J. Am. Chem. Soc.* 124 (2002) 11576.
- [74] W.-L. Yu, J. Pei, W. Huang, A.J. Heeger, *Adv. Mater.* 12 (2000) 828.
- [75] S. Setayesh, A.C. Grimsdale, T. Weil, V. Enkelmann, K. Müllen, F. Meghdadi, E.J.W. List, G. Leising, *J. Am. Chem. Soc.* 123 (2001) 946.
- [76] K.-T. Wong, Y.-Y. Chien, R.-T. Chen, C.-F. Wang, Y.-T. Lin, H.-H. Chiang, P.-Y. Hsieh, C.-C. Wu, C.H. Chou, Y.O. Su, G.-H. Lee, S.-M. Peng, *J. Am. Chem. Soc.* 124 (2002) 11576.
- [77] W.-Y. Wong, G.-L. Lu, K.-H. Choi, J.-X. Shi, *Macromolecules* 25 (2002) 3506.
- [78] M.S. Khan, M.R.A. Al-Mandhary, M.K. Al-Suti, B. Ahrens, M.F. Mahon, L. Male, P.R. Raithby, C.E. Boothby, A. Köhler, *Dalton Trans.* (2003) 74.
- [79] G.-J. Zhou, W.-Y. Wong, D. Cui, C. Ye, *Chem. Mater.* 17 (2005) 5209.
- [80] W.-Y. Wong, K.-H. Choi, G.-L. Lu, J.-X. Shi, *Macromol. Rapid Commun.* 22 (2001) 461.
- [81] W.-Y. Wong, L. Liu, S.-Y. Poon, K.-H. Choi, K.-W. Cheah, J.-X. Shi, *Macromolecules* 37 (2004) 4496.
- [82] K. Haskins-Glusac, M.R. Pinto, C. Tan, K.S. Schanze, *J. Am. Chem. Soc.* 126 (2004) 14964.
- [83] N. Chawdhury, A. Köhler, R.H. Friend, W.-Y. Wong, J. Lewis, M. Younus, P.R. Raithby, T.C. Corcoran, M.R.A. Al-Mandhary, M.S. Khan, *J. Chem. Phys.* 110 (1999) 4963.
- [84] J. Lewis, N.J. Long, P.R. Raithby, G.P. Shields, W.-Y. Wong, M. Younus, *J. Chem. Soc. Dalton Trans.* (1997) 4283.
- [85] J. Cornil, D. Beljonne, D.A. dos Santos, Z. Shuai, J.L. Brédas, *Synth. Met.* 78 (1996) 209.
- [86] D. Beljonne, J. Cornil, J.L. Brédas, R.H. Friend, *Synth. Met.* 76 (1996) 61.
- [87] P. Li, B. Ahrens, N. Feeder, P.R. Raithby, S.J. Teat, M.S. Khan, *Dalton Trans.* (2005) 874.
- [88] N. Chawdhury, M. Younus, P.R. Raithby, J. Lewis, R.H. Friend, *Opt. Mater.* 9 (1998) 498.
- [89] K.A. Buntin, A.K. Kakkar, *J. Mater. Chem.* 5 (1995) 2041.
- [90] K.A. Buntin, A.K. Kakkar, *Macromolecules* 29 (1996) 2885.
- [91] N. Chawdhury, A. Köhler, R.H. Friend, M. Younus, N.J. Long, P.R. Raithby, J. Lewis, *Macromolecules* 31 (1998) 722.
- [92] M.S. Khan, M.R.A. Al-Mandhary, M.K. Al-Suti, A.K. Hisahm, P.R. Raithby, B. Ahrens, M.F. Mahon, L. Male, E.A. Marseglia, E. Tedesco, R.H. Friend, A. Köhler, N. Feeder, S.J. Teat, *J. Chem. Soc. Dalton Trans.* (2002) 1358.
- [93] W.-Y. Wong, S.-M. Chan, K.-H. Choi, K.-W. Cheah, W.-K. Chan, *Macromol. Rapid Commun.* 21 (2000) 453.
- [94] M.S. Khan, M.R.A. Al-Mandhary, M.K. Al-Suti, N. Feeder, S. Nahar, A. Köhler, R.H. Friend, P.J. Wilson, P.R. Raithby, *J. Chem. Soc. Dalton Trans.* (2002) 2441.
- [95] M. Younus, A. Köhler, S. Cron, N. Chawdhury, M.R.A. Al-Mandhary, M.S. Khan, J. Lewis, N.J. Long, R.H. Friend, P.R. Raithby, *Angew. Chem. Int. Ed.* 37 (1998) 3036.
- [96] M.S. Khan, M.K. Al-Suti, M.R.A. Al-Mandhary, B. Ahrens, J.K. Bjernemose, M.F. Mahon, L. Male, P.R. Raithby, R.H. Friend, A. Köhler, J.S. Wilson, *Dalton Trans.* (2003) 65.
- [97] J.S. Wilson, A. Köhler, R.H. Friend, M.K. Al-Suti, M.R.A. Al-Mandhary, M.S. Khan, P.R. Raithby, *J. Chem. Phys.* 113 (2000) 7627.

- [98] J.S. Wilson, N. Chawdhury, M.R.A. Al-Mandhary, M. Younus, M.S. Khan, P.R. Raithby, A. Köhler, R.H. Friend, *J. Am. Chem. Soc.* 123 (2001) 9412.
- [99] J.S. Wilson, A.S. Dhoot, A.J.A.B. Seeley, M.S. Khan, A. Köhler, R.H. Friend, *Nature (London)* 413 (2001) 828.
- [100] C.-H. Tao, K.M.-C. Wong, N. Zhu, V.W.-W. Yam, *New J. Chem.* 27 (2003) 150.
- [101] F. Matsumoto, N. Matsumi, Y. Chujo, *Polym. Bull.* 48 (2002) 119.
- [102] R. Gleiter, W. Schäfer, H. Sakurai, *J. Am. Chem. Soc.* 107 (1985) 3046.
- [103] K.D. Kim, J.S. Park, H.K. Kim, T.B. Lee, K.T. No, *Macromolecules* 31 (1998) 7267.
- [104] H.K. Kim, M.K. Ryu, S.M. Lee, *Macromolecules* 30 (1997) 1236.
- [105] H.K. Kim, M.K. Ryu, K.D. Kim, S.M. Lee, S.W. Cho, J.W. Park, *Macromolecules* 31 (1998) 1114.
- [106] W.-Y. Wong, C.-K. Wong, G.-L. Lu, K.-W. Cheah, J.-X. Shi, Z. Lin, *J. Chem. Soc. Dalton Trans.* (2002) 4587.
- [107] W.E. Douglas, D.M.H. Guy, A.K. Kar, C. Wang, *Chem. Commun.* (1998) 2125.
- [108] B.F.G. Johnson, A.K. Kakkar, M.S. Khan, J. Lewis, A.E. Dray, R.H. Friend, F. Wittmann, *J. Mater. Chem.* 1 (1991) 485.
- [109] J. Lewis, M.S. Khan, B.F.G. Johnson, T.B. Marder, H.B. Fyfe, F. Wittmann, R.H. Friend, A.E. Dray, *J. Organomet. Chem.* 425 (1992) 165.
- [110] W.-Y. Wong, C.-K. Wong, G.-L. Lu, A.W.-M. Lee, K.-W. Cheah, J.-X. Shi, *Macromolecules* 36 (2003) 983.
- [111] W.-Y. Wong, S.-Y. Poon, A.W.-M. Lee, J.-X. Shi, K.-W. Cheah, *Chem. Commun.* (2004) 2420.
- [112] W.-Y. Wong, C.-K. Wong, S.-Y. Poon, A.W.-M. Lee, T. Mo, X. Wei, *Macromol. Rapid. Commun.* 26 (2005) 376.
- [113] A.K. Kakkar, M.S. Khan, N.J. Long, J. Lewis, P.R. Raithby, P. Nguyen, T.B. Marder, F. Wittmann, R.H. Friend, *J. Mater. Chem.* 4 (1994) 1227.
- [114] S. Yamaguchi, K. Tamao, *J. Chem. Soc. Dalton Trans.* (1998) 3693.
- [115] S.-Y. Poon, W.-Y. Wong, K.-W. Cheah, J.-X. Shi, *Chem. Eur. J.* 12 (2006) 2550.
- [116] H. Zhang, A.W.-M. Lee, W.-Y. Wong, M.S.-M. Yuen, *J. Chem. Soc. Dalton Trans.* (2000) 3675.
- [117] W.-Y. Wong, W.-K. Wong, P.R. Raithby, *J. Chem. Soc. Dalton Trans.* (1998) 2761.
- [118] N.J. Long, A.J. Martin, R. Vilar, A.J.P. White, D.J. Williams, M. Younus, *Organometallics* 18 (1999) 4261.
- [119] O. Lavastre, M. Even, P.H. Dixneuf, A. Pacreau, J.P. Vairon, *Organometallics* 15 (1996) 1530.
- [120] W.-Y. Wong, G.-L. Lu, K.-F. Ng, K.-H. Choi, Z. Lin, *J. Chem. Soc. Dalton Trans.* (2001) 3250.
- [121] A. Ferri, G. Polzonetti, S. Licocchia, R. Paolesse, D. Favretto, P. Traldi, M.V. Russo, *J. Chem. Soc. Dalton Trans.* (1998) 4063.
- [122] K.H. Chang, C.C. Haung, Y.H. Liu, Y.H. Hu, P.T. Chou, Y.C. Lin, *Dalton Trans.* (2004) 1731.
- [123] P. Leonì, F. Marchetti, L. Marchetti, M. Pasquali, *Chem. Commun.* (2003) 2372.
- [124] G. Iucci, G. Infante, G. Polzonetti, *Polymer* 43 (2002) 655.
- [125] R. Saha, M.A. Qaium, D. Debnath, M. Younus, N. Chawdhury, N. Sultana, G. Kociok-Köhn, L.L. Ooi, P.R. Raithby, M. Kijima, *Dalton Trans.* (2005) 2761.
- [126] N.J. Long, A.J.P. White, D.J. Williams, M. Younus, *J. Organomet. Chem.* 649 (2002) 94.
- [127] T.J. Meyer, *Prog. Inorg. Chem.* 30 (1983) 389.
- [128] C.J. Adams, S.L. James, P.R. Raithby, *Chem. Commun.* (1997) 2155.
- [129] N. Matsumi, Y. Chujo, O. Lavastre, P.H. Dixneuf, *Organometallics* 20 (2001) 2425.
- [130] O. Lavastre, J. Plass, P. Bachmann, S. Guesmi, C. Moinet, P.H. Dixneuf, *Organometallics* 16 (1997) 184.
- [131] Y. Zhu, D.B. Millet, M.O. Wolf, S.J. Rettig, *Organometallics* 18 (1999) 1930.
- [132] N.J. Long, A.J. Martin, A.J.P. White, D.J. Williams, M. Fontani, F. Laschi, P. Zanello, *J. Chem. Soc. Dalton Trans.* (2000) 3387.
- [133] Q.Y. Hu, W.X. Lu, H.D. Tang, H.H.Y. Sung, T.B. Wen, I.D. Williams, G.K.L. Wong, Z. Lin, G. Jia, *Organometallics* 24 (2005) 3966.
- [134] A.M. McDonagh, M.G. Humphrey, M. Samoc, B. Luther-Daviers, *Organometallics* 18 (1999) 5195.
- [135] S.K. Hurat, M.P. Cifuentes, M.G. Humphrey, *Organometallics* 21 (2002) 2353.
- [136] T. Ren, *Organometallics* 24 (2005) 4854.
- [137] A.S. Blum, T. Ren, D.A. Parish, S.A. Trammell, M.H. Moore, J.G. Kushmerick, G.-L. Xu, J.R. Deschamps, S.K. Pollack, R. Shashidhar, *J. Am. Chem. Soc.* 127 (2005) 10010.
- [138] G.-L. Xu, C.-Y. Wang, Y.-H. Ni, T.G. Goodson III, T. Ren, *Organometallics* 24 (2005) 3247.
- [139] G. Xu, T. Ren, *Inorg. Chem.* 40 (2001) 2925.
- [140] G.-L. Xu, G. Zou, Y.-H. Ni, M.C. DeRosa, R.J. Crutchley, T. Ren, *J. Am. Chem. Soc.* 125 (2003) 10057.
- [141] K.-T. Wong, J.-M. Lehn, S.-M. Peng, G.-H. Lee, *Chem. Commun.* (2000) 2259.
- [142] K.D. John, M.D. Hopkins, *Chem. Commun.* (1999) 589.
- [143] P.K. Sahoo, S.K. Swain, *J. Polym. Sci. Part A: Polym. Chem.* 37 (1999) 3899.
- [144] R.J. Puddephatt, *Chem. Commun.* (1998) 1055.
- [145] R.J. Puddephatt, *Coord. Chem. Rev.* 216/217 (2001) 313.
- [146] V.W.W. Yam, K.K.W. Lo, K.M.C. Wong, *J. Organomet. Chem.* 578 (1999) 3.
- [147] M.J. Irwin, J.J. Vittal, R.J. Puddephatt, *Organometallics* 16 (1997) 3541.
- [148] M.J. Irwin, G. Jia, N.C. Payne, R.J. Puddephatt, *Organometallics* 15 (1996) 51.
- [149] M.J. Irwin, L. Manojlović-Muir, K.W. Muir, R.J. Puddephatt, D.S. Yufit, *Chem. Commun.* (1997) 219.
- [150] D. Eisler, W. Hong, M.C. Jennings, R.J. Puddephatt, *Organometallics* 21 (2002) 3955.
- [151] H.Y. Chao, W. Lu, Y. Li, M.C.W. Chan, C.M. Che, K.K. Cheung, N. Zhu, *J. Am. Chem. Soc.* 124 (2002) 14696.
- [152] W. Lu, H.-F. Xiang, N. Zhu, C.-M. Che, *Organometallics* 21 (2002) 2343.
- [153] C.-M. Che, H.-Y. Chao, V.M. Miskowski, Y. Li, K.-K. Cheung, *J. Am. Chem. Soc.* 123 (2001) 4985.
- [154] B. Ahrens, K.-H. Choi, M.S. Khan, P. Li, P.R. Raithby, P.J. Wilson, W.-Y. Wong, *Cryst. Eng. Commun.* 4 (2002) 405.
- [155] W. Lu, N. Zhu, C.-M. Che, *J. Organomet. Chem.* 670 (2003) 11.
- [156] J. Vicente, M.T. Chicote, M.D. Abrisqueta, M.M. Alvarez-Falcón, *J. Organomet. Chem.* 663 (2002) 40.
- [157] J. Vicente, M.-T. Chicote, M.M. Alvarez-Falcón, *Organometallics* 23 (2004) 5707.
- [158] J. Vicente, M.T. Chicote, M.M. Alvarez-Falcón, *Organometallics* 24 (2005) 2764.
- [159] V.W.-W. Yam, W.-Y. Lo, C.-H. Lam, W.K.-M. Fung, K.M.-C. Wong, V.C.-Y. Lau, N. Zhu, *Coord. Chem. Rev.* 245 (2003) 39.
- [160] M.I. Bruce, B.C. Hall, B.W. Skelton, M.E. Smith, A.H. White, *J. Chem. Soc. Dalton Trans.* (2002) 995.
- [161] Y.-Y. Lin, S.-W. Lai, C.-M. Che, K.-K. Cheung, Z.-Y. Zhou, *Organometallics* 21 (2002) 2275.
- [162] J. Vicente, M.-T. Chicote, M.M. Alvarez-Falcon, *Organometallics* 22 (2003) 4792.
- [163] J.R. Johnson, W.L. McEwen, *J. Am. Chem. Soc.* 48 (1926) 469.
- [164] A.S. Hay, *J. Org. Chem.* 25 (1960) 1275.
- [165] W.-Y. Wong, L. Liu, J.-X. Shi, *Angew. Chem. Int. Ed.* 42 (2003) 4064.
- [166] W.-Y. Wong, K.-H. Choi, G.-L. Lu, J.-X. Shi, P.-Y. Lai, S.-M. Chan, Z. Lin, *Organometallics* 20 (2001) 5446.
- [167] N.G. Pschirer, U.H.F. Bunz, *Macromolecules* 33 (2000) 3961.
- [168] S.J. Faville, W. Henderson, T.J. Mathieson, B.K. Nicholson, *J. Organomet. Chem.* 580 (1999) 363.
- [169] P. Pykkö, *Chem. Rev.* 97 (1997) 597.
- [170] W.-Y. Wong, G.-L. Lu, L. Liu, J.-X. Shi, Z. Lin, *Eur. J. Inorg. Chem.* (2004) 2066.
- [171] D. Hertel, S. Setayesh, H.G. Nothofer, U. Scherf, K. Müllen, H. Bässler, *Adv. Mater.* 13 (2001) 65.

- [172] A.P. Monkman, H.D. Burrows, L.J. Hartwell, L.E. Horsburgh, I. Hamblett, S. Navaratnam, *Phys. Rev. Lett.* 86 (2001) 1358.
- [173] Y. Liao, J.K. Feng, L. Yang, A.M. Ren, H.X. Zhang, *Organometallics* 24 (2005) 385.
- [174] W.-Y. Wong, K.-H. Choi, G.-L. Lu, Z. Lin, *Organometallics* 21 (2002) 4475.
- [175] D. Rais, D.M.P. Mingos, R. Vilar, A.J.P. White, D.J. Williams, *Organometallics* 19 (2000) 5209.
- [176] D.M.P. Mingos, R. Vilar, D. Rais, *J. Organomet. Chem.* 641 (2002) 126.
- [177] L. Liu, M.-X. Li, W.-Y. Wong, *Aust. J. Chem.* 58 (2005) 799.
- [178] L. Liu, Y.-W. Lam, W.-W. Wong, *J. Organomet. Chem.* 691 (2006) 1092.
- [179] F. Hide, M.A. Díaz-García, B.J. Schwartz, A.J. Heeger, *Acc. Chem. Res.* 30 (1997) 430.